uOttawa

L'Université canadienne
Canada's university

FACULTÉ DES ÉTUDES SUPÉRIEURES ET POSTOCTORALES

uOttawa

L'Université canadienne
Canada's university

FACULTY OF GRADUATE AND POSDOCTORAL STUDIES

Kirsty Malone

AUTEUR DE LA THÈSE / AUTHOR OF THESIS

M.Sc. (Neuroscience)

GRADE / DEGREE

Department of Cellular and Molecular Medicine

FACULTÉ, ÉCOLE, DÉPARTEMENT / FACULTY, SCHOOL, DEPARTMENT

Astrocytes Contribute to the Reelin/ApoER2 Signalling Pathway in the Adult Brain

TITRE DE LA THÈSE / TITLE OF THESIS

D. Park

DIRECTEUR (DIRECTRICE) DE LA THÈSE / THESIS SUPERVISOR

CO-DIRECTEUR (CO-DIRECTRICE) DE LA THÈSE / THESIS CO-SUPERVISOR

EXAMINATEURS (EXAMINATRICES) DE LA THÈSE / THESIS EXAMINERS

S. T. Hou

M. Sikoska

Gary W. Slater

LE DOYEN DE LA FACULTÉ DES ÉTUDES SUPÉRIEURES ET POSTDOCTORALES /
DEAN OF THE FACULTY OF GRADUATE AND POSTDOCORAL STUDIES

# Astrocytes Contribute to the Reelin/ApoER2 Signalling Pathway in the Adult Brain

Kirsty Malone

This thesis submitted as partial fulfillment
of the M.Sc. Program in Neuroscience

Submitted on January 2005
To the Department of Cellular and Molecular
Biology
Faculty of Medecine
University of Ottawa

*Your file Votre référence*
*ISBN: 0-494-11337-5*
*Our file Notre référence*
*ISBN: 0-494-11337-5*

# ABSTRACT

Reelin is 400 kDa, secreted glycoprotein that signals via the lipoprotein receptors ApoER2 and VLDLR, and the cytosolic adaptor protein Dab1 in target cells. This Reelin signalling pathway has been shown to be essential for the formation of the radial glia scaffold and subsequent layering of the cortex during neural development. Reelin's role in the adult brain has not been clearly established, however, recent studies have implicated Reelin as an obligatory component of LTP in neurons of the adult rodent brain. To investigate a possible role for the Reelin/ApoER2/Dab1 signalling pathway in mature, human astrocytes the NT2 cell model system was utilized. Here we show for the first time, using a combination of molecular and cell biology techniques such as RT-PCR, immunoblotting and immunohistochemistry, the presence of Reelin, its receptor (ApoER2) and downstream signalling components in mature NT2 astrocytes (NT2/A). Treatment of pure 15-week-old NT2/A cells with recombinant Reelin induced the tyrosyl phosphorylation of Dab1 on residues Y198 and Y220. Furthermore, our results showed that the membrane ruffling induced by serum deprivation in NT2/A is significantly reduced in the presence of recombinant Reelin in culture. Our findings support a model in which the secreted glycoprotein Reelin is required in NT2/A cells to maintain astrocytic morphology. In light of recent studies, which have identified the importance of astrocytes in the modulation of synaptic transmission, Reelin signalling in NT2/A cells could potentially play a role in altering the dynamics of synaptic transmission in the adult brain via modulation of the cytoskeleton.

# Dedication

I dedicate this thesis to my Grandfather, the late Douglas Wilson Malone,
who shall forever hold a special place in my heart.

# Table of Contents

# List of Tables

# List of Figures

# List of Abbreviations

| | |
|---|---|
| AD: | Alzheimer's disease |
| ANOVA: | Analysis of variance |
| ApoER2: | Apolipoprotein E receptor 2 |
| BCP: | 1-Bromo-3-chloro- propane |
| bp: | Base pairs |
| BSA: | Bovine serum albumin |
| Cdk-5: | Cyclin-dependent kinase 5 |
| cDNA: | Complementary DNA |
| CFDA/PI: | Carboxyfluorescein diacetate/ propidium iodide |
| CNRs: | Cadherin-related neuronal receptors |
| CNS: | Central nervous system |
| $CO_2$: | Carbon dioxide |
| CoIP: | Co-Immunoprecipitation lysis buffer |
| C-R: | Cajal Retzius |
| CR: | Complement-type repeat domains |
| CRMP2: | Collapsin response mediator protein-2 |
| Dab1: | Disabled 1 |
| $ddH_2O$: | Double distilled water |
| DEAE: | Diethylaminoethanol |
| DEPC: | Diethyl pyrocarbonate |
| DMSO: | Dimethylsulfoxide |
| DNA: | Deoxyribonucleic acid |

| | |
|---|---|
| dNTPs: | Deoxyribonucleoside triphosphate |
| DTT: | Dithiothreitol |
| EDTA: | Ethylenediaminetetraacetic acid |
| EGF: | Epidermal growth factor |
| ER Buffer: | Endotoxin removal buffer |
| FBS: | Fetal bovine serum |
| FHAS: | Fetal human astrocytes |
| GDP: | Guanosine diphosphate |
| GEF: | Guanine-nucleotide exchange factor |
| GFAP: | Glial fibrillary acidic protein |
| GLAST-1: | Astrocyte specific glutamte and aspartate transporters |
| GLT-1: | Glutamate transporter- 1 |
| GSK-3β: | Glycogen synthase kinase-3 |
| GTP: | Guanosine triphosphate |
| HEK: | Human embryonic kidney cells |
| HG/DMEM: | High glucose Dubecco's modified Eagle's medium |
| IP: | Immunoprecipitation |
| JIP 1 /2: | c-Jun amino-terminal kinase-interacting proteins |
| kDa: | Kilo Daltons |
| LDL: | Low-density lipoprotein |
| LRP: | LDL receptor-related protein |
| LTP: | Long term potentiation |
| M: | Molarity |

| | |
|---|---|
| MAP: | Microtubule associated protein |
| MZ: | Marginal zone |
| NaOH: | Sodium hydroxide |
| NMDA: | N-methyl-D-aspartate glucose receptor |
| NT2/A: | Differentiated NT2 astrocytes (sometimes NT2-A) |
| NT2/D1: | Human Ntera2 precursor cell line |
| NT2/N: | Differentiated NT2 neruonal cells (sometimes NT2-N) |
| OD: | Optical density |
| ORF: | Open reading frame |
| PAGE: | Polyacrylamide gel electrophoresis |
| PBS: | Phosphate-buffered saline |
| pH: | $-\log[H^+]$ |
| PI3K: | Phosphatidylinositol 3-kinase |
| PID: | Protein interaction domain |
| PKB/Akt: | Protein kinase B |
| PTK: | Protein tyrosine kinase |
| RA: | All-trans-retinoic acid |
| RAP: | Receptor associated protein |
| RIPA: | Radio-Immunoprecipitation cell lysis buffer |
| RNA: | Ribonucleic acid |
| RT-PCR: | Reverse transcriptase- polymerase chain reaction |
| SDS: | Sodium dodecylsulfate |
| SFKs: | Src family of non-receptor tyrosine kinases |

| | |
|---|---|
| SFM: | Serum free media |
| SH3: | Src homology sequence |
| ssDNA: | Single stranded DNA |
| TAE: | Tris-acetate buffer |
| TBST: | Tris-buffered saline with .05% Tween |
| TE: | Tris-EDTA buffer |
| VLDLR: | Very low density lipoprotein receptor |
| VZ: | Ventricular zone |
| WT: | Wild type |

# Acknowledgements

First and foremost I would like to thank Dr. PR Walker from the bottom of my heart for being an exceptional supervisor, for answering all of those 'quick' and not so 'quick' questions, for sitting and discussing my thesis, results, and daily ponderings. I would not be where I am today if weren't for the continual support, encouragement, and guidance from him throughout the duration of this thesis, with all the ups and downs that come along with it.

I would like to thank Dr. M Sikorska, for all of her support, guidance and direction for the duration of my thesis; for answering all those unanswerable questions and for helping me get back on track whenever my foot should slip from the path.

I would also like to thank Dr. H Fang, for her patience in helping me get started in my thesis, and struggling through with me for the first year; Dr. M Bani for his guidance and support; Dr. M Ribecco for teaching me so many of my laboratory skills, and for answering all of my questions; Dr. JK Sandhu for her guidance, support and teaching of lab techniques; Roger Tremblay for his support and for helping me get through my thesis with many a lunch hour run; Angele Byrd for her friendship, support and for answering my questions; Angele Desbois for her friendship, continual support, for believing in my ability when things weren't going well, and for teaching and sharing with me her lab techniques; to everyone one else in the Walker/Sikorska lab, and the M-54 building who have helped me out by answering my many questions and have helped me out whenever I was in need.

I would like to give special thanks to Tom Devecseri, the Adobe Photoshop God, to whom all credit must go for producing such amazing figures. If it weren't for Tom, I would still be trying to figure out how the resizing tool works in Adobe Photoshop.

I would like to thank my brother Douglas Malone for his patience and help in explaining to me the theory behind the statistical analysis done in my thesis.

I would like give special thanks to Dr. T Curran, Dr. J Nimpf, & Dr. U Beffert who all generously donated ApoER2 and Dab1 specific antibodies, without which this thesis would not have been possible.

And lastly I would like to thank my friends and family for their continuous support for the duration of this degree and for being there for me around the clock; their love and encouragement is what has gotten me to the end of this long and arduous journey.

**Thank-you.**

# 1.0 Introduction

## 1.1 Discovery of Reelin

Reelin, now known to play an essential role in the development of the brain, was first discovered in the late 1990s following studies on the phenotype of the *Reeler* mouse. The *Reeler* mouse first appeared as a spontaneous mutation in a stock of mice in a Scottish laboratory in 1951 and was described as having locomotor abnormalities, a Reeling gait, a trembling effect as well as aberrant neuronal layering (Falconer DS 1952). The *reeler* phenotype was found to be an autosomal recessive mutation, in which neurons are generated normally, but are abnormally placed (D'Arcangelo G et al. 1997). More specifically, severe migration abnormalities were seen, particularly in laminated regions such as the neocortex, the hippocampus and the cerebellum (Rakic P et al. 1995). In the *reeler* neocortex, cortical plate neurons were aligned in an inverted fashion and migrating cortical neurons failed to split the preplate into the subplate and marginal zone; in the hippocampus migrating granule and pyramidal cells failed to find their correct positions; and in the cerebellum, Purkinje cells did not migrate to their proper location within the neuroepithelium and, as a direct consequence, the granule cells of the cerebellum failed to proliferate (Trommsdorff M et al. 1999).

The human Reelin gene has been cloned and mapped to chromosome 7q22 and its product shares a 94.2% identity at the amino acid level to mouse Reelin, suggesting a highly conserved function (DeSilva U et al. 1997). The Reelin gene contains an open reading frame (ORF) of about 10,383 base pairs (bp) and consists of 65 exons (Royaux I et al. 1997). In humans, the gene is expressed in Cajal-Retzius (C-R) neurons in the immature brain and in pyramidal and interneurons of the mature cortex (Deguchi K et al. 2003). The expression of Reelin in the pyramidal neurons of the cortex is unique to

humans and higher primate species, as this pattern of expression has not been observed within the rodent brain (Deguchi K et al. 2003).

Subsequent work identified the gene product as a large, 400 kDa extracellular glycoprotein, which was called Reelin. Reelin is secreted by a discrete population of cells during neural development (D'Arcangelo G et al. 1997) identified as C-R cells in both the marginal zone of the cortical plate and in the outer molecular layer of the developing hippocampus and post mitotic granule cells in the cerebellum. Reelin is also expressed in the brain, spinal cord, liver, and kidney throughout embryonic development and is transiently expressed in many developing organs such as the optic cup, blood vessels, precartilage, stomach, pituitary, vibrissae, tooth germ, and in cells along growing nerve fibers (Ikeda Y et al. 1997).

Several isoforms of Reelin protein have been found in brain extracts and in the supernatant of primary neuronal cultures that arise via cleavage of full-length Reelin (~400 kDa) into two smaller proteins of approximately 250 and 180 kDa (Royaux I et al. 1997). The N terminus of Reelin contains a cleavable signal peptide and a region of similarity with F-spondin (F-spondin is a secreted protein produced by floor plate cells that controls cell migration and neurite outgrowth) (Royaux I et al. 1997). The main body of the Reelin protein consists of a series of eight internal repeats comprising of 350-390 amino acids (Royaux I et al. 1997). Each Reelin repeat contains two related sub-domains called A &B, separated by a stretch of 30-reserved cystein residues harbouring an epidermal growth factor-like motif (Royaux I et al. 1997). The protein terminates with a basic stretch of 33 amino acids; a region rich in arginine residues near the carboxy terminus that is required for secretion (Royaux I et al. 1997). A monoclonal antibody

named CR-50 recognizes an epitope defined to amino acids 230-346 on the N-terminus of the protein (Ogawa M et al. 1995). CR-50 functions as a blocking antibody, both *in vitro* and *in vivo*, and is able to neutralize the affects of Reelin and to mimic the *reeler* phenotype (Ogawa M et al. 1995).

## 1.2 Components of Reelin Signal Transduction

### 1.2(a) Reelin Receptors

The low-density lipoprotein (LDL) receptor gene family specifies a group of highly related membrane proteins engaged in receptor-mediated endocytosis of a variety of independent ligands (Schneider WJ et al. 1997). This family shares structural homology with the LDL receptor, a prototype receptor responsible for cellular uptake of lipoproteins (May P & Herz J 2003). Specific members of this gene family are capable of mediating signal transduction in addition to endocytosis; the Apolipoprotein E receptor 2 (ApoER2) and the very-low-density-lipoprotein receptor (VLDLR), in particular, are two receptors that are capable of such a dual function (Anderson OM et al. 2003). Both of these receptors have been shown to function as Reelin receptors during embryonic neuronal development, since the absence of both ApoER2 and VLDLR leads to a phenotype that is indistinguishable from that observed in Reelin-deficient (*reeler*) mice (Trommsdorff M et al. 1999). In addition, the cadherin-related neuronal receptors (CNRs) (Senzaki K et al. 1999) and the $\alpha 3\beta 1$-integrin receptors (Dulabon L et al. 2000) have also been considered as candidate receptors for Reelin.

### 1.2(b) The ApoE Receptor 2

The apolipoprotein E receptor-2 (apoER2), also called LR7/8b (the chicken homologue), is predominantly expressed in the brain (Kim, DH et al. 1996) in humans,

mouse, rabbit, rat and chicken. ApoER2 expression has also been found in the placenta of humans and mouse, in the testes and to a lesser extent in ovaries of both rabbit and rat (Kim, DH et al. 1996); (Novak S et al. 1996); (Stockinger W et al. 1998). The predicted domain structure of ApoER2 (see Fig 1) is the same as that of the LDL receptor and the VLDLR, consisting of five functional domains. The first domain is an amino-terminal ligand-binding domain composed of a 40 amino acid cysteine-rich module that is repeated eight times (also called complement-type repeat (CR) domains). These CR-domains are responsible for mediating receptor/ ligand interactions and are characterized by three internal disulfide bridges and a number of conserved acidic residues that form an octahedral cage around a central co-ordinated $Ca^{2+}$ ion (Andersen OM et al. 2003). The second domain is an epidermal growth factor (EGF) precursor homology domain, which contains three growth factor repeats (A-C) and mediates the acid-dependent dissociation of the ligand. The third domain is an O-linked sugar domain; the fourth is a transmembrane domain; and the fifth is a cytoplasmic domain that contains the NPxY-motif that comprises an internalization signal (Kim, DH et al. 1996).

### 1.2(c) The ApoER2 Gene and Its Splicing Variants

The ApoER2 gene maps to human chromosome 1p34, spans ~ 60 kb, contains 19 exons and produces a gene product that consists of 922 amino acids with a protein molecular weight of ~100 kDa (Kim DH et al. 1997). The ApoER2 transcripts are subject to complex differential splicing that is species and tissue specific (Brandes C et al. 1997). Four distinct human ApoER2 splicing variants were established by ribonuclease protection assays (Korschineck I et al. 2001):

## Figure 1: The Human ApoER2 Gene

The human ApoER2 gene consists of 19 exons that produces 5 functional protein domains: an amino terminal ligand-binding domain composed of multiple cysteine rich repeats (1 – 7a) (exons 2 – 6a); an epidermal growth factor precursor homology domain (A – C) (exons 7 - 14); an O-linked sugar domain with clustered serine & theronine residues (exon 15); a transmembrane domain (exon 16); and a cytoplasmic domain (exons 17 – 19) containing both an NPxY motif and a proline rich insertion of 59 aa (encoded by exon 18) with two potential SH3 binding sites.

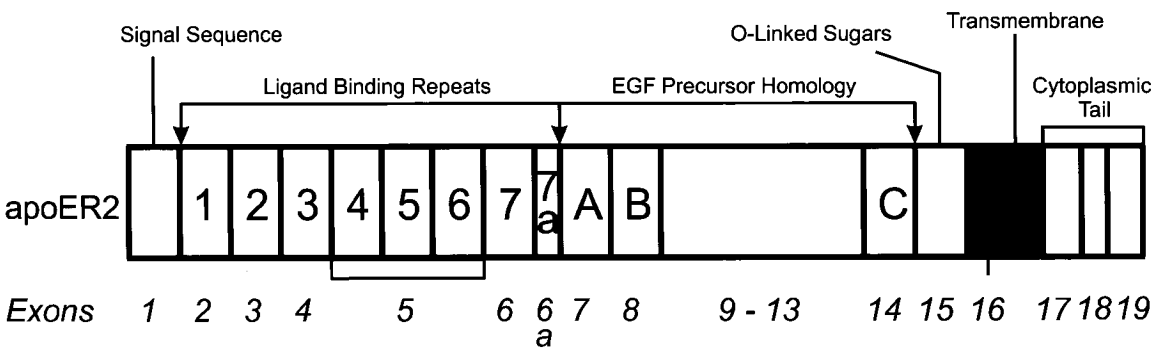
Signal Sequence
O-Linked Sugars
Transmembrane
Ligand Binding Repeats
EGF Precursor Homology
Cytoplasmic Tail
apoER2
1
2
3
4
5
6
7
7a
A
B
C
Exons
1
2
3
4
5
6
6a
7
8
9 - 13
14
15
16
17
18
19

I) full length fragments, with or without exon 5, which contain CR binding domains 4, 5, & 6;

II) full length transcripts, with both exon 15, which encodes the *O*-linked sugar domain, and exon 18, which encodes a novel 59 amino acid, proline rich insertion in the cytoplasmic tail containing two potential SH-3 binding motifs;

III) full length transcripts lacking exon 18 but including exon 15; and

IV) full length transcripts lacking exon 15, but including exon 18.

Similar results were obtained for both brain and placenta samples (Korschineck I et al. 2001). This 59 amino acid insertion in the cytoplasmic tail is thought to allow the receptor to interact with certain intracellular adapter proteins like Dab1, and c-Jun amino-terminal kinase-interacting proteins JIP-1 and JIP-2 (Stockinger W et al. 2000). Brandes C et al. (1997) have also found four other distinct human ApoER2 splicing variants. The first variant lacks exon 7, which encodes repeat A (the first cysteine rich repeat of the EGF precursor homology domain), but contains the remaining 19 exons. The second variant is a full-length variant containing exons 1 through 19. The third variant contains a full-length transcript that has a 73 base pair insertion between exons 7 and 8 (between the cysteine rich repeats A and B); this insertion introduces a frame shift that leads to a premature stop codon. And lastly, the fourth variant consists of a full-length transcript that has a 39 base pair insertion between exons 6 and 7 (between CR domain 7 and repeat A in the EGF precursor homology domain). This insertion fragment is highly basic and contains a consensus signal for precursor cleavage catalyzed by furin (Brandes C et al. 1997).

For the most part, the specific function of each splice variant is not known. Furthermore, recent advances have been made by Koch S et al. (2002), who demonstrated that post-transcriptional furin-dependent processing generates a soluble fragment that consists of the entire ligand-binding domain of ApoER2. This soluble fragment was secreted by ApoER2 expressing murine neuronal cells and was shown to have the ability to act as a dominant-negative receptor that inhibited the Reelin-signalling pathway (Koch S et al. 2002).

### 1.2(d) A Reelin-ApoER2 Connection is Established

The generation of receptor-deficient mice by Trommsdorff M et al. (1999) led to the discovery that mice lacking both the VLDLR and ApoER2 presented a neurological phenotype identical to the *reeler* animals. Using gene-targeting techniques the authors showed that both of these receptors are required for cortical layering, cerebellar foliation, and the migration of Purkinje cells. It was also interesting to note that the Purkinje cells in the cerebellum of double knockout animals also had impaired dendritic trees relative to wild-type controls. These findings suggested that ApoER2/VLDLR function in a co-ordinated and partially overlapping fashion as potential mediators of the Reelin signal. In 1999, D'Arcangelo G et al. (1999) established that Reelin was a ligand for VLDLR and ApoER2 and that the three isoforms of Reelin (400, 250 and 180 kDa) were able to associate with the two receptors in a calcium dependent manner. This association was inhibited in a dose-dependent manner by the monoclonal antibody CR-50.

Direct biochemical evidence for receptor binding was provided by Andersen OM et al. (2003) who unveiled the mechanism by which Reelin interacts with ApoER2. They showed that Reelin-mediated cross-linking of receptors is essential for the ligand to

achieve a high-affinity interaction with its receptor. Andersen OM et al. (2003) further established that Reelin makes an essential contact with the CR-binding domain-1 of ApoER2 and is also able to recognize the CR-binding domain 3. However, results showed that the fingerprint residues in the other CR-binding domains of the receptor were not essential for Reelin binding.

### 1.2(e) Receptor Adapter Proteins: the *Scrambler* and *Yotari* Phenotypes

The next breakthrough in unmasking the Reelin/ApoER2 signalling pathway came from the identification of two new autosomal recessive mouse mutations, *scrambler* and *yotari* that exhibited a phenotype identical to *reeler* (Sweet HO et al. 1996 & Yoneshima H et al. 1997). Molecular genetic studies by Ware ML et al. (1997) revealed that the *scrambler* and *yotari* phenotypes arose from independent mutations in the Dab1 gene. These mutations caused aberrant splicing of Dab1 mRNA that resulted in the synthesis of little or no Dab1 protein (Ware ML et al. 1997). Dab1, like Reelin is necessary for the formation of the laminar structure in the developing brain (Rice DS et al. 1998). In mice that lack Dab1, laminar organization of the cortex, hippocampus and cerebellum is abnormal; neurons are generated normally, but they align abnormally within these cortical structures (Rice DS et al. 1998). In the cortex, migrating cortical plate neurons fail to split the preplate; in the cerebellum, granule cells, which arise from the external germinal layer (EGL) are reduced in number and Purkinje cells do not migrate to their proper location within the neuroepithelium; and in the hippocampus, migrating granule and pyramidal cells fail to find their correct positions (Rice DS et al. 1998).

The first study to establish a biochemical link between Reelin and Dab1 was carried out by Rice DS et al. (1998) who found that Dab1 protein levels, but not mRNA levels were elevated in ectopic neurons of *reeler* and *scrambler* mice. Based on its biochemical properties, Dab1 was thus thought to function as an adaptor molecule in the transduction of protein kinase signals (Rice DS et al. 1998).

### 1.2(f) The Cytosolic Adaptor Protein Dab1

Mouse disabled (mDab1) was first described as a *Src* binding protein that was cloned based upon its interaction with *Src* in a yeast two-hybrid screen (Howell BW et al. 1997). *Src* belongs to a family of non-receptor protein tyrosine kinases (PTK) and is highly expressed in the developing mammalian system (Maness PF 1992). Relatives of the Src PTK family include Fyn, Yes and Abl (Maness PF 1992). The mDab1 gene is expressed in the nervous system as a variety of spliced mRNAs and three main isoforms of mDAb1 have been isolated representing 555, 217 and 271 specific transcripts (Howell WB et al. 1997a). Immunoblot analysis of lysates from differentiated P19 cells found three main mDab1 isoforms of 60, 80 and 120 kDa, which were found to be tyrosine phosphorylated during differentiation prior to neurite extension (Howell WB et al. 1997a). Moreover mDab1 p60 and p80 isoforms were found to interact with the non-receptor PTK Src (Howell WB et al. 1997a). Trommsdorff M et al. (1998) reported that mDab1 interacted via it's Protein Interaction Domain (PID) with sequences containing NPxY motifs in the cytoplasmic tails of the LDL and the LDL receptor-related protein (LRP). In light of this study, and the findings of the similarities of *reeler*, *scrambler/yotari*, and ApoER2/VLDLR double knockout phenotypes, a linear Reelin

signalling pathway was proposed, were the Reelin signal is relayed through the ApoER2/VLDLR receptors to the intracellular adaptor protein Dab1.

### 1.2(g) Reelin Induces Dab1 Tyrosine Phosphorylation

The next advance in deciphering the Reelin/ApoER2/Dab1 signalling pathway came from a study by Hiesberger T et al. (1999) who were the first to establish that Dab1 phosphorylation is Reelin/ApoER2 dependent. This study utilized the receptor-associated protein (RAP), which is a 39 kDa protein that associates with many members of the LDL receptor gene family, including ApoER2 (Herz J et al. 1991). RAP was shown to not only block Reelin from binding to both ApoER2 and VLDLR, but it also prevented the Reelin-induced tyrosine phosphorylation of Dab1 in cultured primary embryonic neurons, clearly placing ApoER2 and VLDLR between Reelin and Dab1 in the signalling pathway. Furthermore, this study established that in *reeler* as well as *vldlr/apoER2* double mutant mice, the phosphorylation level of the microtubule-stabilizing protein tau was significantly increased, suggesting that tau phosphorylation is regulated by the Reelin/ApoER2/VLDLR/Dab1 signalling pathway. Tau regulates microtubule assembly and disassembly during neuronal differentiation and is regulated by phosphorylation at many different sites (Merrick SE et al. 1997). Hypophosphorylated tau binds to and stabilizes microtubules, whereas hyperphosphorylation of tau leads to its dissociation from the microtubules and disruption of the axonal cytoskeleton in neurons (Merrick SE et al. 1997). Thus, the tyrosine phosphorylation of Dab1 likely primes cytoplasmic kinase cascades that control cell shape by remodelling and stabilizing the neuronal cytoskeleton (Trommsdorff M et al. 1999). Significantly, abnormally high levels of tau phosphorylation in adult brains are

associated with various neurological pathologies. In humans, hyperphosphorylated tau is prone to form paired helical filaments which are responsible for the tangles seen in neuronal cell bodies in the brains of patients afflicted with Alzheimer's Disease (AD) (Matsuo ES et al. 1994). In further support of the findings by Hiesberger T et al. (1999), Brich J et al. (2003) used a phenylalanine mutant allele of Dab1 ($Dab1^{5F}$), which lacks tyrosine phosphorylation sites (and has been shown by Howell BW et al. (2000) to be defective in Reelin signalling), to show that mutations preventing the Reelin-dependent induction of Dab1 tyrosine phosphorylation results in tau hyperphosphorylation in the hippocampus.

In order to determine whether tyrosine phosphorylation of Dab1 is critical for its function, Howell BW et al. (2000) generated mice that expressed either the wild-type Dab1 p80 protein or a mutant protein that lacked the tyrosine phosphorylation sites from the endogenous *dab1* promoter. They showed that animals expressing wild-type Dab1 developed normally, but animals producing only the unphosphorylated mutant Dab1 ($Dab1^{5F}$) showed aberrant brain development that phenocopied the null mutant. This study thus established that the tyrosine phosphorylation of Dab1 is critical to its role in Reelin signalling, that binding of Reelin to lipoprotein receptors triggers the tyrosyl phosphorylation of Dab1 in neurons and these tyrosine phosphorylation sites are required to transmit the developmental signal for neuronal positioning.

To identify the specific sites of phosphorylation within Dab1, Keshvara L et al. (2001) generated GST-Dab1 fusion proteins containing single phenylalanine substitutions at tyrosines 185 (185F), 198 (198F), 200 (200F), 220 (220F), and 232 (232F). Their results suggested that Tyr198 and Tyr220 were the major *in vitro* Src phosphorylation

sites, and Tyr185, Tyr200 and Tyr232 were the minor *in vitro* Src phosphorylation sites. They also demonstrated that Tyr198 and Tyr220 are phosphorylated in response to Reelin treatment and despite the elevated levels of Dab1 protein found in *reeler* mice, tyrosyl phosphorylation of Dab1 was significantly diminished in these animals (Keshvara L et al. 2001). These studies clearly demonstrate that Reelin binds to its receptors, ApoER2/ VLDLR in target neurons resulting in the phosphorylation of the cytosolic adapter protein Dab1 by the Src family of non-receptor tyrosine kinases (SFKs) on specific tyrosine residues- 198 and 220 (Keshvara L et al. 2001; Pawson T & Scott JD 1997).

### 1.2(h) Signalling Downstream of Dab1 Tyrosine Phosphorylation

A recent study by Beffert U et al. (2002) provided genetic and biochemical evidence that the signalling cascade induced by Reelin downstream of Dab1 phosphorylation results in the activation of phosphatidylinositol 3-kinase (PI3K) and inhibition of glycogen synthase kinase-3 (GSK-3β). PI3K activation results in the stimulation of protein kinase B (PKB/Akt) by phosphorylation on $Ser^{473}$, and subsequent inactivation of GSK-3β by phosphorylation on $Ser^{9}$ (Beffert U et al. 2002). This cascade was shown to be dependent upon the presence of ApoER2, VLDLR and Dab1. The Reelin-induced suppression of GSK-3β activity could potentially block the phosphorylation of GSK-3β substrates such as the microtubule-associated protein tau. Thus in this model, failure to suppress GSK-3β activity could explain the observed increases in tau phosphorylation seen in different mutant mouse strains (i.e. mice with defects in Reelin, VLDLR, ApoER2 and Dab1) by Hiesberger T et al. (1999).

Several recent studies have suggested that the non-receptor tyrosine kinase Src, or one of its close relatives Fyn, might catalyze Dab1 tyrosine phosphorylation. Studies by

Arnaud L et al. (2003) and Bock HH et al. (2003) both found that Reelin induced Dab1 tyrosine phosphorylation was dependent upon the SFKs. Even though $fyn^{-/-}$ mice do not have a *reeler* phenotype, homozygous Fyn mutants have been reported to have several defects, including abnormal hippocampal architecture, impaired spatial learning, reduced long-term potentiation and behavioural problems (Grant SG et al. 1992). A study by Bock HH & Herz J (2003) additionally demonstrated that Reelin-induced the aggregation of both its lipoprotein receptors and Dab1 at the plasma membrane, generating a 'supercritical' density that appears to be necessary for the mutual activation of Dab1 and its effectors the SFKs (Src family of non-receptor tyrosine kinases) (Bock HH & Herz J 2003).

A study by Balif BA et al. (2003) further analyzed the Reelin/Dab1 signalling pathway in primary neuronal cultures from various mutant mice, and found that the tyrosine phosphorylation of Dab1 was required for Reelin-induced activation of PKB/Akt and SFKs. These findings were later confirmed by Bock HH et al. (2003a), who showed that the activation of PI3K in neurons was indeed regulated by a Reelin-dependent interaction of phosphorylated Dab1 with the PI3K regulatory subunit p85α and that PI3K's activity was a requirement for the formation of a normal cortical plate. Bock HH et al. (2003a) suggested that the Reelin-induced tyrosine phosphorylation of Dab1 could induce a conformational change that exposes proline rich sequences within Dab1, which could foster an interaction with the Src homology-3 (SH3) domain of p85α. The PI3K is a class 1 kinase that consists of a regulatory subunit- p85α, and a catalytic subunit- p110 (Cantley LC 2002). Binding of the regulatory subunit to activated membrane-associated proteins usually occurs at phosphorylated tyrosine residues and relieves the inhibition on

P110 and brings the complex into proximity to its substrate in the membrane (Cantley LC 2002).

### 1.2(i) The Current Reelin Signal Transduction Pathway

Upon secretion, full length Reelin forms a disulfide-linked homodimer of ~800 kDa (Kubo KI et al. 2002). A chemical cross-linking experiment on secreted Reelin confirmed that only dimers are formed by the full length protein and such dimerization is required to elicit proper Reelin induced Dab1 phosphorylation (Kubo KI et al. 2002). Interestingly, chemical cross-linking of the N-terminal-truncated Reelin resulted in the formation of larger complexes, in addition to dimers, suggesting that the tertiary structure required for the proper and stable assembly/dimerization was altered by truncation (Kubo KI et al. 2002). Although the truncated protein bound well to the receptors, it failed to induce efficient tyrosine phosphorylation of Dab1. These findings helped to further reveal the molecular mechanisms of Reelin signalling. Jossin Y et al. (2004) further advanced the field by finding that the N-terminal moiety of Reelin is not involved in binding to the ApoER2 and the VLDLR. Their results showed that the central fragment of Reelin, consisting of repeats 3-6, was able to bind to ApoER2/VLDLR in neuronal cultures and trigger Dab1 phosphorylation. Thus the N-terminal region of Reelin is not required for receptor binding but rather mediates aggregation, and the formation of homopolymers, which increases the ability of Reelin to stimulate Dab1 phosphorylation.

Benhayon D et al. (2003), using a cell based binding assay, showed that Reelin interacts with ApoER2 with a higher affinity than with VLDLR. Furthermore, this study confirmed that Reelin does not induce tyrosine phosphorylation of Dab1 in the absence of the ApoER2 and the VLDLR (Benhayon D et al. 2003). Thus no other receptor was able

to compensate for the loss of ApoER2 and VLDLR, since no Reelin-induced tyrosine phosphorylation was observed in neurons form ApoER2$^{-/-}$: VLDLR$^{-/-}$ animals. Subsequently, Strasser V et al. (2004) showed that in order for Dab1 phosphorylation to occur, a bivalent ligand must bind to either ApoER2 or VLDLR, which results in receptor clustering and subsequent Src dependent Dab1 phosphorylation on tyrosine residues 198 and 220. The authors thus concluded that the primary effect of ligand binding was receptor clustering on the surface of target cells and that the interaction of the receptors with a bivalent agent was sufficient to induce Dab1 phosphorylation. Their experiments further confirmed recent reports demonstrating that activation of PKB/Akt is a direct consequence of Dab1 phosphorylation and does not involve additional PI3K activation by another pathway (Balif BA et al. 2003)(Bock HH et al. 2003(a)).

The most recent model of Reelin action has been postulated by Strasser V et al. (2004) whereby "Reelin is secreted by specialized cells as a disulfide-linked homodimer, which binds to ApoER2 and VLDLR on target cell surfaces, thereby inducing the clustering of the receptors. As a consequence Dab1 becomes dimerized or oligomerized on the cytoplasmic side of the plasma membrane and thus constitutes an active substrate for Src family members" (Strasser V et al. 2004) as depicted in Figure 2.

## 1.3 Reelin Function in Development

Observations of the *Reeler* phenotype suggest a role for Reelin in the spatial organization of the developing cortex since neurons, although produced in the correct number, are not properly placed. Cortical plate development is a critical early stage in the formation of the cortex.

## Figure 2: Proposed Reelin Signalling Pathway

Reelin is secreted by both NT2/A and NT2/N. Secreted Reelin forms homodimers with prior to binding to the lipoprotein receptors. Ligand binding results in receptor clustering and triggers not only the phosphorylation of Dab1 on tyrosyl residues 198 and 220, but also the homodimerization of Dab-1 and the activation of Fyn (a member of the Src non-receptor tyrosine kinase family). Upon Dab1 phosphorylation, a kinase signalling pathway is activated which results in the activation of PI3K that activates PKB/Akt, and in turn inhibits the activity of GSK-3β (a kinase that phosphorylates and destabilizes the microtubule stabilizing protein tau).

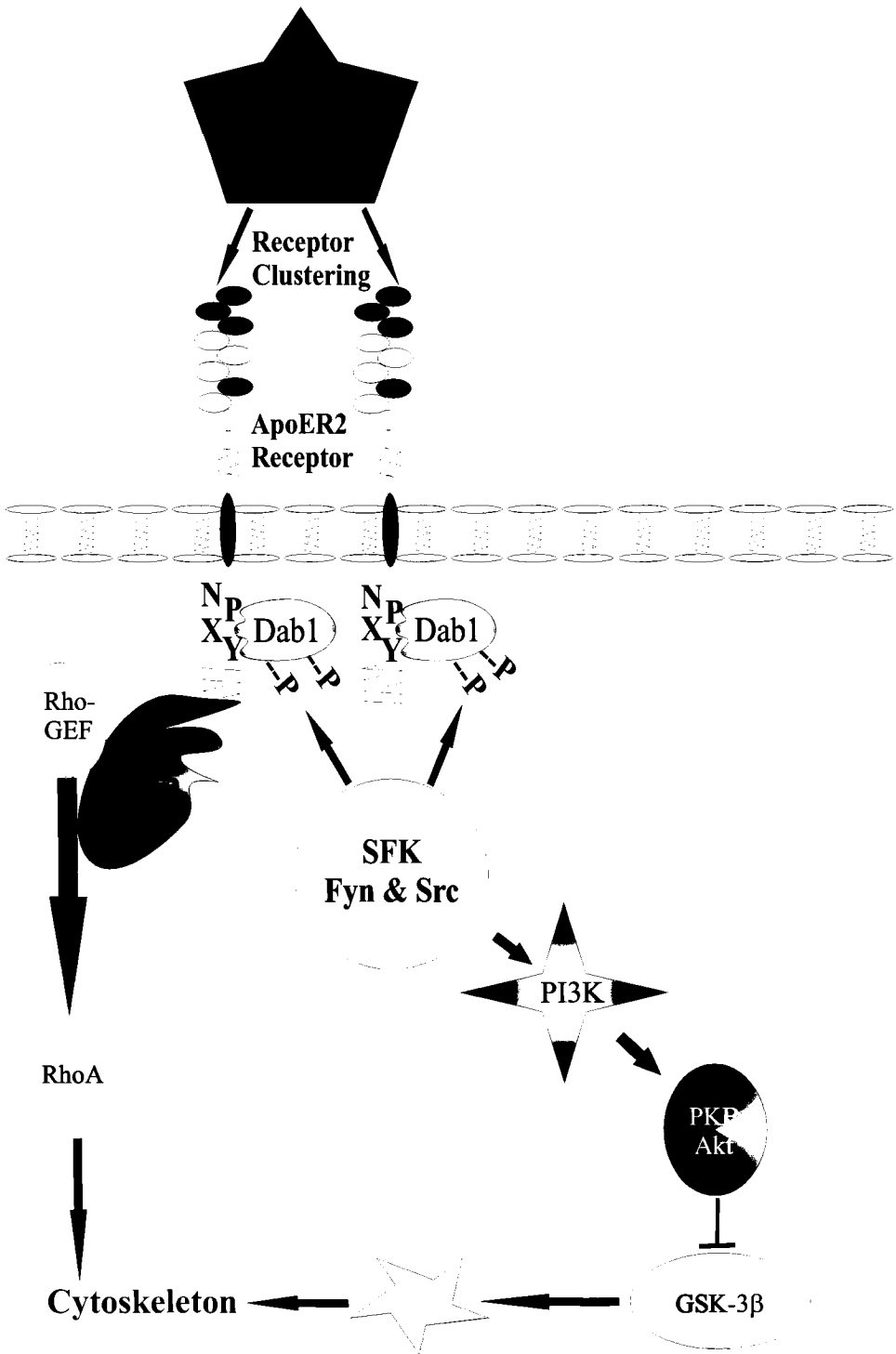
Receptor
Clustering
ApoER2
Receptor
NPXY
Dab1
-P
-P
NPXY
Dab1
-P
-P
Rho-
GEF
SFK
Fyn & Src
PI3K
RhoA
PKB
Akt
Cytoskeleton
GSK-3β

### 1.3(a) Cortical Plate Development

Neocortical development begins with the appearance of the preplate, which consists of Cajal Retzius cells and the subplate neurons. The Cajal Retzius (C-R) cells are amongst the earliest cells to be generated in the neocortex and are the first cells to migrate out of the ventricular zone into the cell-sparse marginal zone (Ogawa M et al. 1995). As described above, the C-R cells are an important source of Reelin production in the developing cortex. The C-R cells reside in the marginal zone throughout development where they maintain a superficial position close to the pial matter and actively signal other cells to migrate (Caviness VS & Rakic P 1978). The next cells to migrate are the radial glial cells, which are characterized by long radial processes that extend from the ventricular zone to the pial surface (Luque JM et al. 2003). Immature neurons use these radial glial processes as a scaffold on which to exit from the ventricular zone to the cortical plate (Luque JM et al. 2003). Upon reaching the cortical plate, neurons differentiate and undergo axonal growth and development (Marin-Padilla M 1978). As new cortical plate neurons migrate past the subplate neurons they insert themselves directly beneath the C-R cells forming the cortical plate, where they become arranged in an inside-first outside-last manner, such that early born cells settle in the deepest layers of the cortex and later-born cells reside in more superficial layers (D'Arcangelo G et al. 1997); (Marin-Padilla M 1978).

The majority of research on the Reelin signalling pathway thus far has been concentrated on a direct effect of Reelin on neuronal migration and positioning, however recent evidence has shown that Reelin is capable of binding to receptors on target radial glial cells and that Reelin signalling is required for proper glial morphology and

biochemical maturation during development (Weiss KH et al. 2003). Forster E et al., (2002) were the first to show that a regular glial scaffold fails to form in the dentate gyrus of *reeler* and *scrambler/yotari* mutants, suggesting that the neuronal migration defects observed in these mutants are caused, in part, by malformations of the radial glial scaffold. This study also demonstrated that Reelin is important for the formation of the radial glial scaffold in the rodent dentate gyrus. Subsequently, in 2003, a study by Luque et al. (2003) provided direct evidence by double-labelling immunofluoresence, using the markers nestin and vimentin, that during cortical development the Reelin receptor machinery, including lipoprotein receptors ApoER2 and VLDLR, along with cytoplasmic adaptor protein Dab1, was located in radial glial precursors as well as in postmitotic neurons. In a similar study, Weiss KH et al. (2003) using glial fibrillary acidic protein (GFAP) as a marker, showed that a regular glial scaffold fails to form in the dentate gyrus not only in *reeler* and *scrambler* mutants, but also in mice lacking both of the Reelin receptors ApoER2 and VLDLR. These results thus confirmed that Reelin signalling via ApoER2, VLDLR and Dab1 is an absolute requirement for the formation of a regular radial glial scaffold in the dentate gyrus of mice (Weiss KH et al. 2003). Furthermore, Frotscher et al. (2003) showed that astrocytes have a preference for Reelin-coated surfaces, whereas neurons do not.

Most recently, Hartfuss et al. (2003) examined the length of radial glia process in wild-type and *reeler* mutant embryos by using the lipophilic dye DiI to trace cells from the ventricular surface (VS) to the marginal zone (MZ). Cells located in the VZ are attached to the VS by an apical process. Hartfuss's group identified four distinct classes of cells according to the length of their basal processes. "The first class of cells, were

long cells with a long basal process reaching into the cortical plate. The second class, were short cells, with a shorter basal process ending underneath the cortical plate. The third cell type, were growth-cone cells, which had a clear growth-cone at the tip of its basal process that appeared to extend towards the pial surface. The fourth group of cells, were club-shaped cells, which consisted of cells with a very short or no basal process of at all." Upon quantification, it was apparent that in wild-type (WT) animals the majority of cells were long cells, whereas the proportion of long cells in the VZ of *reeler* animals was significantly reduced, with the club-shaped cells constituting the largest subpopulation of VZ cells. Moreover, the population of short cells was reduced in the *reeler* cortex to half of their proportion in the wild-type cortex, suggesting that severe problems arise in radial fiber extension and maintenance in the absence of the Reelin protein (Hartfuss et al. 2003).

The finding that Reelin has an effect on the morphology of radial glial cells during development is a novel and exciting discovery. Up until this point it has always been thought that Reelin's effect is conveyed directly through its interaction with receptors upon neurons. These findings raise an interesting question, if Reelin is important for the proper formation of glial scaffolds during development then what is its effect on glial cells in the adult brain?

## 1.4 Reelin in the Adult Brain

After birth, Reelin and its signalling molecules continue to be expressed in the hippocampus where they control the migration of dentate granule cells. Reelin is expressed in all cortical layers by GABAergic interneurons and accumulates on dendritic

spines (Drakew et al. 2002). A study by Niu et al. (2004) demonstrated that Reelin stimulated dendrite outgrowth of hippocampal neurons through the activation of the ApoER2/VLDLR/Dab1 signalling pathway. This dendritic outgrowth was also shown using SFK inhibitors PP2, to be dependent upon the Reelin induced Dab1 tyrosyl phosphorylation mediated by the SFKs. Niu et al. (2004) thus demonstrated that the Reelin-signalling pathway regulates the length and complexity of dendrites. It was also interesting to note from this study that the addition of recombinant Reelin to hippocampal cells from *reeler* mice rescued dendrite outgrowth in these cultures. However, the addition of recombinant Reelin to hippocampal cultures from Dab1 knockout mice failed to rescue the defect and promote dendrite extension in these cultures (Niu et al. 2004). Furthermore, in rodents, Reelin is expressed in the GABAergic interneurons of the adult cerebral cortex and hippocampus, and in glutamatergic cerebellar granule neurons (Pappas et al. 2001). Immunomicroscopy has shown that Reelin is present in the extracellular space surrounding dendrites, dendritic spines and small-unidentified neural profiles in discontinuous areas of the cortex in wild type mice (Pappas et al. 2001). Reelin is thought to play a role in the normal functioning and plasticity of adult neurons (Pappas et al. 2001). Thus Reelin in adult animals via the ApoER2/Dab1 signalling pathway (Beffert et al. 2004), by virtue of its effects on neurons, plays a role in dendritic outgrowth and branching in hippocampal neurons (Niu et al. 2004) and in modulating synaptic plasticity within the hippocampus (Weeber EJ et al. 2002).

Since astrocytes play a vital role in the functioning of neurons, it is tempting to speculate that changes in morphology of astrocytes surrounding neurons could contribute to the loss of synaptic plasticity seen in *reeler* and *yotari/scrambler* mice. In fact, recent

findings by Piet R et al. (2004) show that astrocytes are capable of acting as a third partner in synaptic transmission. However, to date, a functional Reeling signalling pathway has not been established in mature astrocytes.

## 1.5 Astrocyte Structure and Function

Astrocytes in the adult brain fall into two broad classes based on their morphology - protoplasmic astrocytes and fibrous astrocytes. Despite having distinct morphological appearances, protoplasmic and fibrous astrocytes have similar characteristics; both have a well-developed cytoskeleton that is dominated by intermediate filaments and includes microtubules and actin filaments (Nolte J 1999). Fibrous astrocytes have a predominantly star-like morphology, with many cylindrical processes that radiate symmetrically away from the soma and frequently form end-feet on capillaries. These processes extend for long distances and branch infrequently. Protoplasmic astrocytes, on the other hand, have a more complex morphology than fibrous astrocytes. Their processes are highly branched and form membranous sheets that enfold neuronal processes and cell bodies. They also form endfeet on capillaries and at the pial surface.

Since astrocytes can assume stellate shapes *in vitro*, the process-bearing morphology of astrocytes is thought to reflect the intrinsic biochemical and cytoskeletal properties of the cells (Nolte J 1999). Indeed, astrocytes have the potential to acquire very different morphologies, depending on their regional location in the CNS and on their functional interactions with other cell types (Safavi-Abbasi S et al. 2001). Morphological changes between a flat or a fibrous-like and a stellate or process-bearing appearance, can

occur rapidly, requiring subcellular redistribution of most cytoskeletal proteins, but no quantitative modifications of the amount of the respective proteins (Safavi-Abbasi S et al. 2001). In addition to their distinct regional appearance in various parts of the brain, astrocytes have the potential to react with changes of their morphology to interactions with other cells, such as the endothelial cells of capillaries (Mi H et al. 2001) and in response to damage in the central nervous system (CNS) commonly referred to as reactive (astro) gliosis (Wu VW & Schwartz JP 1998). It has been hypothesized that the enormous differences in process growth and distribution that occur on various glial cells represent a predictable adaptation to their specific environment, referring mainly to the activity level of neighbouring neurons (Reichenbach et al. 1992). Thus astrocytes can play a key role in modulating the synaptic environment of their neighbouring neurons (Piet R et al. 2004). To examine the effects of Reelin on LTP induction, Weeber EJ et al. (2002) perfused hippocampal slices with either recombinant Reelin or control medium prior to LTP induction. Their results showed that Reelin significantly augmented LTP induction in hippocampal slices, whereby the ablation of either of Reelin's receptors abrogated this LTP-inducing affect of Reelin. Based on these findings, the following model was put forth by Weeber EJ et al. (2002): "upon the Reelin-mediated tyrosyl phosphorylation of Dab1 and subsequent activation of SFKs, these kinase cascades in the adult brain may directly or indirectly alter the phosphorylation state of the post-synaptic NMDA receptors, or of proteins that regulate the activity of the NMDA receptors, thereby modulating the magnitude of LTP induction" (Weeber EJ et al. 2002). These findings clearly indicated a direct role for Reelin in the modulation of hippocampal synaptic plasticity in the adult brain.

## 1.6 Objectives of Thesis

Based on the above observations, we hypothesised that a functional Reelin signalling pathway may exist in astrocytes. To address this, the human NT2 cell model system was utilized. The NT2 cell is a pluripotent embryonal carcinoma cell line that grows as a monolayer of small and large progenitors and can be differentiated into post-mitotic neurons (NT2/N) and astrocytes (NT2/A) by a 4-week treatment with retinoic acid. This cellular system is an established model of human neuronal differentiation and is known to produce both fibrous and protoplasmic types of astrocytes in addition to neurons (Sandhu et al. 2002). Using a combination of molecular and cell biology techniques, RT-PCR, immunoblotting and immunocytochemistry the presence of Reelin, its receptor ApoER2 and downstream signalling components was examined in NT2/A.

# 2.0 Materials and Methods

## 2.1 Cell Culture Conditions

All cell culture dishes (plates and flasks) were purchased from Beckton Dickinson (NJ, USA). All tissue culture was carried out under sterile conditions. The human NTera-2 (NT2/D1) cell line used in this study is a pluripotent clonal embryonal carcinoma cell line (clone# 21) established by Andrews, et al. (1984). The undifferentiated cells were purchased from Stratagene (La Jolla, CA) and were seeded (2 x $10^6$ cells per T-75 $cm^2$ flask) in high glucose Dubecco's modified Eagle's medium (HG/DMEM, cat# 12100-061, GIBCO BRL®, Burlington, ON) supplemented with 10% heat-inactivated (56°C for 30 minutes) fetal bovine serum (FBS, Wisent Inc., St. Bruno, Que.), sodium bicarbonate (37g /10L, BDH Chemicals, Toronto, ON) and 40 μg/mL Gentamycin sulfate (Cat# 61 098 RF, Multicell, Warwick, RI). The cells were maintained in a humidified environment of 5% $CO_2$/95% air at 37°C. Differentiation of NT2/D1 cells was carried out as previously described by Andrews et al. (1984) and Lee et al. (1986). Briefly, NT2/D1 cells were seeded at a density of 2 x $10^6$ cells per T-75 $cm^2$ and were treated with 1 x $10^{-5}$ M all-trans-retinoic acid (RA, cat# R-2625, Sigma Chemical Co., Oakville, ON) three times a week for four weeks. Following RA treatment, cells from one T75 $cm^2$ flask were replated into three T175 $cm^2$ flasks in order to obtain differentiated astrocytes and neurons. Cells were pre-washed with 1x PBS (phosphate-buffered saline, 137 mM NaCl, 4.3 mM $Na_2HPO_4$, 27 mM KCl, 1.4 mM $KH_2PO4$, pH 7.4) 1mM EDTA (ethylenediaminetetraacetic acid, Sigma Chemical Co., Oakville, ON) solution to remove serum, $Ca^{2+}$ and $Mg^{2+}$ ions, and then were harvested using 0.15% Trypsin (Bovine pancreas, Sigma Chemical Co., Oakville, ON) 1mM EDTA (Sigma Chemical Co., Oakville, ON). Trypsinized cells were spun down at 1000 g for 5 minutes at room

temperature, then resuspended in ~15 ml of HG/DMEM supplemented with 10% FBS and equally dispersed into three T175 $cm^2$ flasks with a final volume of 25 ml per flask. Cells were incubated for 1 week, then differentiated neuronal cells (NT2/N) were separated from the underlying astroglia (NT2/A) by incubating cells with 0.015% Trypsin-1mM EDTA (Sigma Chemical Co., Oakville, ON) for 1 minute followed by gentle shaking. The NT2/A were maintained in HG/DMEM supplemented with 5% FBS and were replated on a weekly basis. For optimal results NT2/A were seeded at the following densities: 2 x $10^6$ cells/flask for T75 $cm^2$ flasks and 5 x $10^6$/flask for T175 $cm^2$ flasks. The collected NT2/N cells were plated at a density of 3 x $10^6$ into T75 $cm^2$ flasks containing 2 x $10^6$ differentiated NT2/A cells. The NT2/N were maintained in HG/DMEM supplemented with 10 % FBS and fed once a week.

Fetal human astrocytes (FHAS) primary cultures were kindly provided by Dr. Abulrob Abedelnasser (Institute for Biological Sciences, Ottawa, ON). FHAS were maintained in HG/DMEM supplemented with 10% FBS and were used after the second passage. Pure NT2 neuronal cultures were kindly provided by Angele Desbois (Institute for Biological Sciences, Ottawa, ON), and were used immediately for RNA extraction as described in section 2.2.

## 2.2 RNA Processing

### 2.2(a) RNA Extraction and Purification

Cultured cells were scraped into media and collected in microfuge tubes. RNA was extracted with TriReagent according to the manufacturer's protocol (1995, Molecular Research Center, Inc., Cincinnati, OH). Briefly, collected cells were

resuspended such that the sample volume did not exceed 10% of the volume of TRI Reagent and lysed. The homogenate was then separated into aqueous and organic phases by the addition of 100 µl of BCP (1-Bromo-3-Chloro- Propane, cat# 203-697-1, SIGMA Chemical Co., Germany) per 1 ml of TRI REAGENT, and centrifuged at 12 000g for 15 minutes at 4°C. The aqueous phase was removed to a fresh tube and the RNA was precipitated from the aqueous phase by the addition of 500µl isopropanol (Propan-2-ol, cat# ACS720-76, BDH Inc., Toronto, ON) per ml of TRI Reagent. Samples were centrifuged at 12,000g for 10 minutes at 4°C and the RNA pellet was washed with 1ml of 75% ethanol (Anhydrous Ethyl alcohol, Commercial Alcohols Inc., Brampton, ON.) in DEPC (Diethyl Pyrocarbonate, cat# D-578, SIGMA Chemical Co, Oakville, ON) -treated water (DEPC-dd$H_2O$). The samples were subsequently centrifuged at 12,000g for 5min at 4°C and the RNA pellet was then allowed to air dry for 30 minutes on ice, before dissolving in 50-100 µl of DEPC-dd$H_2O$ for 30 minutes on ice. Two microliters of RNA was diluted 50x in sterile distilled water and the optical density (OD) was taken at 260 nm on the Beckman Coulter $^{TM}$ 600 series spectrophotometer (Beckman Coulter Inc., Fullerton CA). A single-stranded RNA concentration of 40 µg/ml in pure water corresponds to an absorbance at 260 nm of one in a 1 cm light path, thus 1 OD unit is equal to 40 µg/ml. Therefore the following equation was used to calculate the concentration of RNA per sample: Concentration= (40µg/ml)(Absorbance at 260 nm)(Dilution Factor). One microgram of RNA was then run on a 1% TAE (Tris-acetate buffer, 40 mM Tris acetate, 1 mM EDTA, pH 8.0) agarose (Seakem LE agarose, cat# 50004, BMA, Rockland, ME) gel to assess the integrity of the RNA.

Ten micrograms of RNA in a 50µl volume was cleaned using the Ambion DNA-free RNA cleaning kit (cat# 1906, Ambion, Austin. TX). This kit is designed to remove contaminating DNA from RNA preparations, and to subsequently remove the DNase and divalent cations from the sample. Briefly, 0.1 volume of 10X DNase 1 Buffer (100mM Tris-Cl pH 7.5, 25 mM $MgCl_2$, 1 mM $CaCl_2$) and 1 µl of DNase 1 (2 units/µl) was added to the RNA and incubated at 37°C for 30 minutes. Then, 0.1 volume or 5 µl (whichever was greater) of the DNase Inactivation reagent slurry was added to each sample and samples were incubated at room temp for 2 minutes. Samples were subsequently centrifuged at 10,000g for 1minute to pellet the DNase Inactivation Reagent and RNA was recovered from the liquid phase. The RNA concentration was measured using the Beckman Coulter ™ spectrophotometer 600 series (Beckman Coulter Inc., Fullerton CA), and RNA integrity was reconfirmed on a 1% TAE agarose gel.

**2.2(b) cDNA Synthesis**

Two micrograms of total RNA was prepared in 20µl DEPC-ddH2O for the generation of first strand cDNA. Two microliters of Random primers (0.3 µg/µl, Cat. # 48190-011, Invitrogen, Bethesda, MD) was added to each sample and the samples were heated at 70°C for 3 minutes then placed on ice to denature the RNA. The use of random primers provides priming throughout the length of the RNA for unbiased representation of all regions. Eighteen microliters of reaction buffer (5X first strand buffer (Cat. # 18064-014, Invitrogen), 10 mM dNTPs (100mM stock, Cat. #. 27-2035-01, Amersham Pharmacia, Arlington Heights, IL), 100 mM dithiothreitol (DTT, Cat. #18064-014, Invitrogen, Bethesda, MD), 2µl of RNasin (Cat. # N251B, Promega, Pittsburgh, PA), and 2µl of SuperScript™ II RT (Reverse Transcriptase, Cat. # 18064-014, Invitrogen,

Bethesda, MD) was added to each sample and the samples were then incubated at 42°C for 2 hours. To stop the cDNA synthesis reaction and to hydrolyze RNA templates, 2.5 µl of 50 mM EDTA (cat# E-5134, Sigma Chemical Co., Oakville, ON), and 1 µl of 10N NaOH (cat# B10252-34, EM Science, MERK, Germany) was added to each sample; samples were then incubated at 65°C for 20 minutes. To neutralize NaOH, 2 µl of 5 M acetic acid (cat# AC 5003-78, Acetic Acid Glacial, BDH Inc., Toronto, ON) was added, and then the pH (-log $[H^+]$) was measured using litmus paper (colour pHast Indicator strips, pH 0-14, cat# 9590 EM Science, Merk, Gibbstown, NJ) to ensure the pH range was between 6 and 7.5.

### 2.2(c) cDNA Purification

Newly synthesized cDNA was cleaned with the Promega Wizard PCR Preps DNA Purification System (cat# A7170, Promega Corp. Madison, WI), which purifies DNA from macromolecular contaminants. This purification system uses a purification buffer that has a high salt concentration, which increases both the overall charge of the solution and the charge of the DNA molecules and facilitates the binding of DNA to the DNA purification resin and subsequent binding to the Promega Wizard, Minicolumn. To ~50 µl of aqueous cDNA, 100 µl of Direct Purification Buffer (50 mM KCl, 10 mM Tris-HCl, pH 8.8, 1.5 mM $MgCl_2$, 0.1% Triton® X-100) and 1ml of Wizard PCR Preps DNA Purification Resin were added. The resin/cDNA mixture was pushed with a syringe plunger into the Minicolumn. The Minicolumn was then washed twice with 2 ml of 80% isopropanol, to remove salt, protein and organic contaminants from the purified DNA. The Minicolumn was centrifuged for 2 minutes at 10,000 g to dry the resin. The cDNA

was then eluted from the Minicolumn with 50µl of distilled water (pre-heated to 80°C) and centrifuged for 20 seconds at 10,000g.

### 2.2(d) cDNA Quantitation

The purified cDNA was quantified using the OliGreen ssDNA Quantitation kit (cat# 0-11492, Molecular Probes, Invitrogen, Burlington, ON). OliGreen is an exceedingly sensitive fluorescent nucleic acid stain that can detect small amounts of ssDNA in solution and is provided in the kit as a 1 ml concentrated dye solution in high quality DMSO (dimethylsulfoxide). The dye binds to nucleic acids in solution, and when excitation light of an appropriate wavelength hits the OliGreen dye (fluorescence excitation) a photon of light is emitted (emission wavelength), which can be measured by a standard spectrofluorometer. A ssDNA stock standard solution was prepared by re-constituting 1 mg of calf Thymus Single strand DNA (cat# D8899, Sigma Chemical Co., Oakville, ON) in 1 ml of water that was then diluted to a 2 µg/ml working solution. The ssDNA working solution was then serially diluted to 0, 10, 30, 50, 100, 150, and 200 ng/ml to make a standard curve in a Falcon 96 plate (Beckton Dickinson, NJ, USA) in duplicate. The cDNA samples were diluted to be approximately in the range of 50 ng/ml to 100 ng/ml in 1x TE Buffer (10 mM Tris-HCl, 1 mM EDTA, pH 7.5, Molecular Probes, Invitrogen, Burlington, Ont.). The 200x stock solution of OliGreen dye was diluted to a 1x working solution in 1x TE Buffer and 100µl of the diluted dye was added to each sample, such that the final volume of each sample in the Falcon 96 plate was 200µl. Pipetting up and down to mix the components in each well, and the reactions were incubated for 5 minutes at room temperature. As the OliGreen dye is light sensitive, the assay was carried out in the dark. OliGreen fluorescence was measured using a Cytofluor

2350 fluorescence measurement system (Millipore, Billerica, Massachusetts) with the following parameters: Excitation filter: B (480/20); Emission filter: B (530/25); and Sensitivity: 4 & 5. A standard curve was made in Microsoft EXCEL by plotting the average fluorescence values (minus the blank)(y-axis) as a function of the standard DNA concentrations (ng/ml) (x-axis). The concentration of the unknown cDNA sample was extrapolated from the curve using the equation for the standard curve: $y = mx + b$. Where: y = fluorescence value; m = slope of the line; x = concentration of the unknown sample (μg/μl); and b = x intercept of the line (which was pre-set for zero). The equation was solved for x, and the unknown cDNA concentrations were calculated.

**2.2(e) Reverse Transcriptase Polymerase Chain Reaction (RT-PCR)**

Based on the OliGreen calculations, 15-20 ng of cDNA was prepared for each PCR amplification. Each 25 μl PCR reaction contained 1 x PCR buffer (cat# 18038-042, Invitrogen, Carlsbad, CA), 2 μM primers (Alpha DNA, Montreal, Que.; See table 1 for primer details), 0.2 mM dNTP (dGTP- cat# N04425, dCTP- cat# N04415, dATP- cat# N04405, dTTP- cat# N04435, BioLabs, New England, Beverly, MA), 1.5 mM $MgCl_2$ (cat# 18038-042, Invitrogen, Carlsbad, CA), 2.5 units of *Taq* polymerase (cat# 18038-042, Invitrogen, Carlsbad, CA) and was incubated in a Peltier Thermal Cycler, DNA engine from DYAD (model PTC-220, MJ Research Inc., Waltham, MA). All PCR reactions were performed with one denaturation cycle at 94°C for 5 minutes at the very beginning and had one final extension cycle of 72°C for 5 minutes. The following programs were used: Reelin primers, 26 cycles of 1 minute at 94°C, one minute at 55°C and one minute at 72°C; ApoER2 exon 5, exon 6a, exon F15/R18, and exon F6a/R18 primers, 28 cycles of one minute at 94°C, one minute at 60°C and one minute at 72°C;

VLDLR and α-3 Integrin primers, 30 cycles of one minute at 94°C, one minute at 60°C and one minute at 72°C; β-1 Integrin primers, 25 cycles of one minute at 94°C, one minute at 60°C and one minute at 72°C; Dab1 primers, 29 cycles of one minute at 94°C, one minute at 60°C and one minute at 72°C; and β-Actin primers, 20 cycles of one minute at 94°C, one minute at 60°C and one minute at 72°C. PCR products were analysed by electrophroesis on either a 1.5% (for fragments over 300 base pairs) or 2% (for fragments under 200 base pairs) agarose (Seakem LE agarose, cat# 50004, BMA, Rockland, ME) gel containing ethidium bromide (cat# 161-0433, Bio-Rad laboratories, Hercules, CA), and were visualized by using the Ultra Lum gel documentation system (Claremont, CA).

### 2.2(f) Primers for RT-PCR

The full length coding sequence for the genes of interest were retrieved from the NCBI (http://www.ncbi.nlm.nih.gov) or the UCSC genome browser (http://genome.ucsc.edu). Specific exons were chosen and primers were designed specifically for them using the Primer 3 Software package (Howard Hughes Medical Institute & the National Institutes of Health, http://www-genome.wi.mit.edu/cgi-bin/primer/primer3. Primers were chosen that contained a low guanidine and cytosine content and an annealing temperature of either 60°C or 55°C. The primers were 'blasted' at the NCBI Blast web site (http://www.ncbi.nlm.nih.gov/blast/Blast.cgi) to ensure specificity. Primers were generated by Alpha DNA (Montreal, Que.). The sequences of the used primers are shown in Table 1.

**Table 1: Primers used for RT-PCR Analysis**

| Gene | Primer Sequence | Expected PCR Product Size (Base Pairs- bp) |
|---|---|---|
| Reelin | F: CTGCTGGACTTCTCTACGGAT<br>R: CAGTAGAGGTGGAAGGATGCC | 385 bp |
| ApoER2-exon 5 | F: CAGAGAAGCTGAGCTGTGGA<br>R: TCATCACTCCCATCTGGACA | 604 bp with exon 5<br>217 bp without |
| ApoER2-exon 6a | F: CCAGATGGGAGTGATGAAGC<br>R: CATTGTTGTGCAGACACTCG | 102 bp with exon 6a<br>61 bp without |
| ApoER2-exon F15/R18 | F: TCCTCAGATCTCCAGCCACT<br>R: GTGATCCCATCCTCAGGGTA | 784 bp with both exons; 382 bp without both<br>607 bp with 15/without 18; 559 bp with 18/without 15 |
| ApoER2- exon F6a/R18 | F: CCAGATGGGAGTGATGAAGC<br>R: GTGATCCCATCCTCAGGGTA | 1971 bp has 6a, 15, 18; 1932 bp has 15 & 18<br>1746 bp has 6a & 18; 1707 bp has 18; 1530 bp lacks all |
| VLDLR | F: GAGGTCAACTGTCCCTCTCG<br>R: ACTTCATCGGAACCATCGAC | 122 bp |
| α-3 Integrin | F: CTACGAAGTCAGCAATGGCA<br>R: CCCAGGGTCAGAAAGAGTGA | 130 bp |
| β-1 Integrin | F: GGTGGTGCACAAATTCAACA<br>R: CTGGCTTGAGCTTCTCTGCT | 185 bp |
| Dab1 | F: TCCAGGTGATGCCTTTATCC<br>R: ACCCATGACCATCTGCTGTT | 175 bp |
| β-Actin | F: TCACCCACACTGTGCCCATC<br>R: CAGCGGAACCGCTCATTGCC | 400 bp |

## 2.3 Protein Processing

### 2.3(a) Protein Extraction & Western Blotting

Proteins were extracted by homogenization of harvested cells in RIPA buffer (50 mM Tris-HCl, pH 7.4, 150 mM NaCl, 2 mM EDTA, 1% Triton X-100, 0.1% sodium dodecylsulfate (SDS), 1% sodium deoxycholate) containing 1x Protease inhibitor cocktail (Roche Diagnostics, Laval, Que) and 1 M sodium fluoride (cat# S-1504, Sigma Chemical Co., Germany) was freshly added to obtain a final concentration of 10 mM. Samples were sonicated briefly, prior to quantitation. The extracted protein was quantitated using the BIO-RAD Bradford Protein Assay (Cat # 500-0005, Bio-Rad laboratories, Hercules, CA). The Bradford Assay is a protein concentration determination method that involves the binding of Coomassie Brilliant Blue G-250 dye to proteins (Bradford MM 1976). The dye exists in three forms: cationic (red), neutral (green), and anionic (blue)(Compton SJ & Jones CG 1985). Under acidic conditions, the dye is predominantly in the doubly protonated red cationic form. However, when the dye binds to protein, it is converted to a stable unprotonated blue form. The blue form is detected at 595 nm in the assay using a spectrophotometer. Bovine serum albumin (BSA) is the protein standard used in this assay (Bio-Rad Laboratories, Hercules, CA). The BSA stock solution of 1.45 mg/ml is serially diluted to a working concentration of 100 μg/ml from which the following concentrations were prepared: 5, 10, 20, and 30 μg/ml. Samples were diluted 100x and the absorbance of each was read at 595nm on a spectrophotometer (Beckman Coulter Inc., Fullerton, CA). A standard curve was constructed by plotting the average absorbance at 595 nm (y-axis) as a function of protein concentration (x-axis). The concentration of the unknown protein sample was extrapolated from the curve using the

equation for the line: y = mx + b. Where: y = Absorbance at 595 nm; m = slope of the line; x = concentration of the unknown sample (μl); and b = x intercept of the line (was pre-set to zero). The equation was solved for x and protein samples were prepared according to the calculated volumes.

A 5x Laemmli SDS-PAGE Sample Buffer (62.5 mM Tris-HCl, pH 6.8, 2% SDS, 25% Glycerol, 0.01% Bromophenol Blue, 1% β-Mercaptoethanol (2-mercaptoethanol, cat# M-7154, Sigma Chemical Co., Germany)) was added to each sample before being boiled for 5 minutes. The samples were loaded onto the gel (75 μg/lane) and subjected to sodium dodecylsulfate-polyacrylamide gel electrophoresis and electrophoretically transferred to a nitrocellulose membrane (cat# RPN203E, Amersham Pharmacia Biotech, Baie d'Urfe, Que) for 1 hour at 80 volts at 4°C using BIO-RAD mode 3000 Xi, a computer controlled electrophoresis power supply. The full-range Rainbow, Recombinant Protein Molecular Weight Marker (cat# RPN800, Amersham Pharmacia Biotech, Baie d'Urfe, Que.), with individually coloured recombinant proteins ranging from10 (red) – 250 (blue) kDa was used. Whatman Blotting Paper (cat#3003917, Raymond A Lamb LTD, Apex, NC) was used in the transfer. Membranes were stained with Ponceau S (cat # P-3504, Sigma Chemical Co., Oakville, ON) and incubated with rotation for 10 minutes at 25 rpm before the image was scanned using an EPSON Expression 636 scanner (EPSON America, Long Beach, CA).

Detection of specific antigens was carried out by blocking the membranes with TBST (10 mM Tris-HCl, 150 mM NaCl, .05% Tween-20, pH 8.0) containing 5% non-fat Carnation milk (Loblaws, Ottawa, ON) for one hour at room temperature on a shaker. The membranes were probed with the following primary antibodies overnight at 4°C on a rotator: anti-Reelin

142 (1:500, mouse monoclonal, Chemicon International Inc., Temecula, CA); anti-ApoER2 (1:2000, rabbit polyclonal directed against last 13 amino acids of the receptor protein, a kind gift from Dr. Uwe Beffert, Department of Molecular Genetics, University of Texas Southwestern Medical Centre, Dallas, Texas); anti-ApoER-220 (1: 1000, rabbit polyclonal directed against the first 14 amino acids of the ligand binding domain (exon 2), a kind gift from Dr. Johannes Nimpf, Institute of Medical Biochemistry, Department of Molecular Genetics, BioCenter and University of Vienna, Vienna, Austria); anti-Dab1 CY38 (1:5000), PY198 (1:100), PY220 (1:1000) antibodies (all anti-Dab1 antibodies were a kind gift from Dr. Tom Curran, Department of Developmental Neurobiology, St Jude Children's Research Hospital, Memphis, Tennessee); anti-β-Actin (1:5000, Sigma Chemical Co., Germany). Antibodies were diluted in TBST containing 5% non-fat Carnation milk (Loblaws, Ottawa, ON). Membranes were washed with TBST and then incubated with a 1:5000 dilution of horseradish peroxidase-conjugated goat anti mouse or goat anti rabbit IgG secondary antibodies (Jackson ImmunoResearch Laboratories, Inc., West grove, PA) in TBST containing 5% non-fat milk for 45 minutes at room temperature. Peroxidase was detected using the ECL plus chemiluminescence kit (cat# RPN2133, Amersham Pharmacia Biotech, Arlington Heights, IL). The resulting light was detected on autoradiography film (Kodak Biomax MS film, cat#829 4985, Amersham Bioscineces Inc., Baie d'Urfe, Que.). As necessary, blots were then stripped in stripping buffer (62.5mM Tris, pH6.8, 2%SDS, 100mM ∃-mercaptoethanol- added freshly,) for 30 minutes at 70°C and then washed thoroughly in TBST before being re-probed.

To demonstrate the specificity of the ApoER2 antibody directed against the last 13 amino acids of the protein, an ApoER2 blocking peptide was synthesized by Dr.

Gordon Willick (Peptide Synthesis Faculty, IBS, NRC, Ottawa, ON), consisting of the last 13 amino acids of the ApoER2 protein- KRVALSLEDDGLP. Twenty-seven milligrams of the blocking peptide was dissolved in 2.7 ml of sterile, distilled water to give a final concentration of 10 μg/μl. For the rabbit polyclonal ApoER2 antibody, ten microlitres of the blocking peptide was used for every 3 ml of diluted primary (1:2000) antibody. The primary was incubated with the blocking peptide for 2 hours at room temperature on a rotator, prior to being incubated with the blot overnight at 4°C on a rotator. As a control the same blot was stripped and re-probed with the same primary, but this time it was incubated with 100 μg of the CRMP2 (Collapsin response mediator protein-2, which is a cytosolic phosphoprotein that is involved in neuronal differentiation during the development of the nervous system) blocking peptide (also synthesized by Dr. Gordon) to show the specificity of the antibody for the ApoER2 blocking peptide.

## 2.4 Immunoprecipitation (IP)

Immunoprecipitation is a highly specific and effective technique for the analytical separation of target antigens from crude cell lysates. Cells were washed twice with PBS and placed in serum free medium (SFM) for two or four days prior to IP, since serum is known to contain Reelin. The media was then collected and concentrated using the AMICON Ultra-15 PLHK centrifugal filter unit (100 kDa, cat# UFC9 100 24, Millipore, Billerica, MA). The approximate concentration of protein in the media was quantitated using the BIO-RAD Bradford Protein Assay (Bio-Rad laboratories, Cat # 500-0005, Hercules, CA). For each IP, 1 mg of protein was used at a final concentration of 2 μg/μl in 500 μl total volume. A 50% slurry was made with either Protein G or Protein A

Sepharose™ 4 Fast Flow beads (Immunoprecipitation starter pack, cat# 17-6002-35, Amersham Biosciences, Baie d'Urfe, Que.) in CoIP (Co-Immunoprecipitation) lysis buffer (0.05 M Tris, pH 8.0, 0.137 M NaCl, 1% (v/v) NP-40, 5% (v/v) Glycerol and 1x freshly added Protease Inhibitor Cocktail). Protein G Sepharose 4 fast flow beads were used when the IP antibody was monoclonal and Protein A sepharose 4 fast flow beads were used when the IP antibody was polyclonal. The lysates were pre-cleared with 40 µl of 50% slurry for one hour at 4°C on a rotator. IP's were carried out in pairs, where one sample was treated with an anti-Reelin 142 antibody (1:100, mouse monoclonal, Chemicon International Inc., Temecula, CA) and the other was used as control in which no primary antibody was added. Samples were incubated overnight at 4°C on a rotator. Forty microlitres of the 50% slurry was then added to each sample and samples were further incubated for one hour at 4°C on the rotator. Samples were then washed 5 times with 500 µl of CoIP lysis buffer, before resuspending the beads in 35 µl of CoIP lysis buffer. Samples were then prepared for Western blotting as described previously (section 2.3) and subjected to 7% or 10% sodium dodecylsulfate-polyacrylamide gel electrophoresis. Proteins were electrophoretically transferred to a nitrocellulose membrane (Amersham Pharmacia, Baie d'Urfe, Que.), which was either probed with an anti-ApoER-220 antibody (1: 1000, rabbit polyclonal directed against the first 14 amino acids of the ligand binding domain [exon 2]) or with an anti-Reelin 142 antibody. Primary antibodies were detected as described in section 2.3.

## 2.5 Immunohistochemistry

### 2.5(a) NT2 Cell Cultures

NT2/D1, fourteen week old NT2/A or NT2 co-cultures (1.5 x $10^5$ cells/well in 12-well falcon plates) were grown on glass coverslips pre-coated with high-molecular weight poly-D-lysine (cat# P-1149, Sigma Chemical Co., Germany) at a concentration of 10 μg/ml for 1 week, washed with PBS and fixed for 10 minutes at room temperature with the methanol/ethanol fixative Genofix™ (DNA Genotek Inc, Ottawa, ON). Fixed cells were rinsed with PBS then blocked for 15 minutes with either 10% normal goat serum (Sigma Chemical Co., Oakville, ON) or with universal blocking solution (DAKO Diagnostics Canada Inc. Mississauga, ON) in a humidity chamber. Excess liquid was drained and cells were incubated for 1 hour at room temperature with primary antibodies diluted in antibody diluting buffer (DAKO Diagnostics Canada Inc., Mississauga, ON). The following primary antibodies were used: anti-glial fibrillary acidic protein (1:100, GFAP, mouse monoclonal clone GA-5, Neomarkers, Lab Vision Corporation, Fremont, CA); anti- glutamine synthase (1:100, mouse monoclonal, Chemicon International Inc., Temecula, CA); anti- vimentin (1:25, mouse monoclonal, clone V9, Sigma Chemical Co. Oakville, ON); anti-β3-Tubulin (1:10, mouse monoclonal, a kind gift from Dr. David Brown, Department of Biology, University of Ottawa, Ottawa, ON); anti-Reelin 142 (1:100, mouse monoclonal, Chemicon International Inc., Temecula, CA); anti-ApoER2 (1:100, rabbit polyclonal, a kind gift from Dr. Uwe Beffert); anti-Dab1 CY38 (1:50, rabbit polyclonal, a kind gift from Dr. Tom Curran); anti-MAP 2a+2b (1:50, mouse monoclonal, Sigma Chemical Co., Germany) The coverslips were then washed with PBS and incubated with Rhodamine or Alexa 488-conjugated goat anti-mouse or anti-rabbit

IgG secondary antibodies (1:600, Molecular Probes, Inc., Eugene, OR) for 45 minutes at room temperature. Negative controls with omission of primary or secondary antibodies were included. All coverslips were washed with PBS and mounted in DAKO fluorescent mounting media (DAKO Diagnostics Canada Inc., Mississauga, ON). Immunofluorescent cells were viewed with an Axiovert 220M (Zeiss, Germany) fluorescence microscope equipped with a Zeiss Axiocam (Zeiss, Germany) camera. The images were captured using Carl Zeiss Vision, Axio Vision Viewer 3.0 software (Zeiss, Germany).

### 2.5(b) P20 Mouse Cortical Brain Sections

Paraffin embedded postnatal day 20 (P-20) mouse cortical brain slices (kindly provided by Dr. M. Bani, IBS, NRC, Ottawa, ON) were serially washed in the organic solvent Xylene (cat# X0250, ACP, Montreal, Que.) to dissolve the paraffin, before being hydrated and fixed sequentially in 100%, 90%, and 75% ethanol 5 minutes each (Anhydrous Ethyl alcohol, Comercial Alcohols Inc., Brampton, ON). Coverslips were washed twice in PBS and blocked for 30 minutes with 10% normal goat serum (Sigma Chemical Co., Oakville, ON). Excess liquid was drained and cells were incubated for 1 hour at room temperature with primary antibodies diluted in antibody diluting buffer (DAKO diagnostics Canada Inc., Mississauga, ON). The following primary antibodies were used: anti-glial fibrillary acidic protein (1:100, mouse monoclonal clone GA-5, Neomarkers, Lab Vision Corporation, Fremont, CA); anti-ApoER2 (1:100, rabbit polyclonal, a kind gift from Dr. Uwe Beffert); anti-MAP 2a+2b (1:50, mouse monoclonal, Sigma Chemical Co., Germany). The coverslips were then washed with PBS and incubated with Rhodamine or Alexa 488-conjugated goat anti-mouse or anti-rabbit IgG secondary antibodies (1:600, Molecular Probes, Inc., Eugene, OR) for 45

minutes at room temperature. Negative controls with omission of primary or secondary antibodies were included. All coverslips were washed with PBS and mounted in DAKO fluorescent mounting media (DAKO Diagnostics Canada Inc., Mississauga, ON). Immunofluorescent cells were viewed with an Axiovert 220M (Zeiss, Germany) fluorescence microscope equipped with a Zeiss Axiocam (Zeiss, Germany) camera. The images were captured using Carl Zeiss Vision, Axio Vision Viewer 3.0 software (Zeiss, Germany).

## 2.6 Preparation of Recombinant Reelin

The mouse pCrl recombinant reelin plasmid was kindly provided by Gabriella D'Arcangelo (Curran T et al. 1995). The recombinant reelin pCrl vector contains the cytomegalovirus promoter expression vector and has a full length Reelin ORF of ~10.6 Kb from nucleotide number 188 of the GenBank Reelin cDNA; accession number U24703. The plasmid carries ampicillin resistance and contains KpnI digestion sites at ~1, 5.9, and 6.6 Kb. See Figure 3.

### 2.6(a) Transforming Competent Cells

DH5α Competent E. coli (cat# 18265-017, Invitrogen, Carlsbad, CA) were transformed with the recombinant reelin pCrl construct. A vial of the DH5α competent cells was defrosted upon dry ice, then 100 ng of the recombinant reelin pCrl plasmid was added. The mixture was incubated on ice for 30 minutes (to ensure that the bacteria don't replicate while the plasmid is being absorbed) then heat shocked at 37°C for 20 seconds to trigger uptake of the plasmid DNA and incubated on ice for another 2 minutes. The

## Figure 3: The pCrl Recombinant Reelin Plasmid

The mouse pCrl recombinant reelin plasmid confers ampicillin resistance and contains KpnI restriction sites at ~1, 5.9, and 6.6 Kb. The recombinant reelin pCrl vector contains the cytomegalovirus promoter expression vector, and has a full length Reelin ORF of ~10.6 Kb from nucleotide number 188 of the GenBank cDNA; accession number U24703. DH5α Competent E. coli were transformed with the recombinant reelin pCrl plasmid. See Section 2.6 for details.

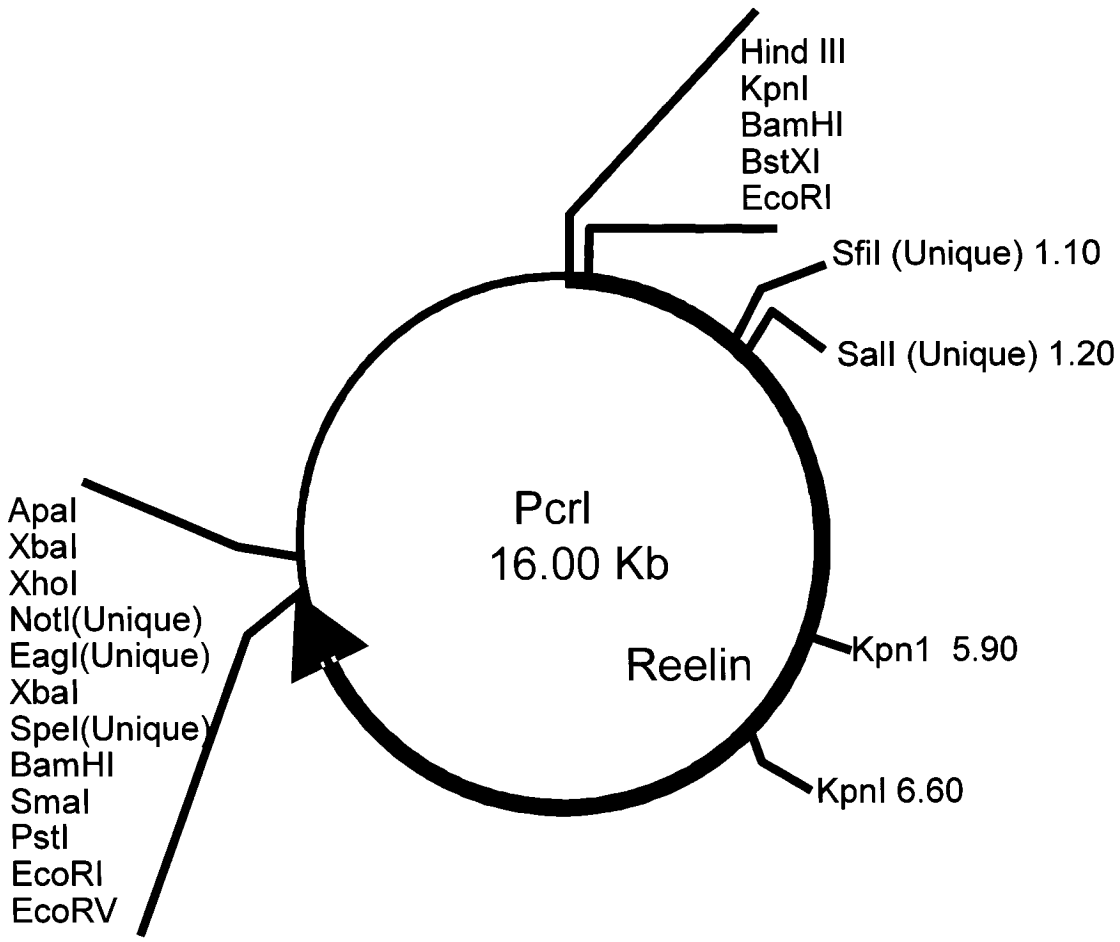
Hind III
KpnI
BamHI
BstXI
EcoRI
SfiI (Unique) 1.10
SalI (Unique) 1.20
ApaI
XbaI
XhoI
NotI(Unique)
EagI(Unique)
XbaI
SpeI(Unique)
BamHI
SmaI
PstI
EcoRI
EcoRV
Pcrl
16.00 Kb
Reelin
Kpn1 5.90
KpnI 6.60

cell slurry was placed in a tube containing pre-warmed LB Broth and incubated on a rotator for 1 hour at 37°C and 250 rpm. The cells were subsequently plated onto LB (1 L contains: 10 g Bacto Tryptone [Cat# 0118-17-0, Difco Lab, Becton Dickinson, Sparks, MD], 5g Bacto™ yeast extract [Difco Lab] and 10 g sodium chloride) – agar (Bacto™ Agar, cat# 214010, Difco Lab) - ampicillin (stock 100 mg/ml; working 100 μg/ml, cat# A9518, SIGMA, Oak. ON) plates, which were incubated overnight at 37°C.

### 2.6(b) Inoculation of Positive Colonies

Individual colonies were picked and inoculated into 5 ml of LB Broth supplemented with ampicillin (100 μg/ml) and grown for 7-8 hours at 37°C at 300 rpm. The inoculated colonies were checked for growth, diluted into 250ml of LB Broth/ ampicillin (100 μg/ml) and grown for 12-16 hours at 37°C at 300 rpm. Flasks were checked for growth and the plasmid DNA was purified using a QIAGEN EndoFree Plasmid Maxi kit (cat# 12362, QIAGEN Inc., Mississauga, ON) according to the manufacturers protocol.

### 2.6(c) Purification of Plasmid DNA

Cells were harvested by centrifugation at 6000 g for 15 minutes at 4°C. The supernatant was discarded and the pellet was re-suspended in 10 ml of Buffer P1 (50 mM Tris-Cl, pH 8.0, 10 mM EDTA, 100 μg/ml RNase A). The bacterial cells were lysed for 5 minutes in 10 ml of Buffer P2 (200 mM NaOH, 1% SDS w/v). The lysates are neutralized by the addition of 10 ml of acidic potassium acetate (Buffer P3, 3.0 M potassium acetate, pH 5.5). The high salt concentration of this buffer causes SDS to precipitate and causes the denatured proteins, chromosomal DNA and cellular debris to

become trapped in salt-detergent complexes. Plasmid DNA, being smaller and covalently closed, renatures correctly and remains in the clear supernatant. The precipitated debris was then removed by centrifugation (10 minutes at 15 000g at 4°C) followed by filtration with a QIAfilter Cartridge, producing cleared lysates that are then incubated on ice for 30 minutes with 2.5 ml of endotoxin removal (ER) buffer. ER Buffer is a specific endotoxin removal buffer that prevents endotoxins from binding to the resin in the QIAGEN-tips. The lysates were loaded onto a pre-equilibriated QIAGEN cartridge, which contains an anion-exchange resin. The QIAGEN Resin consists of defined silica beads that allow plasmid DNA to tightly bind to the DEAE (diethylaminoethanol) groups on the surface of the resin over a wide range of salt concentrations. Impurities such as RNA, protein, carbohydrates and small metabolites are washed from the QIAGEN resin with medium ionic strength buffers, while plasmid DNA remains bound until eluted with a high salt buffer. The QIAGEN cartridge was then washed twice with 30 ml of Buffer QC (1 M NaCl, 50 mM MOPS-3- (N-morpholino) propanesulfonic acid), pH 7.0, 15% isopropanol v/v) a medium ionic strength buffer which completely removed any residual contaminants, such as traces of RNA or protein, in addition to nucleic acid binding proteins. The plasmid DNA was then efficiently eluted from the QIAGEN cartridge with the addition of 15 ml of a high-salt buffer (1.6 M NaCl, 50 mM MOPS, pH 7.0, 15% isopropanol v/v).

The eluted plasmid DNA was then desalted and concentrated by the addition of 10.5 ml of isopropanol. Precipitation was carried out at room temperature to minimize co-precipitation of salt. After centrifugation at 15,000 g for 30 minutes at 4°C, the DNA pellet was washed in 5 ml of endotoxin-free 70% ethanol in order to remove residual salt

and to replace the isopropanol with ethanol, which is more volatile and easily removed. After further centrifugation at 15,000g for 10 minutes at 4°C the pellet was air dried for 10 minutes and resuspended in an appropriate volume of endotoxin free, TE buffer (1 mM EDTA, 10 mM Tris-Cl, pH 8.0). Two microliters of DNA was diluted 50x in sterile distilled water and the OD was taken at 260 nm on the Beckman Coulter ™ spectrophotometer 600 series (Beckman Coulter Inc., Fullerton CA). To confirm plasmid quality and integrity, 1 μg of DNA was digested with the restriction enzyme KpnI in a 20 μl reaction buffer (2 μl of 1 x Reaction Buffer 4 (cat# B70045, Biolabs, New England, Beverly, MA), 1 μl of KpnI (cat# 15232-036, Invitrogen, Carlsbad, CA), & 16 μl of $ddH_2O$) for 2 hours at 37°C. The restriction sites of KpnI on the mReelin pCrl vector are shown in Figure 3. KpnI digestion produces three fragments, 700 bp, 5,300 bp and 10,000 bp, which can be visualized on a 1% agarose, ethidium bromide stained gel (cat# 50004, Seakem LE agarose, BMA, Rockland, ME). See Figure 4A.

### 2.6(d) Transfection of Human Embryonic Kidney (HEK) 293 Cells

In order to generate recombinant reelin protein, HEK 293 cells (cat# CRL-1573 American Type Culture Collection, Manassas, VA) were plated (the night before transfection) at a density of $2.2 \times 10^6$ cells per 10 $cm^2$ dish (Beckton Dickinson, NJ). Prior to transfection, cells at 80% confluency were given fresh serum free media (SFM). Each 10-$cm^2$ dish received 10 μg of the purified mReelin pCrl plasmid and 20 μl of lipofectamine ™ reagent diluted in 500 μl of SFM and were left for 6 hours at 37°C. Transfection was terminated by removal of the medium and the cells were given 7 ml of fresh SFM. Media was collected daily for the next 72 hours and concentrated using an

**Figure 4: KpnI Digestion of the pCrl Recombinant Reelin Plasmid**

(A) To confirm plasmid quality and integrity purified plasmid DNA was digested with the restriction enzyme KpnI. KpnI digestion produces three fragments: a 700 bp fragment, a 5300 bp fragment and a 10 000 bp fragment, which were visualized on a 1% agarose gel containing ethidium bromide. KpnI digested samples 1′- 6′; non-digested plasmid 1 – 6.

(B) 10 μg of the purified pCrl recombinant reelin plasmid was transfected into the HEK 293 cells, plated at a density of $2.2 \times 10^6$ cells per 10 $cm^2$ dish. Media from transfected cultures was collected daily for a 72-hour period before being concentrated using an AMICON Ultra-15 PLHK centrifugal filter unit. Twenty microlitres of the concentrated media was then separated by SDS/PAGE on a 7% gel, transferred to a nitrocellulose membrane and incubated overnight with a mouse monoclonal anti-Reelin primary antibody (142). After a 45-minute incubation with a peroxidase labelled anti-mouse IgG secondary antibody, bound antibody was then detected by chemiluminesence, with 1-minute exposure to film. The positions of molecular mass markers (kDa) are shown and prominent bands indicate the expected size of Reelin (~400, 200-300, 180 kDa).

A

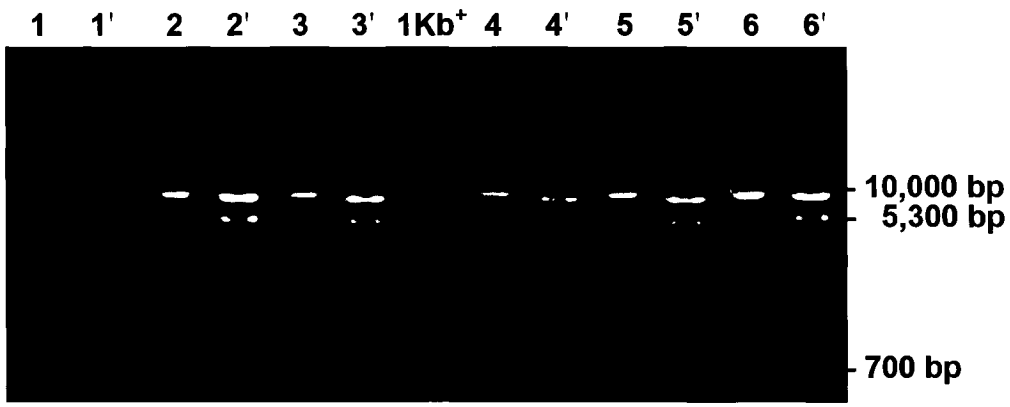
1
1'
2
2'
3
3'
1Kb+
4
4'
5
5'
6
6'
10,000 bp
5,300 bp
700 bp

B

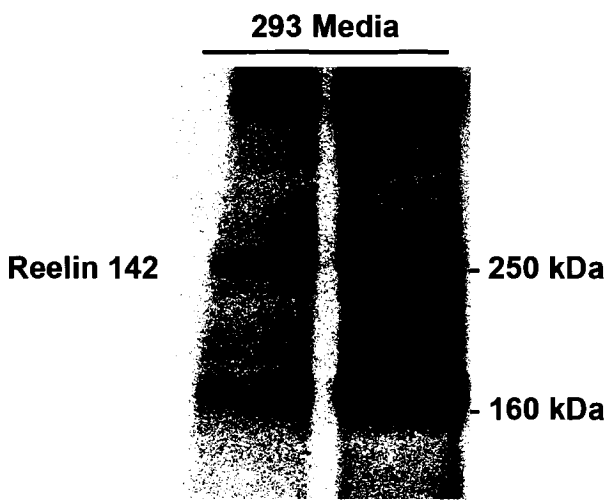
293 Media
Reelin 142
250 kDa
160 kDa

AMICON Ultra-15 PLHK centrifugal filter unit (100 kDa cut-off, cat# UFC9 100 24, Millipore, Billerica, MA). The presence of recombinant reelin in the concentrated media was confirmed by Western blot. See Figure 4B.

## 2.7 Treatment Conditions

### 2.7(a) Recombinant Reelin

Pure fifteen week old NT2/A cells grown in T75 $cm^2$ flasks were pre-washed twice in PBS, then treated with either of the following for 20 minutes:

I) SFM; control cells.

II) SFM supplemented with 75 µl of recombinant reelin enriched 293 cell media, daily (as described in section 2.5 (d)); Reelin treated cells.

Following incubation the cells were homogenized in RIPA buffer and processed for Western blotting according to the protocol described in section 2.3.

### 2.7(b) λ-Phosphatase

Pure fifteen week old NT2/A cells grown in T25 $cm^2$ flasks were divided into two main groups: 1A) Control cells incubated with normal SFM for 20 minutes; 1B) Control incubated with λ-Phosphatase; 2A) Treated cells incubated with SFM supplemented with 75 µl of 293 cell media enriched with recombinant reelin at 37°C, for 20 minutes; and 2B)Treated cells incubated with λ-Phosphatase (each group was done in triplicate). Cells were pre-washed with 1x PBS-EDTA solution to remove serum, $Ca^{2+}$ and $Mg^{2+}$ ions, and harvested using 0.15% Trypsin (Bovine pancreas, Sigma Chemical Co., Oakville, ON) - 1mM EDTA. Trypsinized cells were neutralized in SFM, centrifuged for 5 minutes at 1000g, and homogenized in 100 µl of Alkaline Phosphatase Lysis Buffer (50mM TRIS-

Cl, pH 7.4, 1% NP40 [cat# 155942, MP Biomedicals Inc., Irvine, CA], 150mM NaCl, 50x Protease Inhibitor cocktail [Roche Diagnostics, Laval, Quebec], added fresh). Lysates were incubated on ice for 25 minutes, sonicated briefly then spun down for 20 minutes at 14,000g at 4°C. Half of the control and treated cell extracts were then incubated with λ-Phosphatase reaction buffer (1 x λ-Phosphatase Reaction Buffer, 2 Mm $MnCl_2$, 800 units of λ-Phosphatase, all sold together- cat# P0753L, Biolabs, New England, Beverly, MA) for 30 minutes at 30°C. Following the incubation, the protein content of each lysate was determined with the Bio-Rad Bradford assay and diluted with 5x Laemmli SDS-PAGE Sample Buffer (62.5 mM Tris-HCl, pH 6.8, 2% SDS, 25% Glycerol, .01% Bromophenol Blue, 1% β-Mercaptoethanol) and subjected to sodium dodecylsulfate-polyacrylamide gel electrophoresis and subsequent immunoblotting (See section 2.3 for details).

### 2.7(c) Determination of Cell Viability

Pure fourteen week old NT2/A were grown in 6 well plates pre-coated with high-molecular weight poly-D-lysine (cat# P-1149, Sigma Chemical Co., Germany) at a concentration of 10 μg/ml, for 1 week, pre-washed with PBS then treated with either of the following for 72 hours:

I) HG/DMEM supplemented with 5% heat-inactivated FBS (Wisent Inc., St. Bruno, Que.), sodium bicarbonate (37g /10L)(BDH Chemicals, Toronto, ON) and with 40 μg/mL Gentamycin sulfate (Cat# 61 098 RF, Multicell, Warwick, RI); control cells

II) SFM only; SFM

III) SFM supplemented with 75 µl of recombinant reelin enriched 293 cell media, daily (as described in section 2.6 (d)); Reelin Treated cells

Following the 72-hour incubation at 37°C, cells were subjected to either i) fixation followed by staining for β-tubulin and GFAP (Section 2.5) or ii) the cells were used in the CFDA/PI viability assay (Section 2.8).

## 2.8 Carboxyfluorescein Diacetate/ Propidium Iodide Cell Viability Assay

Cell viability is commonly determined by the carboxyfluorescein diacetate (CFDA)/propidium iodide (PI) assay, where non-fluorescent CFDA is taken up by diffusion and converted via cytoplasmic esterase-catalyzed hydrolysis to carboxyfluorescein, a negatively charged fluorescent molecule that is retained by the cell (Massaro EJ et al. 1989). It is generally accepted that the viable cell excludes basic dyes, such as PI (a red-fluorescent nuclear and chromosome counterstain), and uptake is indicative of irreversible cellular injury (Massaro EJ et al. 1989). Stock PI (cat# P1304MP, Molecular Probes, Burlington, ON) 1 mg/ml, was diluted 50x with 0.1M Sodium Phosphate buffer (50 ml of 0.5M Dibasic-Sodium Phosphate anhydrous, cat# ACS 807, was gradually added to 150 ml of 0.5M Monobasic-Sodium Phosphate, cat# ACS 795, BDH Inc., Toronto, ON, to bring the pH of the solution to 7.4, final volume brought to 1L with $dH_20$); stock CFDA (Molecular Probes, Burlington, ON) 2.5 mg/ml in DMSO (Dimethyl Sulfoxide, cat# B10323-74, Sigma Chemical Co., Oakville, ON) was diluted 200x with 0.1M Sodium Phosphate buffer. To a 6-well plate, 100µl of diluted CFDA, and 30µl of diluted PI was added to each well and the cells where incubated at

37°C for 10 minutes and washed in 2 ml of 0.1M Sodium Phosphate buffer. Fluorescent cells were viewed within a 30-minute time frame, with the Axiovert 220M (Zeiss, Germany) fluorescence microscope equipped with a Zeiss Axiocam (Zeiss, Germany) camera. The images were captured using Carl Zeiss Vision, Axio Vision Viewer 3.0 software (Zeiss, Germany).

## 2.9 Statistical Analysis

An F-test was carried out using a one-way ANOVA table to see if there was any difference amongst treatments. Then multiple comparisons where carried out using Tukey tests, in order to control the probability of any false rejection amongst all comparisons made. A Tukey test was used instead of a T-test as the level of significance in a t-test only applies to each individual test; whereas the Tukey test controls the level of significance for all treatments tested at the same time. All statistical analysis was done with SIGMA plot 6.0 (Systat Software, Inc. Point Richmond, CA).

# 3.0 RESULTS

## 3.1 The NT2 Cell Model System

### 3.1(a) NT2 Cells as a Model System for Studying Human Glial and Neuronal Cell Function

The human NTera-2 (NT2/D1) cell line used in this study is a pluripotent clonal embryonal carcinoma cell line (clone# 21) established by Andrews, et al (1984). This cell model system generates both human neuronal and glial cells and is widely studied (Hartley RS et al. 1999; Tamagno E et al. 2000; Sandhu JK et al. 2002). NT2/D1 cells (Fig 5A) were differentiated as described by Andrews et al (1984) and Lee et al. (1986) and appear as monolayer of morphologically distinct cells. Briefly, NT2/D1 cells were seeded at a density of 2 x $10^6$ cells per T-75 $cm^2$ and were treated with 1 x $10^{-5}$ M all-trans-retinoic acid (RA) three times a week for four weeks to produce a multi-layered structure of differentiating cells as seen under light microscopy (Fig 5B). Following the RA treatment, cells from one T75 flask were replated into three T175 $cm^2$ flasks in order to separate the astrocytes from the neurons (see Section 2.1 for details). Cells were maintained for 1 week, then differentiated neuronal cells (NT2/N) were separated from the underlying astroglia (NT2/A) by incubating cells with 0.015% Trypsin-1mM EDTA for 1 minute followed by gentle mechanical shaking. At this point, cells are considered to be one week old. The NT2/A were replated on a weekly basis at the following densities: 2 x $10^6$ cells for T75 flasks and 5 x $10^6$ for T175 flasks, generating pure glial populations (Fig 5C & 5C′) that were grown in culture for a total of 15 weeks before being processed for RNA or protein extraction. The collected NT2/N cells were plated at a density of 3 x $10^6$ into T75 flasks containing 2 x $10^6$ four weeks old, pure NT2/A cells, producing NT2 co- cultures (Fig 5D & 5D′) that were allowed to grow in culture for a total of 15 weeks

## Figure 5: The NT2 Cell Model System

NT2/D1 precursor cells, not treated (A) or treated with 10 μM retinoic acid (RA) for 4 weeks (B). Cells were replated and then allowed to mature for one week prior to being harvested and separated into either pure NT2/A (C & C′) or into NT2 Co-cultures (D & D′). Magnification x 50 for C & D; x 400 for A, B, C′, & D′

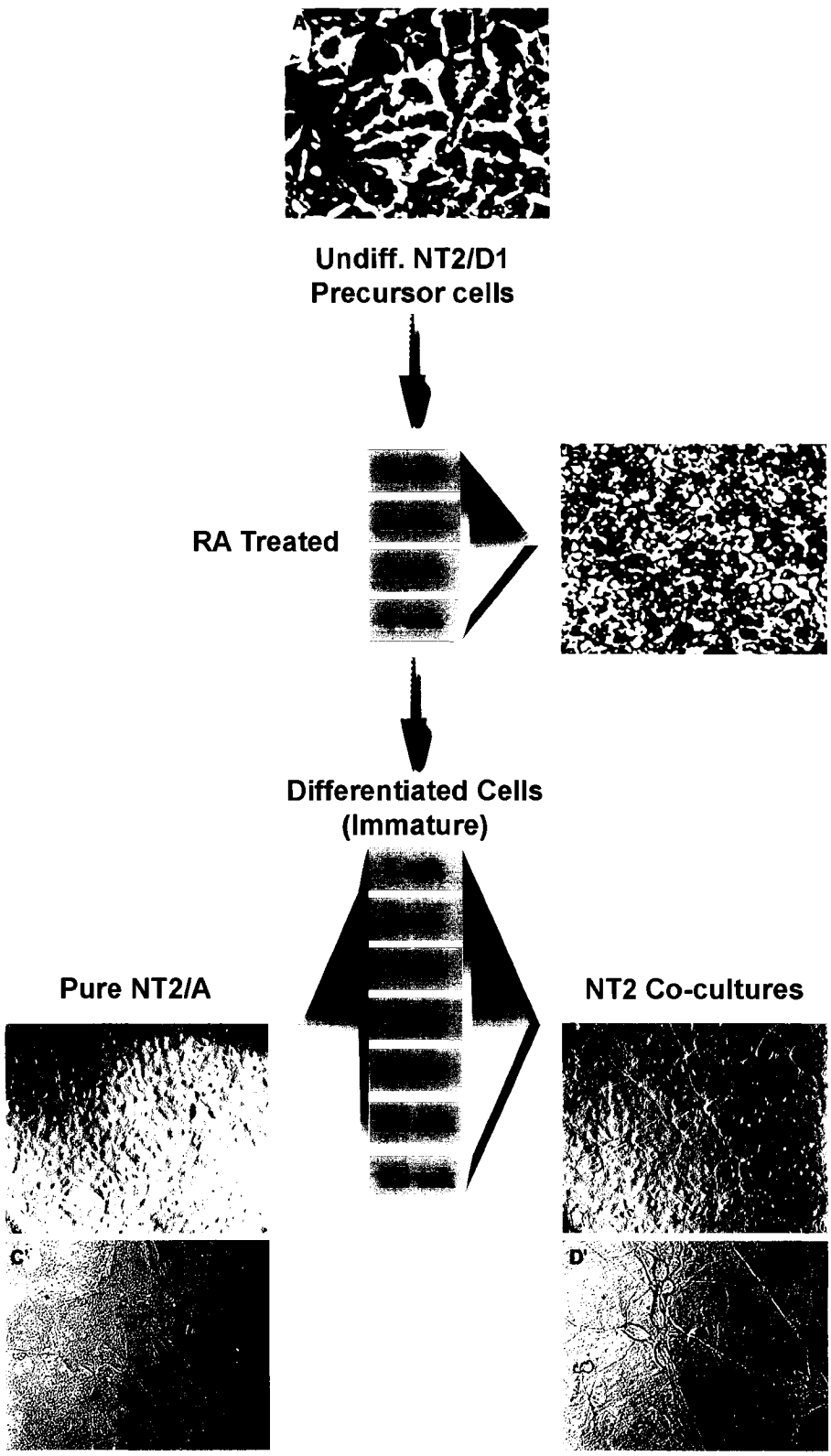
A
Undiff. NT2/D1
Precursor cells
RA Treated
B
Differentiated Cells
(Immature)
Pure NT2/A
NT2 Co-cultures
C'
D'

before being processed. Neurons were removed separately from co-cultures producing fairly pure neuronal protein and mRNA extracts. Co-cultures were mainly used for obtaining neuronal mRNA and protein in this study, however it was necessary to use pure neuronal NT2 cultures (cells that were allowed to mature in culture in the absence of astrocytes; these cells were kindly provided by Angele Desbois), in addition in order to demonstrate the specificity of findings per cell type for some experiments (Fig 9 & Fig 11).

### 3.1(b) Characterization of the NT2 Cell Model System

As described above, the human NT2/D1 cells undergo neuronal and glial differentiation in response to treatment with retinoic acid. The resulting glial cells have been shown to differentiate into two types of astrocytes - star-shaped fibrous astrocytes and large, flat polygonal astrocytes (Sandhu JK et al. 2002), both of which expressed markers of mature astroglial cells and have been shown to possess functional glutamate transport systems (Sandhu JK et al. 2002). NT2/A cells in our cultures were shown to stain positively for the astrocyte-specific enzyme glutamine synthase (an enzyme involved in the breakdown of toxic intracellular glutamate to non-toxic glutamine). In all cells, the protein was localized to the cytoplasm (Fig 6A). To further characterize NT2/A cells, pure cultures of 15 week old astrocytes were examined for the production of glial-specific intermediated filament proteins expressed by astrocytes in the CNS (Fig.6). By indirect immunofluoresence, both the GFAP and vimentin antibodies decorated intra-cytoplasmic filaments within the entire cell population (Fig 6C, 6D, 6E & 6F). As a positive control, sections of mouse cortical brain from postnatal day 20 (P-20) were stained with both glial (GFAP green) and neuronal markers (the microtubule associated

## Figure 6: Characterization of NT2/A

Immunofluoresence staining for glial proteins in pure cultures of 15 week old astrocytes (NT2/A). The cells showed immunoreactivity for the following: the astrocyte-specific enzyme glutamine synthase (A), the intermediate filaments GFAP (C & D) and vimentin (E & F); and the building blocks of microtubules, β-Tubulin (G & H). As a control, sections of mouse cortical brain from postnatal day 20 (P-20) were stained with either GFAP (B) or for both GFAP (B′, green) and MAP 2a + 2b (B′, red). Also shown are the phase-contrast micrographs (A′, C′-H′). Immunohistochemistry was performed as described in material methods. Either Alexa 488 (green), or Rhodamine (red) conjugated secondary antibodies were used. Representative images are shown from triplicate results. Magnification x200 for A, C, E, G and x400 for B, D, F, and H.

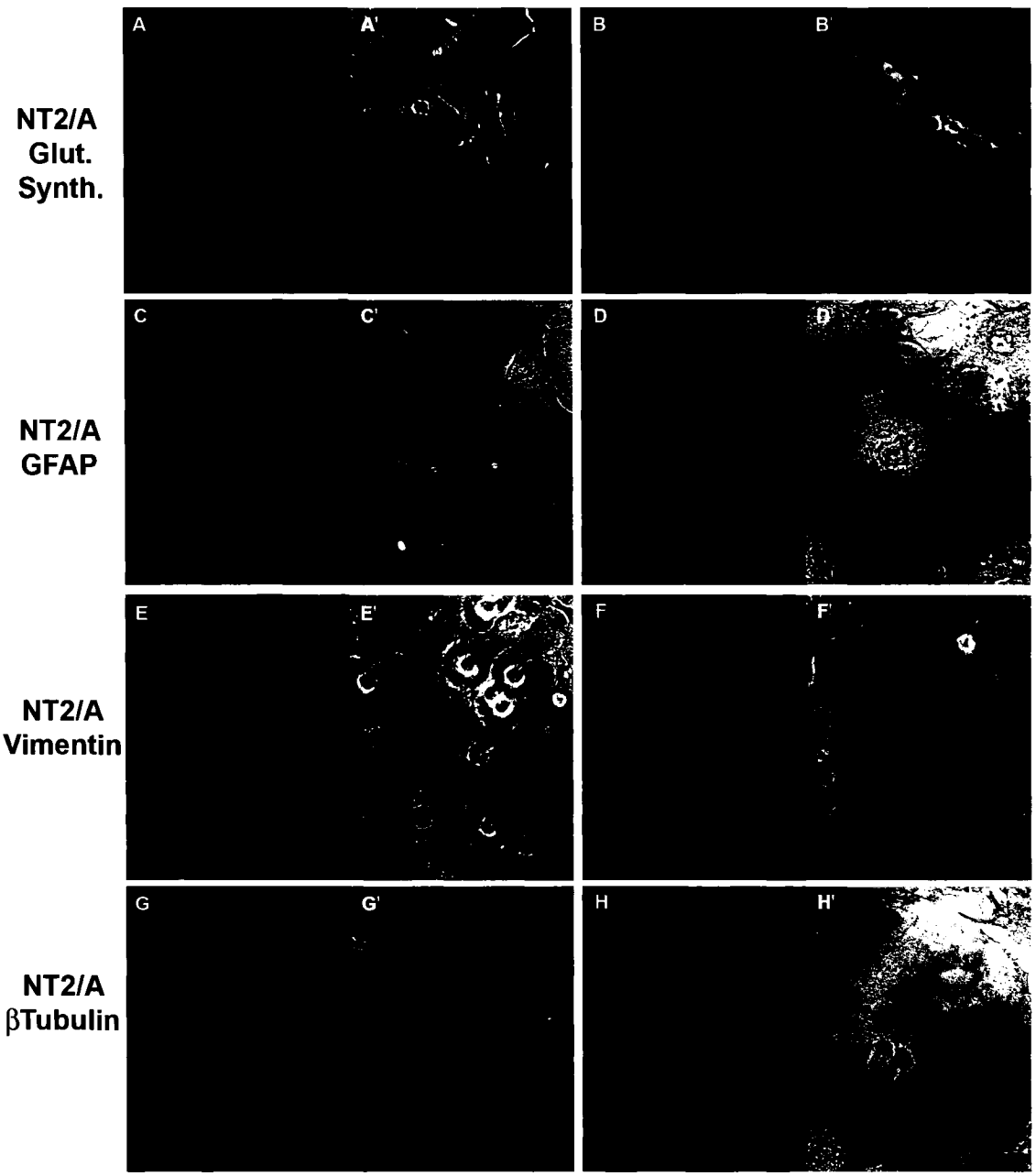
NT2/A
Glut.
Synth.
NT2/A
GFAP
NT2/A
Vimentin
NT2/A
βTubulin
A
A'
B
B'
C
C'
D
D'
E
E'
F
F'
G
G'
H
H'

protein [MAP 2a+2b] red, Fig 6B & 6B'). It was interesting to note that at 15 weeks of maturation, the majority of astrocytes maintained a large, flat polygonal morphology as well as an extensive microtubule network that spanned the entire surface area of the cell, staining the cytoplasm in distinct, punctate fibre bundles (Fig 6G & 6H).

NT2/N's grown as mixed cell co-cultures were also examined. Figure 7A and 7B show the typical morphology of NT2/N grown in culture, where neurons establish elaborate connections between each other that are capable of synaptic transmission (Hartley RS et al. 1999). Neurons were stained with the neuronal-specific marker MAP 2a+2b. As above, mouse cortex from P-20 was stained as a positive control for both glial and neuronal markers (GFAP green, and MAP 2a+2b red, Fig 7D & 7D'). As a negative control cells were incubated with 10% horse serum instead of with the MAP 2a+2b primary antibody, before being probed with a rhodamine conjugated secondary (Fig 7C). These results showed that both astrocytes (NT2/A) and neurons (NT2/N) could be readily produced from NT2/D1 precursor cells by the treatment with retinoic acid.

## 3.2 **Reelin and Its Receptors In NT2/A and NT2/N Cells**

Reelin is a large glycoprotein of approximately 400 kDa. In rodents, Reelin is known to be expressed in the GABAergic interneurons of the adult cerebral cortex and hippocampus and in glutamatergic cerebellar granule neurons (Pappas GD et al. 2001). In the Human brain, Reelin and Dab1 are co-expressed in Cajal Retzius neurons of the

## Figure 7: Characterization of NT2/N

Fifteen week old NT2 co-cultures were stained with the neuronal-specific marker, microtubule associated protein (MAP 2a+2b), (A & B). As a control, subsets of cells were treated with 10% horse serum in place of primary antibody (C). Additionally, as a positive control, sections of mouse cortical brain from postnatal day 20 (P-20) were stained with either MAP 2a + 2b (D, red) or both MAP 2a + 2b and GFAP (green) (D′). Also shown are the phase-contrast micrographs (A′-C′). Immuncytochemistry was performed as described in material and methods. Either Alexa 488 (green), or Rhodamine (red) conjugated secondary antibodies were used. Representative images are shown from triplicate results. Magnification x200 for A, & C; x400 for B, & D.

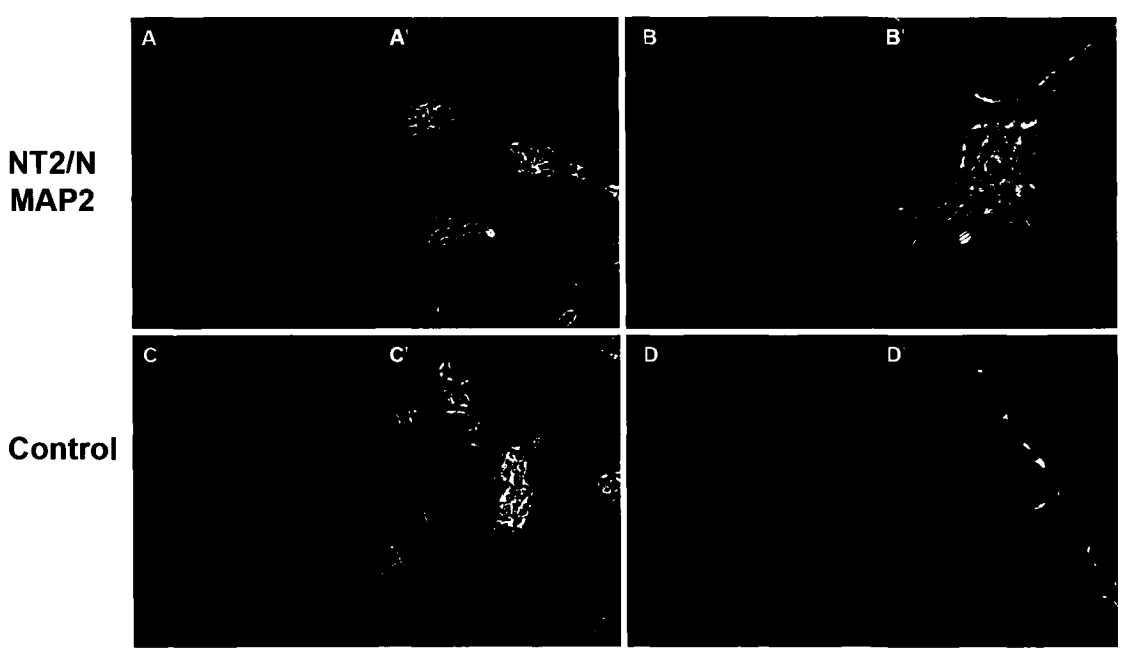
NT2/N
MAP2
Control
A
A'
B
B'
C
C'
D
D'

immature brain and in pyramidal and interneurons of the mature cortex (Deguchi K et al. 2003). To determine whether Reelin and its gene products are expressed and translated in the NT2 cell model system, we utilized RT-PCR, Western blotting and immunohistological techniques (Fig 8). For RT-PCR, primers specific for Reelin were generated that produced a 385 bp fragment. As an internal control, to demonstrate equal loading, primers were used against β-Actin, which generated a 400 bp fragment (Fig 8A). For both Western blotting and immunostaining procedures a mouse monoclonal anti-Reelin 142 antibody was used that is specific for the N-terminal region of the protein (between amino acids 164 and 189). Both the Reelin transcript and Reelin protein were expressed at similar levels in NT2 astrocytes and neurons, but no transcript was detected in FHAS at this stage of development (Fig 8A & 8B). However, we have found (Walker et al., unpublished observations) that Reelin is expressed in embryonic cells and fully differentiated cells, but not in cells at intermediate stages of development. Thus, "fetal" astrocytes may not be expressing Reelin yet.

At the protein level, consistent with previous findings (Beffert U et al. 2004), three isoforms of Reelin were identified of approximately 400, 300, and 180 kDa on Western blots of both the total cell lysates of 15 week old NT2/A and NT2/N cells, using the anti Reelin 142 antibody (Fig 8B). In addition to the total cell protein lysates, we also tested the media from NT2 glial and neuronal cultures for the presence of Reelin. Fifteen week old NT2/A and NT2/N cultures where washed twice with PBS, before being given fresh SFM. After 36 hours of incubation at 37°C, the media was collected and was subjected to Western blotting on a 7% polyacrylamide gel under denaturing

## Figure 8: Expression of Reelin In the NT2 Cell Model System

(A) RT-PCR: Total RNA was extracted from 1, 5, or 15, week old NT2/A, NT2/N, and FHAS was used for cDNA synthesis with reverse transcriptase (as described in materials and methods). The resulting cDNAs were used for the RT-PCR amplification using either Reelin specific primers or β-Actin specific primers as an internal control (see Table 1 for primer details). Amplified products were separated on 1% agarose gels, stained with ethidium bromide. The respective sizes of amplified products are indicated on right hand side of the panel (base pairs- bp).

(B) Western Blotting: Protein extracts (80 μg per lane) from 15 week old (15 wk) NT2/A and NT2/N and 40 μl of serum free media (SFM) obtained from 15 week old NT2/A (SFM) and NT2/N (SFM) cultures (which were pre-washed in PBS, then given fresh SFM; media was collected 24 hours later) were separated by SDS/PAGE on a 7% gel, transferred to a nitrocellulose membrane and incubated overnight with a monoclonal mouse anti-Reelin 142 primary antibody. After a 45-minute incubation with peroxidase labelled anti-mouse IgG secondary antibody, bound antibody was then detected by chemiluminesence with 1-minute film exposure. The positions of molecular mass markers (kDa) are indicated, and prominent bands indicate expected sizes of Reelin (180, 250-300, 400 kDa bands).

(C) Immunofluoresence: Staining of 15 week old NT2/A cells, with the anti-Reelin 142 antibody (A) and phase contrast photomicrograph (A′). Immunohistochemistry was performed as described in the material methods and the Alexa 488 (green) conjugated secondary antibody was used. Representative images are shown from triplicate results. Magnification x400

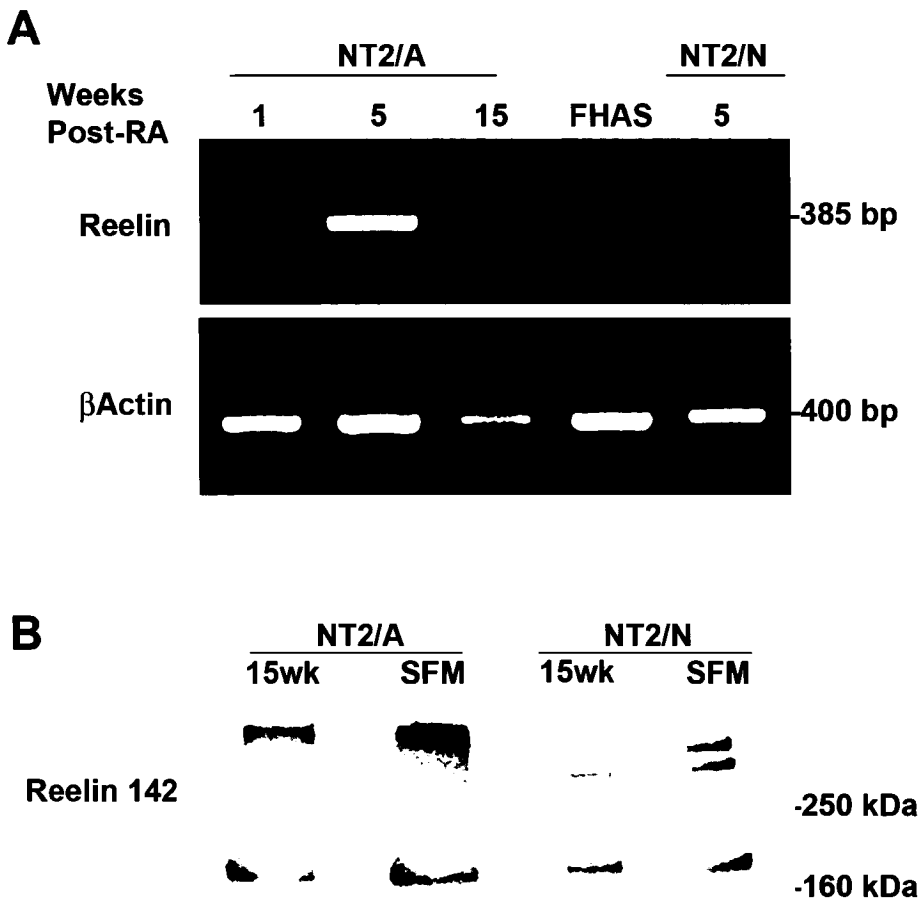
A
NT2/A
NT2/N
Weeks
Post-RA
1
5
15
FHAS
5
Reelin
385 bp
βActin
400 bp
B
NT2/A
NT2/N
15wk
SFM
15wk
SFM
Reelin 142
-250 kDa
-160 kDa
C
A
NT2/A
Reelin 142

conditions (Fig 8B). The 300 and 400 kDa protein bands from glial extracts failed to separate fully and were of a higher molecular weight than what was observed in neuronal extracts, however, the bands migrated in a pattern that was similar to that observed for recombinant Reelin secreted by 293 cells (Fig 4B). Complete separation of the 300 and 400 kDa bands occurred in neuronal samples (Fig 8B), while both glial and neuronal cell types produced a 180-kDa fragment that migrated at the same velocity.

Immunostaining showed that the Reelin protein was localized to distinct puncta throughout the cytoplasm of 15 week old astrocytes (Fig 8C). These results clearly demonstrated that the large secreted glycoprotein Reelin is not only transcribed, but is also abundantly expressed and secreted by both NT2 astrocytes and neurons.

### 3.2(a) Reelin's Receptors are Expressed in the NT2 Cell Model System

Reelin has been shown to bind to two members of the low-density lipoprotein receptor family ApoER2 and VLDLR (Trommsdorff M et al. 1999), the cadherin-related neuronal receptors (CNRs) (Senzaki K et al. 1999) and the $\alpha 3\beta 1$-integrin receptors (Dulabon L et al. 2000). To investigate which of Reelin's receptors where present in the NT2 cell model system, RNA from 15 week old astrocytes and neurons was extracted and used for cDNA synthesis (See section 2.2 for details), which was subjected to RT-PCR using primers specific for the ApoER2, VLDLR and $\alpha 3\beta 1$-integrin receptors (see Table 1 for primer details). The RT-PCR analysis confirmed the presence of ApoER2, producing a fragment of 217 bp; the very low-density lipoprotein receptor (VLDLR), producing a fragment of 122 bp; and the $\alpha$-3, $\beta$-1 Integrin receptors, producing a fragment of either 130 or 185 bp, respectively, in both neuronal and glial cell populations (Fig 9). Primers amplifying $\beta$-Actin were used to generate a 400 bp fragment. Thus,

## Figure 9: Reelin Receptors are Expressed in NT2 Cells

Total RNA from 15-week old NT2/A cells was extracted from either co-cultures (where neurons were shaken off before astrocytes were harvested, Co-Astro) or from pure cultures (Pure Astro) and from pure 8 week old neuronal cultures (Pure Neuron). The extracted RNA was then used for cDNA synthesis with reverse transcriptase as described in materials and methods. The resulting cDNAs were used for RT-PCR amplification using ApoER2, VLDLR, α3 Integrin and β-1 Integrin specific primers, with β-Actin specific primers used as an internal control (see Table 1 for primer details). Amplified products were separated on 1% agarose gels stained with ethidium bromide. The respective expected sizes of amplified products are indicated on right hand side of panel (base pairs- bp).

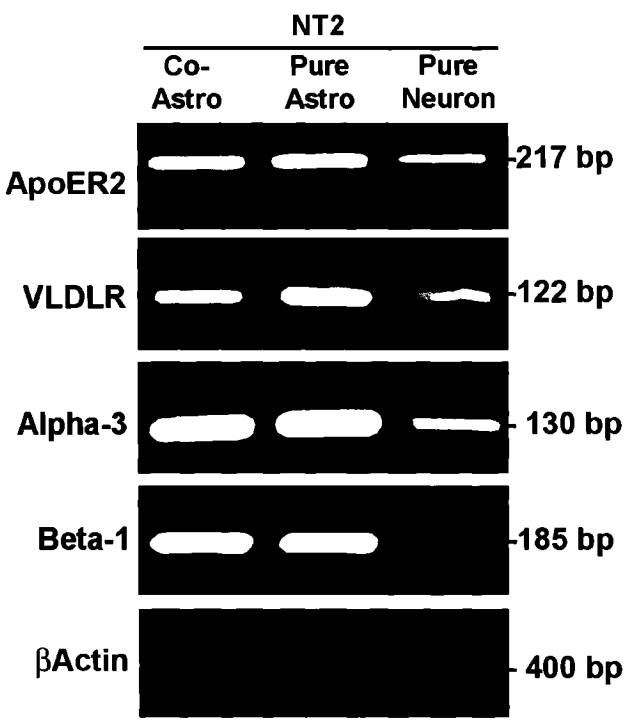
NT2
Co-Astro
Pure Astro
Pure Neuron
ApoER2
217 bp
VLDLR
122 bp
Alpha-3
130 bp
Beta-1
185 bp
βActin
400 bp

Reelin and its receptors were actively transcribed in this cell model system. As the ApoER2 has been shown to play a role in transmission of the Reelin signal to an intracellular kinase-signalling pathway within the brain (D' Arcangelo G et al. 1999), we concentrated on Reelin signalling via ApoER2 as the primary focus for this study. However it is possible that some of Reelin's effects in the NT2 cell model system is dependent on the VLDLR, which has also been shown to be an important component of Reelin signalling in mice (Hiesberger T et al. 1999) and this remains for further study.

### 3.2(b) Timecourse Expression of ApoER2 at the Transcriptional Level

Ten ApoER2 splicing variants have been described in human brain tissues (Kim DH et al. 1997; Sun XM et al. 1999; Brandes C et al 1997). To establish which ApoER2 splicing variants are present in the NT2 cells and at what stages of differentiation, primers specific for the five variants specifically occurring in human cells were used to carry out an RT-PCR analysis on NT2 extracts at various stages of development (Fig 10). ApoER2 transcript expression was fairly constant throughout neuronal development for most of the isoforms and consisted of the following variants (see also Sun XM et al. 1999): a 217 base pair variant lacking exon 5 ubiquitously expressed throughout NT2 development; a 784 base pair variant containing both exon 15 and exon 18 and a 559 base pair variant lacking exon 15, but including exon 18, both of which were consistently expressed throughout NT2 development; a 382 base pair variant lacking both exon 15 and exon 18 that appeared to be down-regulated from it's level of expression in NT2/D1 precursor cells over the course of development (with only a faint band present during later time points); and a 61 base pair variant lacking the 39 base pair insertion fragment that defines a consensus site for furin cleavage as shown in Fig 10. It was interesting to

## Figure 10: The Expression of ApoER2 During NT2 Cell Differentiation

Total RNA was extracted from NT2/D1 precursor cells, cells treated with retinoic acid (RA) for 1, 2, 3 and 4 weeks and from 1, 2, 3, or 4 weeks old NT2/N cells (See materials and methods for details). The RNA was reverse transcribed into cDNA and the resulting cDNAs were used for RT-PCR amplification using primers specific for various ApoER2 transcripts.
ApoER2-Ex5 is a set of primers flanking either side of exon 5 and produces a 217 bp fragment without exon 5 or 604 bp fragment with exon 5.
ApoER2 Ex15/18 is a set of primers that amplify the region between exon 15 and exon 18 of the ApoER2 gene producing a 784 bp fragment with both exons present, a 559 bp fragment with only exon 18 present, and a 382 bp fragment when both exons are spliced out.
ApoER2-Ex6a is a set of primers that flanks either side of the consensus site for furin cleavage site (exon 6 and exon 7) and produces a 102 bp fragment if the furin cleavage site is present and a 61 bp fragment without the furin cleavage fragment.
β-Actinin specific primers were used as an internal control (see Table 1 for primer details). Amplified products were separated on 1.5 % agarose gels stained with ethidium bromide. The respective sizes of amplified products are indicated on right hand side of panel (base pairs- bp)

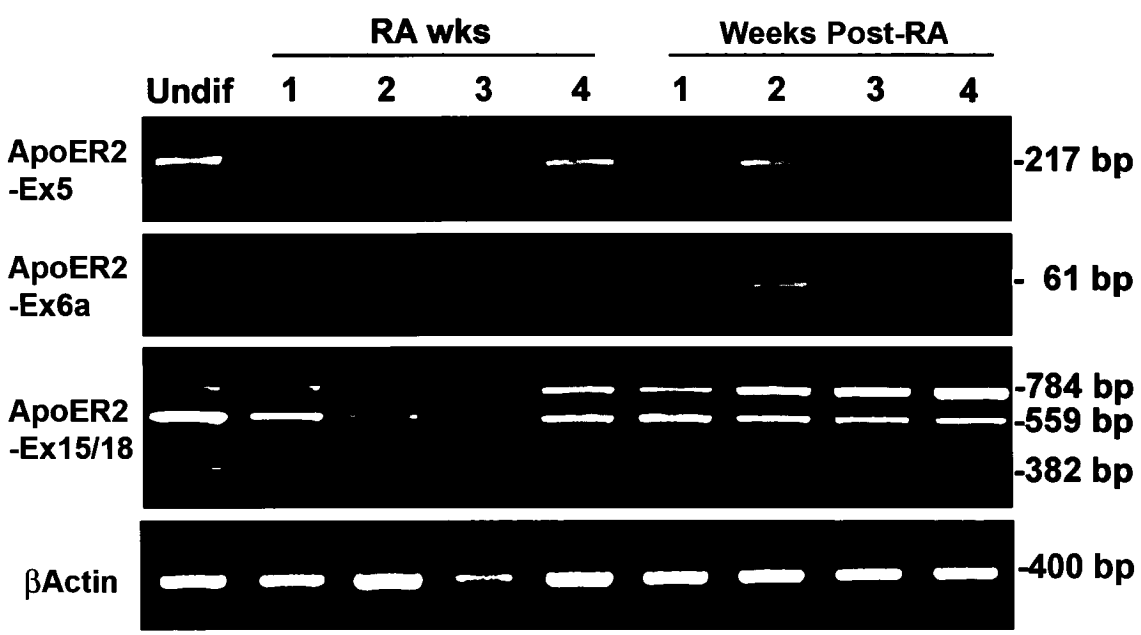
RA wks
Weeks Post-RA
Undif
1
2
3
4
1
2
3
4
ApoER2
-Ex5
-217 bp
ApoER2
-Ex6a
- 61 bp
ApoER2
-Ex15/18
-784 bp
-559 bp
-382 bp
βActin
-400 bp

note that the expression of the ApoER2 variant that contains the consensus site for furin cleavage (primer ApoER2-Ex6b, which would have generated a 102 base pair fragment) was not present in any of the NT2/N extracts, RA treated cells, nor in the NT2/D1 precursor cells. A faint band was seen in the 1 week differentiated samples, however this may be due to the presence of a low level of glial mRNA (see Figure 12). As a standard internal control to demonstrate equal loading primers were used against β-Actin, which generated a 400 bp fragment.

### 3.2(c) ApoER2 Splicing Variants in NT2/A, NT2/N, and FHAS Cells

Having established that ApoER2 is generally expressed throughout differentiation we examined the specific differences in expression pattern of the ApoER2 variants in NT2/A and NT2/N cells (Fig. 11 & Fig 12). Once again, we utilized RT-PCR to distinguish the ApoER2 variants in the following samples: i) astrocytes extracted from a co-culture (enriched astrocytes), ii) pure astrocytes, iii) pure neurons or iv) fetal human astrocytes (see Section 2.1 for tissue culture details). Expression patterns of both the ApoER2-Ex15/EX18 and ApoEx5 were similar between glial and neuronal cultures, both expressing 784 bp, 559 bp and 217 bp fragments, respectively. As was the case in Figure 10, the expression of a 382 base pair variant lacking both exon 15 and exon 18, was only faintly visible in both glial and neuronal cultures. However a 102 base pair variant of ApoER2, containing the consensus site for furin cleavage, appeared to be exclusively expressed in glial cultures but not in neuronal cultures. In contrast the 61 base pair variant lacking this insertion was detected in both cell types (Fig 11). To confirm these findings, RT-PCR was carried out with mRNA extracted from both pure NT2 astrocytes and neurons after 1,2,5 or 15 weeks post-RA. Figure 12 shows without any doubt that the

## Figure 11: ApoER2 Splicing Variants in NT2/A, NT2/N and FHAS

Total RNA from 8 week old NT2/A cells was extracted from either co-cultures (Co-Astro) or from pure cultures (Pure Astro) and from 8 week old NT2/N pure neuronal cultures (Pure Neuron). Total RNA from fetal human astrocytes (FHAS) was extracted once cells had been passaged twice. Extracted RNA was then used for cDNA synthesis with reverse transcriptase (as described in materials and methods). The resulting cDNAs were used for RT-PCR amplification using the same primers as described previously in Fig 5. Amplified products were separated on 1.5 % agarose gels stained with ethidium bromide. The sizes of amplified products are indicated on the right hand side of panel (base pairs- bp).

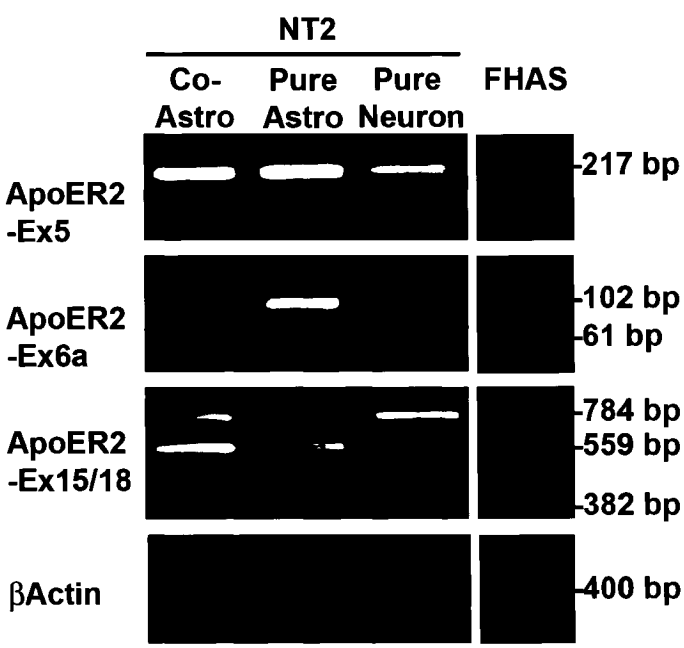
NT2
Co-Astro
Pure Astro
Pure Neuron
FHAS
ApoER2 -Ex5
217 bp
ApoER2 -Ex6a
102 bp
61 bp
ApoER2 -Ex15/18
784 bp
559 bp
382 bp
βActin
400 bp

## Figure 12: ApoER2 Splicing Variants in NT2/A, NT2/N and FHAS During Maturation

Total RNA was extracted from FHAS and from NT2/A and NT2/N at 1, 2, 5, or 15 weeks of maturation. Extracted RNA was then used for cDNA synthesis with reverse transcriptase (as described in materials and methods). The resulting cDNAs were used for RT-PCR amplification using the ApoER2-Ex6a primers and the ApoER2 Ex6a/18 primers. The ApoER2 Ex6a/18 is a set of primers that amplify the region between exon 6a and exon 18 of the ApoER2 gene, producing three transcripts: 1971 bp (containing exons 6a, 15 and 18), 1746 bp (containing exons 6a, and 18) and 1530 bp (containing exon 6a) in NT2/A over the course of maturation; whereas only two transcripts of 1932 bp (containing exons 15 and 18) and 1707 bp (containing exon 18) were expressed by NT2/N. β-Actin specific primers were used as an internal control (see Table 1 for primer details). Amplified products were separated on 1.5 % agarose gels stained with ethidium bromide. The sizes of amplified products are indicated on right hand side of panel (base pairs- bp).

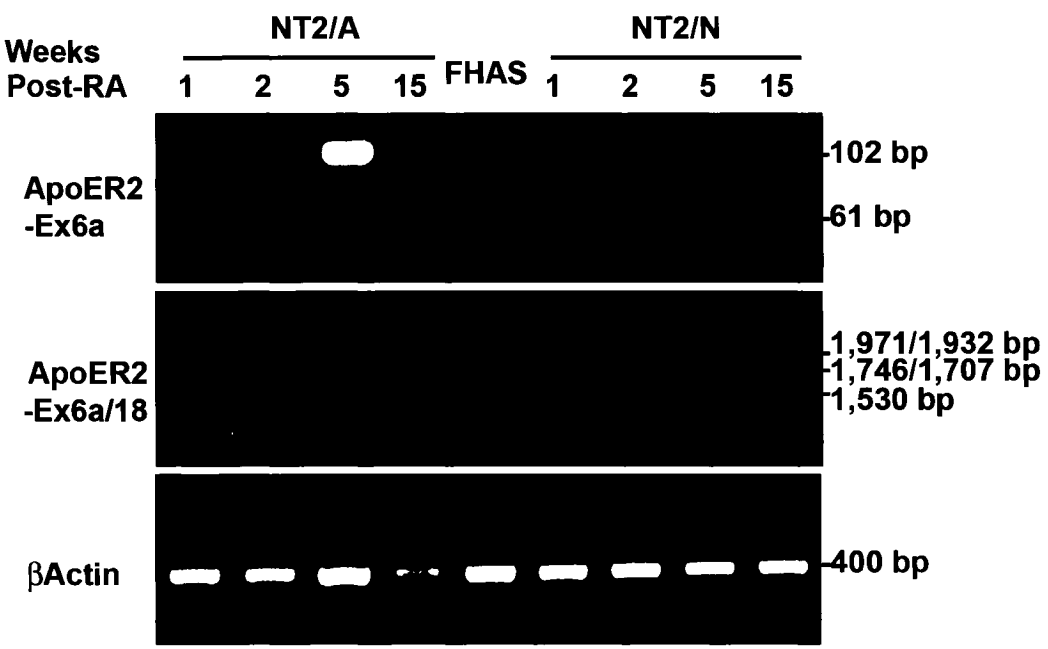
Weeks
Post-RA
NT2/A
1
2
5
15
FHAS
NT2/N
1
2
5
15
ApoER2
-Ex6a
102 bp
61 bp
ApoER2
-Ex6a/18
1,971/1,932 bp
1,746/1,707 bp
1,530 bp
βActin
400 bp

expression of the fragment containing the furin cleavage site (102 bp fragment) was, indeed, unique to mature NT2/A.

In order to observe whether differential splicing of ApoER2 occurs in primary human astrocytes, RT-PCR analysis of the ApoER2 splicing variants was carried out on RNA extracted from fetal human astrocytes (FHAS) (Fig 11 & Fig 12). The expression patterns between NT2/A and FHAS were similar, however there was a much stronger signal in the pure NT2/A than in the FHAS. This may be due to the fact that FHAS have not yet fully matured since, as indicated in Figure 12, there is an increased expression of ApoER2 in NT2/A at either 1 week post-RA or 5 weeks post-RA.

Consistent with our previous findings (Fig 10), three transcripts: a 1971 bp (containing exons 6a, 15 and 18), 1746 bp (containing exons 6a, and 18) and 1530 (containing exon 6a) were expressed by NT2/A over the course of maturation, whereas only two transcripts of a 1932 bp (containing exons 15 and 18) and a 1707 bp (containing exon 18) were expressed by NT2/N cells over the same period of maturation (Fig 12). It should be noted that the sizes of some of the fragments expressed by both glial and neuronal cells are so similar that they are not fully resolved on the gel. These results provide direct evidence that ApoER2 transcripts are spliced differently in the astrocytes and the neurons derived from the NT2 cell model system.

### 3.2(d) Time-course Expression of ApoER2 at the Protein Level

The RT-PCR results indicated that the ApoER2 variants in NT2/A cells are different from those in NT2/N cells. These findings were confirmed by Western blotting using an antibody specific for the last 14 amino acids of the cytoplasmic tail of ApoER2 (Fig 13). In astrocytes, the ApoER2 protein variants migrated with different apparent

## Figure 13: Expression of ApoER2 Protein During NT2/A Maturation

(A) Protein extracts (80μg per lane) from NT2/D1 precursor cells, from 1, 5, 10, and 15 week old NT2/A, from 15 week old NT2/N and from mouse cortical brain (MC adult) were separated by SDS/PAGE on a 8% gel, transferred to a nitrocellulose membrane and incubated overnight with a rabbit polyclonal anti-ApoER2 primary antibody specific for the last 14 amino acids of the cytoplasmic tail of the receptor. After a 45-minute incubation with a peroxidase labelled anti-rabbit IgG secondary bound antibody was then detected by chemiluminesence with 2-minute film exposure. The positions of molecular mass markers (kDa) are indicated, and prominent bands represent the 3 different isoforms of the ApoER2 receptor (160, 148, 110 kDa). As controls, the membrane was stained with Ponceau S, and stripped and re-probed with a mouse monoclonal anti-β-actin antibody to demonstrate equal protein loading.

(B) Protein extracts (80μg per lane) from 5 week old NT2/A and NT2/N and from mouse cortex extracted on embryonic day 13 were separated by SDS/PAGE on an 8% gel and transferred to a nitrocellulose membrane. The ApoER2 antibody was incubated with 100 μg of an ApoER2 blocking peptide (consisting of the last 14 amino acids of the receptors cytoplasmic tail) prior to membrane probing as a control. To confirm the specificity of the blocking peptide, the membrane was stripped and re-probed with the ApoER2 antibody in the presence of 100 μg of the CRMP2 blocking peptide. The positions of molecular mass markers (kDa) are indicated, and the prominent bands represent the different isoforms of ApoER2.

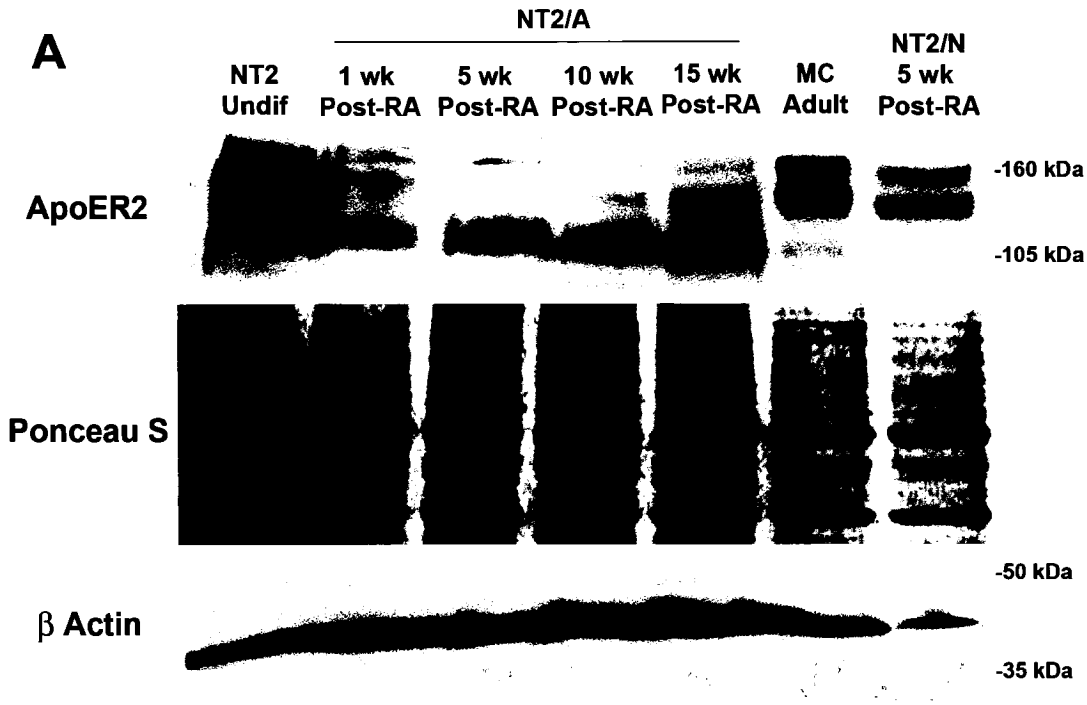
A
NT2/A
NT2 Undif
1 wk Post-RA
5 wk Post-RA
10 wk Post-RA
15 wk Post-RA
MC Adult
NT2/N 5 wk Post-RA
ApoER2
-160 kDa
-105 kDa
Ponceau S
-50 kDa
β Actin
-35 kDa

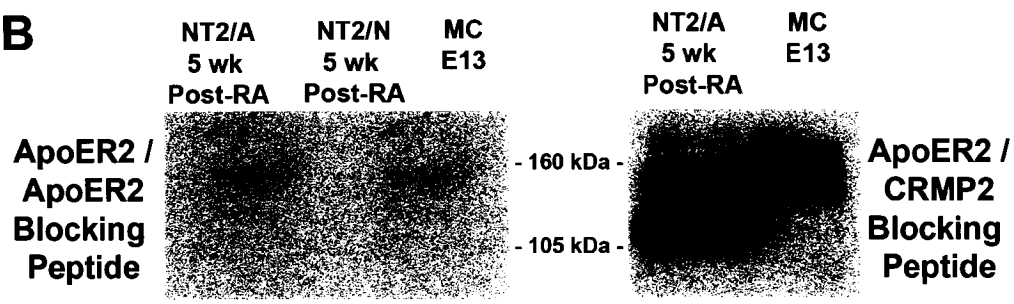
B
NT2/A 5 wk Post-RA
NT2/N 5 wk Post-RA
MC E13
NT2/A 5 wk Post-RA
MC E13
ApoER2 / ApoER2 Blocking Peptide
- 160 kDa -
- 105 kDa -
ApoER2 / CRMP2 Blocking Peptide

molecular masses: these were ~ 160 kDa equivalent to full-length protein, ~148 kDa presumably of the receptor variant containing exon 18, but lacking exon 15; and ~ 110 kDa for the receptor variant lacking both exons 15 and 18 and other exons yet to be identified (see also Sun XM & Soutar AK 1999). However, only two isoforms were expressed in NT2/N and in cortical mouse extracts (Fig 13A). The molecular masses of the migrating proteins, with the exception of the protein lacking the sugar domain (exon 15), were all greater than those predicted from their amino acid sequences, as also seen by Sun XM & Soutar AK (1999), presumably reflecting post-translational modification of the sugar domain. To show the specificity of the ApoER2 antibody, an ApoER2 blocking peptide, consisting of the last 14 amino acids of the receptors cytoplasmic tail was synthesised. The ApoER2 antibody was incubated with 100 μg of the blocking peptide prior to membrane probing, this completely abolished the binding of the ApoER2 antibody to its epitope (Fig 13B). To confirm the specificity of the blocking peptide, the membrane was stripped and re-probed with the ApoER2 antibody in the presence of a non-specific blocking peptide- CRMP2. This peptide failed to inhibitthe antibody binding (Fig 13B). Thus we felt confident that the detected protein bands were representative of different ApoER2 protein isoforms. To demonstrate equal protein loading, membranes were stained with Ponceau S prior to being stripped and re-probed with a mouse monoclonal anti-β-actin antibody (Fig 13A).

### 3.2(e) Sub-cellular Localization of ApoER2

To investigate the sub-cellular localization of ApoER2 in the NT2 cells, immunostaining was carried out on pure 15 week old NT2/A, NT2/N co-cultures and NT2/D1 precursor cells. All cells were cultured as described in Section 2.1. Using the

same antibody described in Fig 13, the NT2/A stained positively for the ApoER2 throughout the cytoplasm of the cell, with a strong signal radiating outwards form the nucleus (Fig 14A & 14B). A similar staining pattern was also observed in both NT2/N co-cultures and in NT2/D1 cultures (Fig 14D & 14C). As a positive control, sections of mouse cortical brain from postnatal day 20 (P-20) were stained with the ApoER2 antibody (Fig 14F). As a negative control, cells were incubated with 10% horse serum instead of the ApoER2 primary antibody, before being probed with the secondary antibody (Fig 14H). Cells were also stained with an anti- ApoER2 primary antibody that had been pre-incubated with the ApoER2 blocking peptide (as described in Fig 13B) to confirm its specificity (Fig 14E & 14G).

## 3.3 A Secreted Soluble Form of ApoER2 is Present in NT2/A

It has previously been reported by Koch S et al. (2002) that furin dependent cleavage of the ApoER2 variant carrying the consensus site for furin cleavage does indeed take place in primary mouse neurons and that the receptor fragment generated, which consists of the entire ligand-binding domain, can be secreted as a soluble peptide of ~28 kDa. To establish whether such a soluble fragment could be secreted by NT2/A or NT2/N cells, cultures were given fresh SFM which was collected 2 or 4-days later and tested for the presence of the secreted soluble fragment, by Western blotting with the anti-AppER2 220 antibody (a kind gift from Dr. Johannes Nimpf). This antibody is specific for the first 13 amino acids of the ligand-binding domain (Fig 15A). A faint band of approximately 28 kDa was detected in media collected from NT2/A but not NT2/N cells (Fig 15A), consistent with our RT-PCR results (Fig 12). In order to confirm these

## Figure 14: Immunolocalization of ApoER2 in NT2/A and NT2/N cells

Fifteen week old NT2/A (A, B, G, & H), NT2/N co-cultures (D & E), NT2/D1 precursor cells (C) and sections of mouse cortical brain (F) from postnatal day 20 (P-20) were fixed and immunostained with the anti-ApoER2 primary antibody- specific for the last 14 amino acids of the receptor (A, B, C, D, F) or they were stained with the anti-ApoER2 primary antibody pre-incubated with an ApoER2 blocking peptide (E, G, H) as a control. Shown also are phase-contrast micrographs (A′- H′). Immunohistochemistry was performed as described in material & methods. Either Alexa 488 (green), or Rhodamine (red) conjugated secondary antibodies were used. Representative images are shown from triplicate results. Magnification x200 for A, C, E, G, and x400 for B, D, F, & H

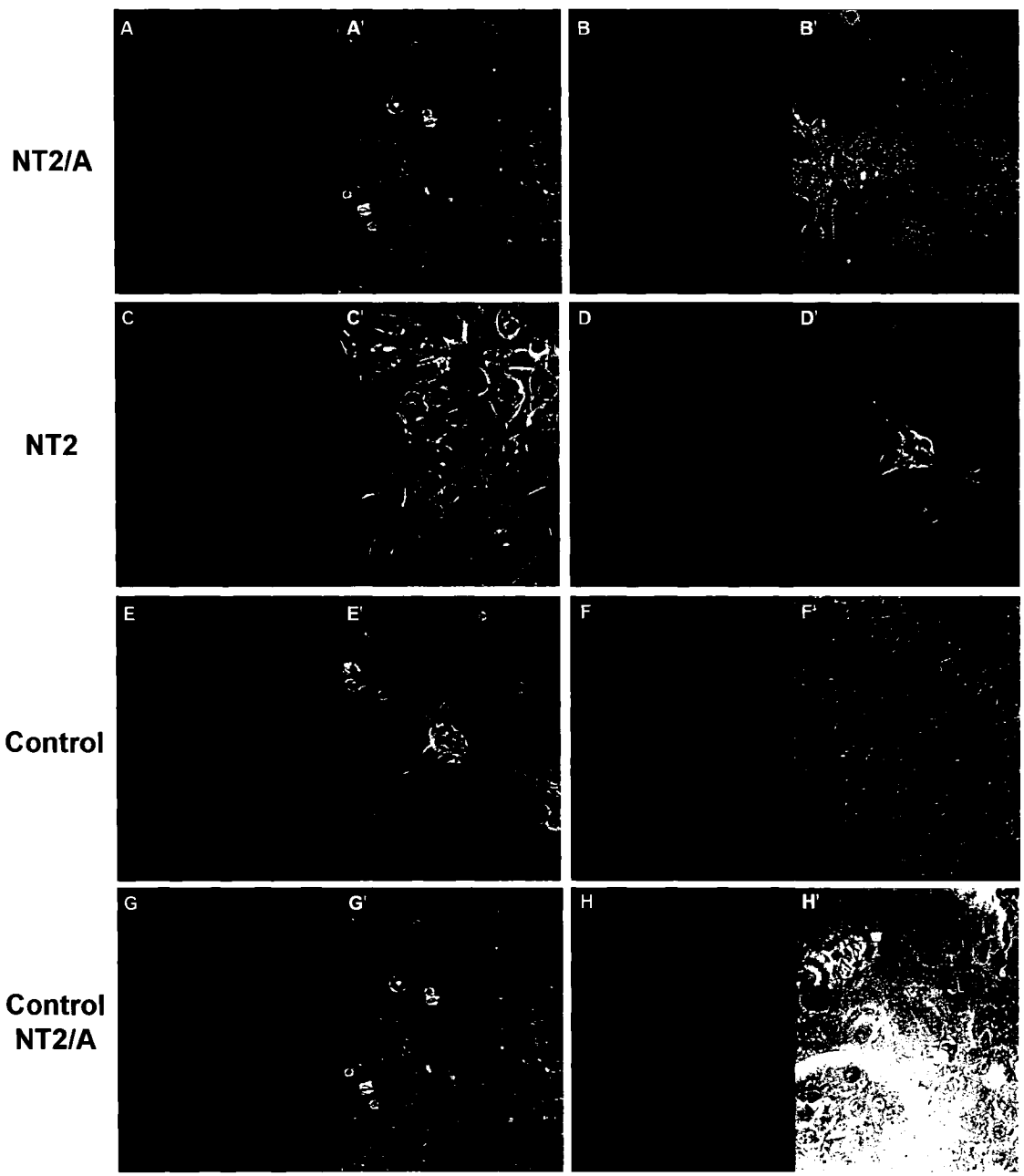
NT2/A
NT2
Control
Control NT2/A
A
A'
B
B'
C
C'
D
D'
E
E'
F
F'
G
G'
H
H'

## Figure 15: A Secreted Soluble Form of ApoER2 is Present in NT2/A

(A) Fifteen week old NT2/A and NT2/N cultures were pre-washed with PBS and then given fresh SFM, which was collected either 24-hours or 36-hours later. Approximately 40 μl of supernatant from these cultures was separated by SDS/PAGE on a 10% gel, transferred to a nitrocellulose membrane and incubated overnight with a rabbit polyclonal anti-ApoER2-220 antibody (directed against the first 14 amino acids of the ligand binding domain (exon 2)). After a 45-minute incubation with a peroxidase labelled anti-rabbit IgG secondary, bound antibody was then detected by chemiluminesence, with 10-minute exposure to film. The position of molecular mass marker (kDa) is indicated, and the 28 kDa band is the predicted size of the prominent band that corresponds to that of the secreted soluble receptor fragment.

(B) The supernatant from either 5 week or 15 week old NT2/A cells was immunoprecipitated with a mouse monoclonal anti-Reelin 142 antibody. Immunocomplexes were precipitated with protein G-Sepharose beads and resolved by SDS/PAGE on a 10 or 7% gel and transferred to a nitrocellulose membrane. Membranes were incubated overnight with either a rabbit polyclonal anti-ApoER2-220 antibody (directed against the first 14 amino acids of the ligand binding domain (exon 2)) or with a mouse monoclonal anti-Reelin 142-antibody. After a 45-minute incubation with either a peroxidase labelled anti-rabbit or anti-mouse IgG secondary, bound antibody was then detected by chemiluminesence with a 10-minute exposure to film. The positions of molecular mass markers (kDa) are indicated. Control lanes contain non-specific bands that were formed by the interaction of the protein G-sepharose beads with the supernatant, in the absence of the primary anti-Reelin 142 antibody.

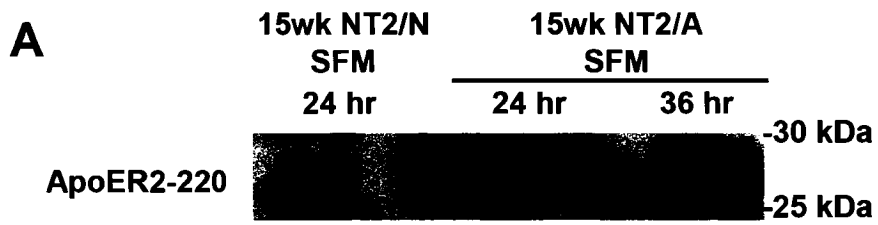
A
15wk NT2/N
SFM
24 hr
15wk NT2/A
SFM
24 hr
36 hr
-30 kDa
ApoER2-220
-25 kDa

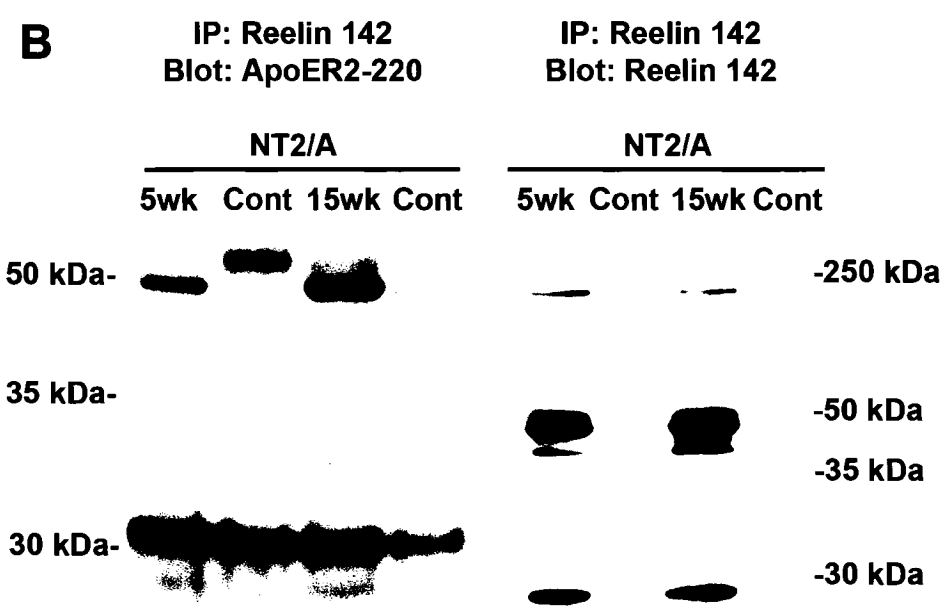
B
IP: Reelin 142
Blot: ApoER2-220
IP: Reelin 142
Blot: Reelin 142
NT2/A
NT2/A
5wk Cont 15wk Cont
5wk Cont 15wk Cont
50 kDa-
35 kDa-
30 kDa-
-250 kDa
-50 kDa
-35 kDa
-30 kDa

results, Reelin was immunoprecipitated from the NT2/A media and the precipitate was tested for the presence of the soluble receptor fragment by Western blotting with the anti-ApoER2 220 antibody (Fig 15B). The ApoER2-220 blot detects both the heavy and light chains of the IgG immunoglobin; the bands at ~28 kDa are representative of the predicted size (Koch S et al 2002) of the secreted soluble receptor fragment. Prominent bands at 50 and 30 kDa in the Reelin 142 blot are the heavy and light chain portions of the IgG immunoglobin (heavy chains 60-200 kDa, and light chains 30-45 kDa); the bands at ~180 kDa are representative of the predicted size of Reelin (Fig 15B). The 300 and 400 kDa bands of Reelin failed to migrate into the gel in this experiment. With this co-precipitation approach, the soluble receptor fragment could clearly be seen in the medium of NT2/A (Fig 15B). Collectively these RT-PCR results have established the presence of Reelin mRNA and the various isoforms of ApoER2 in NT2 derived neurons and astrocytes. They have identified an isoform of ApoER2 that is expressed exclusively in astrocytes and have confirmed by immunoblotting and immunohistochemistry the expression of both Reelin and ApoER2 within NT2/A at the protein level.

## 3.4 Establishment of Reelin Signalling Components in NT2/A and NT2/N

Having established that both Reelin and its key receptor ApoER2 are expressed and translated in NT2 cells, we tested whether the downstream signalling molecule Dab1, a cytosolic adaptor protein, was also expressed and produced within these cells. Both the Dab1 transcript and protein were expressed in NT2/A and NT2/N cells at similar levels (Fig 16A & 16B, respectively). Dab1 specific primers generated a 175 bp fragment (Fig

## Figure 16: Dab1 Expression in NT2/A, NT2/N and FHAS Cells

(A) Total RNA was extracted from 5 or 15 week old NT2/A, NT2/N and from FHAS cells for cDNA synthesis with reverse transcriptase as described in materials and methods. The resulting cDNAs were used for RT-PCR amplification using either Dab1 specific primers or β-Actin specific primers (see Table 1 for primer details). Amplified products were separated on 1.5 % agarose gels and stained with ethidium bromide. The respective sizes of amplified products are indicated on right hand side of panel (base pairs- bp).

(B) Protein extracts (35 μg per lane) from 15 week old NT2/A, NT2/N cells and from adult mouse cortex were separated by SDS/PAGE on a 8% gel, transferred to a nitrocellulose membrane and incubated overnight with a rabbit polyclonal anti-Dab1-CY38 primary antibody. After a 45-minute incubation with a peroxidase labelled anti-rabbit IgG secondary, bound antibody was then detected by chemiluminesence, with 1-minute film exposure. The positions of molecular mass markers (kDa) are indicated and the prominent band is the expected size for Dab1 (~80 kDa). As control, the membrane was stained with Ponceau S to demonstrate equal protein loading.

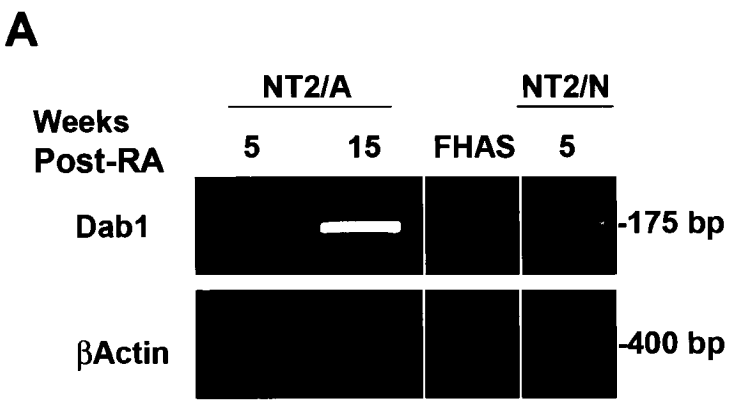
A
NT2/A
NT2/N
Weeks
Post-RA
5
15
FHAS
5
Dab1
-175 bp
βActin
-400 bp


B
NT2/A
15wk
NT2/N
15wk
Adult
MC
-105 kDa
Dab1 CY38
-75 kDa
Ponceau S

16A), whereas the rabbit polyclonal anti-Dab1 CY38 antibody identified a band that migrated at approximately 80 kDa (Fig 16B). As a positive control protein lysates extracted from adult mouse cortex was used and to demonstrate equal protein loading, the membrane was stained with Ponceau S prior to primary incubation (Fig 16B). Cells were stained and the protein was found to be concentrated in a perinuclear location in the NT2/A cells (Fig 17A & 17B), whereas in NT2/N the protein was expressed ubiquitously throughout the cytoplasm (Fig 17C & 17D). As a negative control for this experiment cells were incubated with 10% horse serum instead of the Dab1 primary antibody, before being probed with the secondary antibody (Fig 17E & 17F). These findings established for the first time, the presence of the signalling components of the Reelin pathway in mature, human NT2/A.

## 3.5 Demonstration of Functional Reelin Signalling in NT2/A

Reelin has previously been shown to mediate signals via the ApoER2 and VLDLR resulting in the tyrosyl phosphorylation of Dab1 (Hiesberger T et al. 1999, Balif BA et al. 2003). Since studies by Howell BW et al. 2000 have shown that the tyrosyl phosphorylation of Dab1 plays such a critical role in the transmission of the Reelin signal, we wanted to determine whether Reelin could stimulate the tyrosyl phosphorylation of Dab1 in NT2/A. Since purified Reelin was not commercially available, we used conditioned medium from 293 cells expressing and secreting Reelin (see Section 2.6) as described previously (D'Arcangelo G et al. 1999) to induce Reelin mediated signalling. Specifically, pure 15 week old NT2/A cultures were treated with media containing recombinant Reelin for 15 or 20 minutes (the optimal times for Reelin

## Figure 17: Immunolocalization of Dab1

Fifteen week old NT2/A cells (A, B, & E) and NT2/N co-cultures (C, D, & F) were fixed and immunostained with the anti-Dab1 CY38 primary antibody (A, B, C, D) or, as a control, they were treated with 10% horse serum instead of with a primary antibody (E & F). Shown also are phase-contrast micrographs (A′- F′). Immunohistochemistry was performed as described in material & methods. Either Alexa 488 (green), or Rhodamine (red) conjugated secondary antibodies were used. Representative images are shown from triplicate results. Magnification x200 for A, C, E; x400 for B, D, & F.

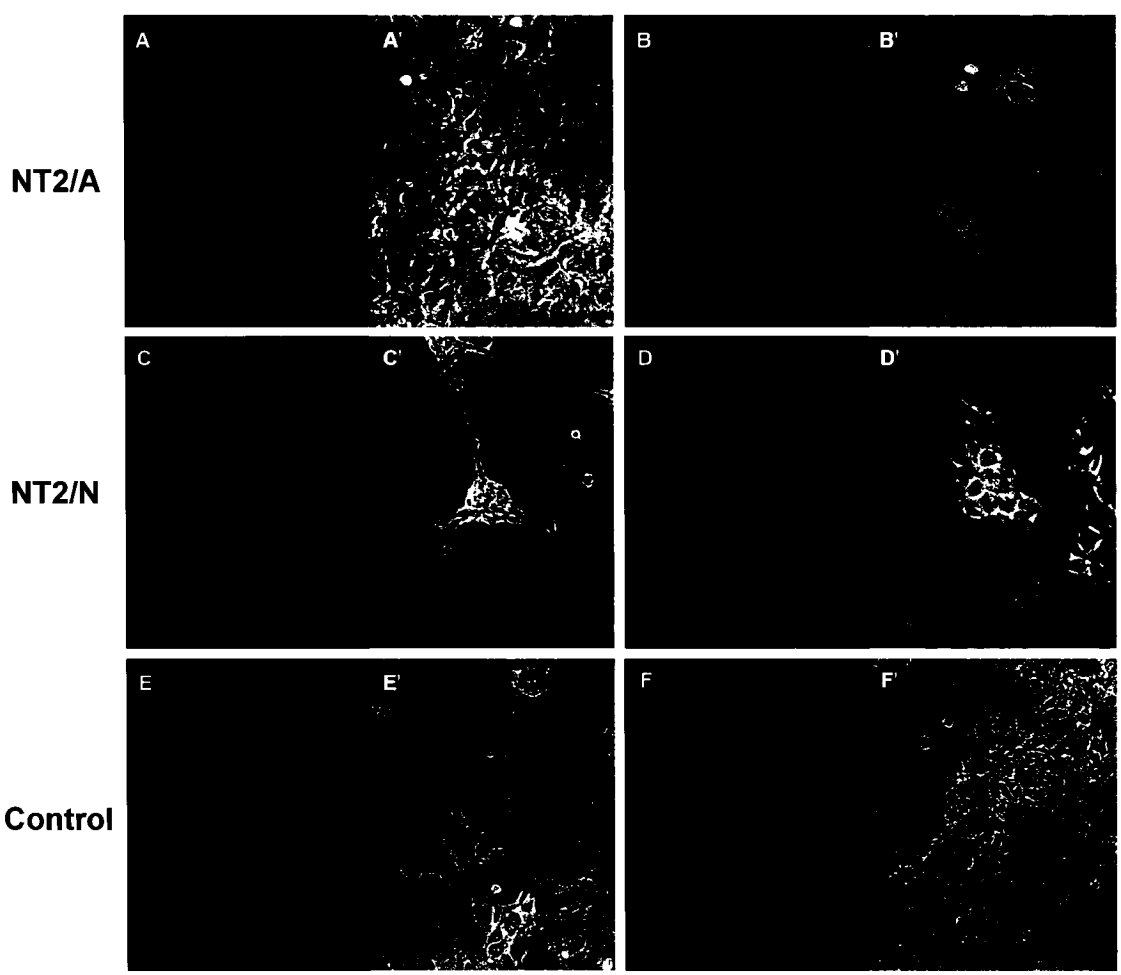
NT2/A
NT2/N
Control
A
A'
B
B'
C
C'
D
D'
E
E'
F
F'

stimulation shown by Befferet U et al. 2002) at 37°C. Lysates were tested by Western blotting using antibodies specific for the tyrosyl residues on Dab1 that have been shown to be phosphorylated in a Reelin dependent manner (Keshvara L et al. 2001). Results are shown in Figures 18 and 19. The identified protein bands migrated at an approximate molecular weight of 80 kDa, consistent with our previous findings (Fig 16) and with the literature (Keshvara L et al. 2001; Befferet U et al. 2002; Balif BA et al. 2003). Our results clearly showed that Reelin induced the phosphorylation of Dab1 on Tyr198 (Fig 18) and Tyr220 (Fig 19) while the total amount of Dab1 protein remained constant. As a positive control protein lysates extracted from mouse embryonic day 16 cortical neurons was used (Fig 18). To demonstrate equal protein loading membranes were stained with Ponceau S prior to primary incubation, in addition to being stripped and re-probed with a mouse monoclonal anti-β-Actin antibody (Fig 18 & Fig 19). As a control to ensure antibody specificity, half of the extracted lysates were treated with λ-phosphatase, an $Mn^{2+}$ dependent, threonine tyrosine phosphatase, which completely abolished the Reelin-induced phosphorylation of Dab1 on tyrosyl residue 220 (Fig 19). Consistent with previous findings (Keshvara L et al. 2001), tyrosyl phosphorylation of Dab1 was very faint in the absence of Reelin and only the anti PY220 antisera reacted against Dab1 from unstimulated astrocytes (Fig 19). Thus in accordance with Keshvara L et al. (2001), our results suggest that Tyr220 is a major site of basal phosphorylation. β-Actin was used as a control to demonstrate equal protein loading for all blots. These findings demonstrate that Reelin is able to signal via its receptors and elicit Dab1 phosphorylation in human, NT2/A.

## Figure 18: Recombinant Reelin Triggers Dab1 Tyrosyl Phosphorylation in Pure, 15wk Old NT2/A

Pure fifteen week old NT2/A cells were pre-washed twice in PBS then treated for 20 or 30 minutes with either 7 ml of SFM supplemented with 75 μl of 293 medium containing recombinant reelin or with 7 ml of SFM only (control). Proteins were extracted in RIPA lysis buffer, as described in materials and methods then were separated (80μg per lane) by SDS/PAGE on a 8% gel, transferred to a nitrocellulose membrane and incubated overnight with a polyclonal rabbit anti-Dab1-PY198 primary antibody, specific for the phosphorylated tyrosyl residue-198 of the Dab1 protein. After a 45-minute incubation with a peroxidase labelled anti-rabbit IgG secondary, bound antibody was then detected by chemiluminesence, with 5-minute film exposure. The positions of molecular mass markers (kDa) are indicated, and prominent band is expected size of phosphorylated Dab1 (~80 kDa). As a control, the membrane was stripped and re-probed with a rabbit polyclonal anti-Dab1-CY38 antibody to demonstrate that the total amount of Dab-1 protein remained constant. To demonstrate equal protein loading, the membrane was stripped again and re-probed with a mouse monoclonal anti-β-actin antibody, in addition to being stained with Ponceau S.

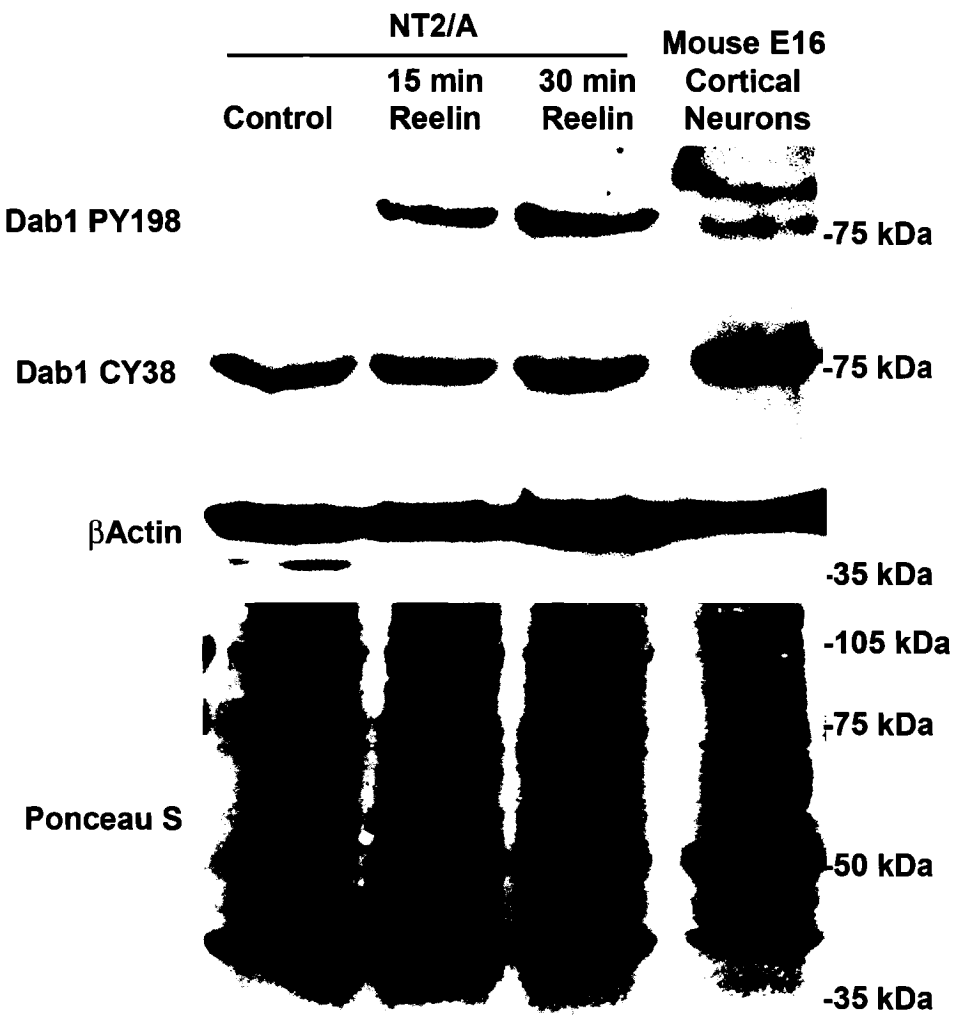
NT2/A
Mouse E16
Control
15 min Reelin
30 min Reelin
Cortical Neurons
Dab1 PY198
-75 kDa
Dab1 CY38
-75 kDa
βActin
-35 kDa
-105 kDa
-75 kDa
Ponceau S
-50 kDa
-35 kDa

## Figure 19: λ-Phosphatase Treatment Abolishes the Reelin Induced Tyrosyl Phosphorylation of Dab1 in NT2/A

Pure fifteen week old NT2/A cells were pre-washed twice in PBS then were treated for 20 minutes with either 7 ml of SFM supplemented with 75 μl of 293 medium containing recombinant reelin or with 7 ml of SFM only (control). Proteins were extracted (80μg per lane) in Alkaline Phosphatase Lysis Buffer as described in materials and methods, then half of the protein lysates were kept as control and the other half were incubated with the λ-Phosphatase reaction buffer for 30 minutes at 30°C, before being separated by SDS/PAGE on a 8% gel and transferred to a nitrocellulose membrane. Membranes were incubated overnight with a rabbit polyclonal anti-Dab1-PY220 primary antibody, specific for the phosphorylated tyrosyl residue-220 of the Dab1 protein. After a 45-minute incubation with a peroxidase labelled anti-rabbit IgG secondary, bound antibody was then detected by chemiluminesence with 5-minute exposure to film. The positions of molecular mass markers (kDa) are indicated and prominent band is expected size of phosphorylated Dab1 (~80 kDa). As a control, the membrane was stripped and re-probed with a rabbit polyclonal anti-Dab1-CY38 antibody to demonstrate that the total amount of Dab-1 protein remained constant. To demonstrate equal protein loading, the membrane was stripped again and re-probed with a mouse monoclonal anti-β-actin antibody, in addition to being stained with Ponceau S

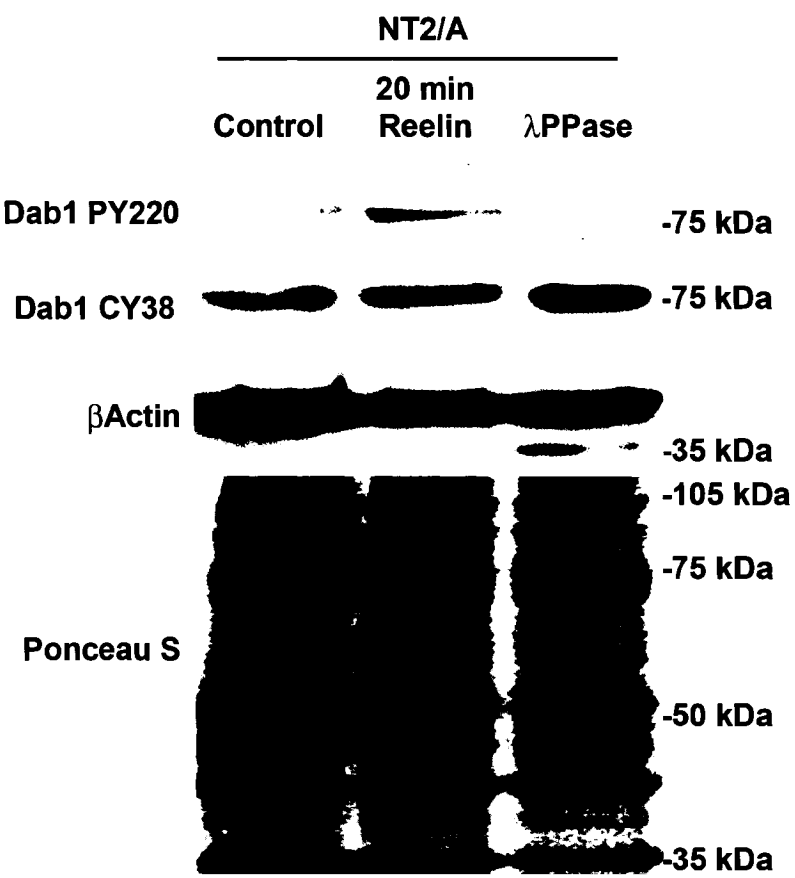
NT2/A
20 min
Control
Reelin
λPPase
Dab1 PY220
-75 kDa
Dab1 CY38
-75 kDa
βActin
-35 kDa
-105 kDa
-75 kDa
Ponceau S
-50 kDa
-35 kDa

## 3.6 Recombinant Reelin Reduces Membrane Ruffling in NT2/A

Having demonstrated the existence of a functional Reelin-signalling pathway in NT2/A we then sought to demonstrate an effect of Reelin on cell functionality. Since it has previously been shown that during development a functional Reelin signalling pathway is an absolute requirement for the formation of a regular radial glial scaffold in the dentate gyrus of mice (Weiss KH et al. 2003), we hypothesized that Reelin may play a role in determining the morphology of mature NT2/A. To test this hypothesis, 15 week old NT2/A were exposed to either SFM for a 72hour period, or were exposed to SFM supplemented with 293 media containing recombinant Reelin, replenished daily for a 72-hour period. SFM conditions have been shown to induce stellate cell morphology in astrocytes (Michler-Stuke A et al. 1984), whereas serum supplemented conditions have been shown (Moonen G et al. 1975) to induce flat polygonal shaped cells. Thus control cells were treated with normal NT2 media, then fixed and stained for either β-tubulin or GFAP and cell morphologies were compared. Figures 20A and 20B, and 21A and 21B illustrate the typical microtubule and intermediate filament arrangement found within normal cells grown in the presence of FBS. In these cells, GFAP immunofluoresence was dispersed in the form of filamentous bundles, arranged in an irregular fashion throughout the cytoplasm (Fig 21A & 21B); whereas β-tubulin staining was concentrated around the nucleus and dispersed in a filamentous form throughout the cytoplasm (Fig 20A & 20B). Serum withdrawal resulted in the alteration of cell morphology from a flat, polygonal shape to a more fibrous, ruffled architecture (Fig 20C & 20D and Fig 21C and 21D), consistent with the findings by Moonen G et al. (1975). However, this alteration in cell morphology was prevented by the presence of recombinant Reelin (Fig 20E, 20F & Fig

## Figure 20: Recombinant Reelin Helps to Maintain NT2/A Protoplasmic Morphology

Pure fifteen week old NT2/A grown in 6-well poly-D-lysine coated plates were pre-washed twice in PBS then treated for 72 hours with the following: 2 ml of SFM supplemented with 5% heat-inactivated FBS (Control, A & B); 2 ml of SFM (Serum Free Media, C & D) or with 2 ml of SFM supplemented with 75 µl of 293 medium containing recombinant reelin (Reelin Treated, E & F), which was added fresh daily. Following the 72-hour incubation at 37°C, cells were fixed and immunostained for the microtubule protein β-Tubulin, with a mouse monoclonal anti-β-Tubulin primary antibody (A, B, C, D, E, & F). Shown also are phase-contrast micrographs (A′- F′). Immunohistochemistry was performed as described in materials and methods and Rhodamine (red) conjugated secondary antibodies were used. Representative images are shown from triplicate results. Magnification x200 for A, C, & E; x400 for B, D, & F.

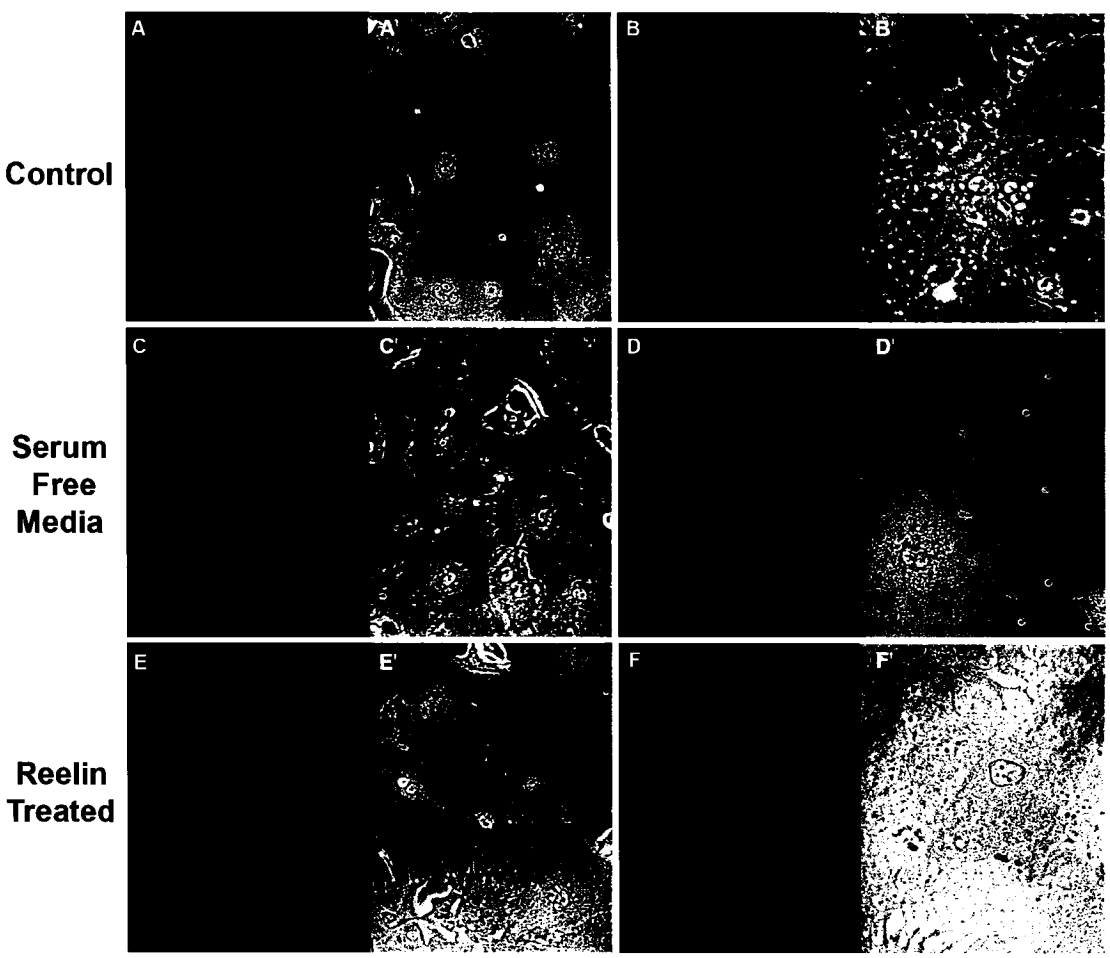
Control
Serum Free Media
Reelin Treated
A
A'
B
B'
C
C'
D
D'
E
E'
F
F'

## Figure 21: Recombinant Reelin Minimizes the Effects of SFM on NT2/A Cells

Pure fifteen week old NT2/A grown in 6-well poly-D-lysine coated plates were pre-washed twice in PBS then treated for 72 hours with the following: 2 ml of SFM supplemented with 5% heat-inactivated FBS (Control, A & B); 2 ml of SFM (Serum Free Media, C & D) or with 2 ml of SFM supplemented with 75 µl of 293 medium containing recombinant reelin (Reelin Treated, E & F) which was added fresh daily. Following the 72-hour incubation at 37°C, cells were fixed and immunostained for the intermediate filament protein GFAP, with a mouse monoclonal anti-GFAP primary antibody (A, B, C, D, E, & F); or as a control they were treated with 10% horse serum instead of with a primary antibody (G). Shown also are phase-contrast micrographs (A′-G′). Immunohistochemistry was performed as described in material and methods, and Alexa 488 (green) conjugated secondary antibodies were used. Representative images are shown from triplicate results. Magnification x200 for A, C, E, G; x400 for B, D, & F.

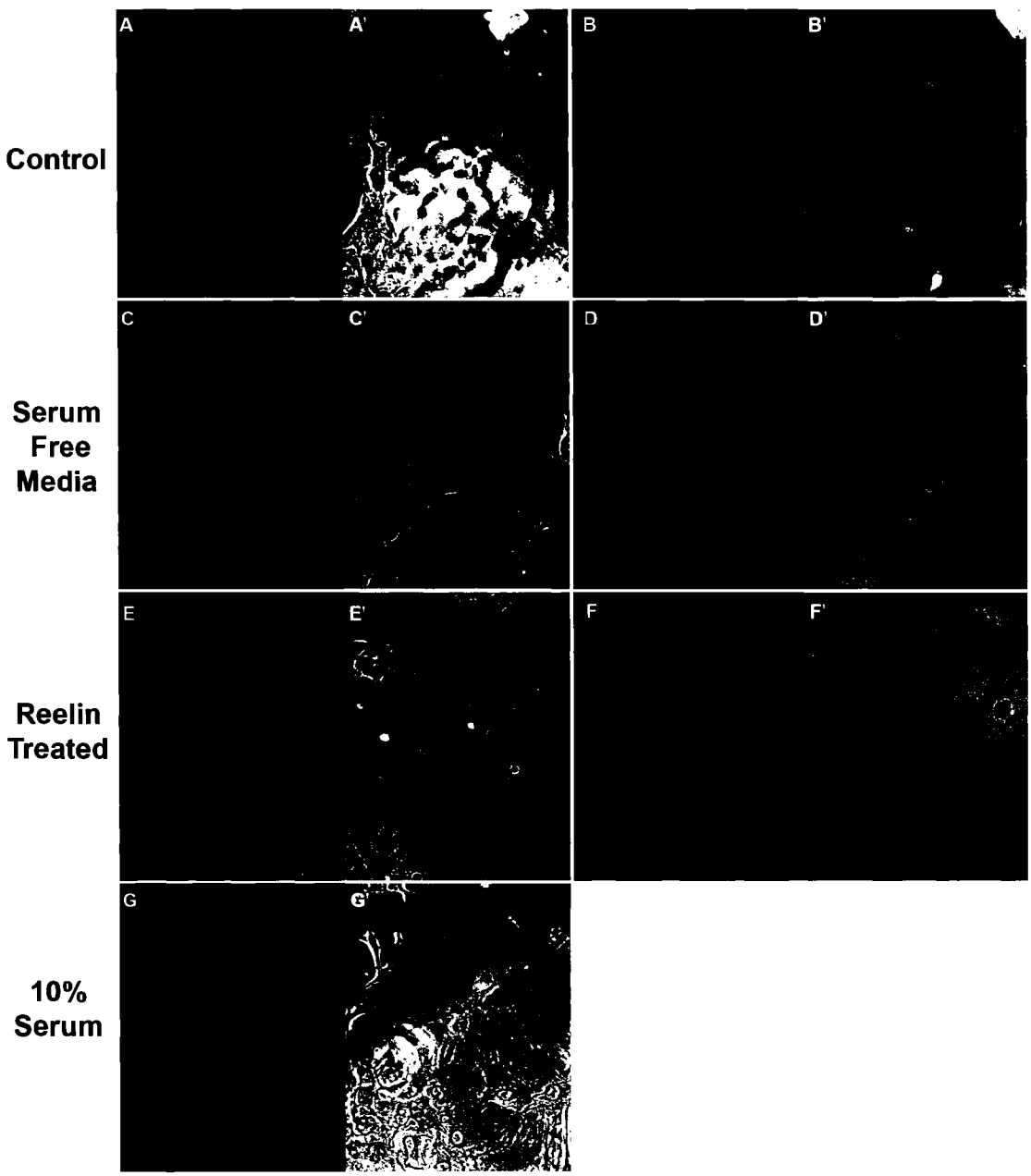
Control
Serum Free Media
Reelin Treated
10% Serum
A
A'
B
B'
C
C'
D
D'
E
E'
F
F'
G
G'

21E & 21F), which appeared to maintain normal cell morphology. Supportive of these findings, a recent study by Ramakers GJ & Moolenaar WH (1998) established that the blood borne mitogen lysophosphatidic acid could also cause the rapid reversal of astrocyte stellation through the activation of the small GTP- binding protein RhoA, a possible target of Reelin signalling. It was interesting to note that the microtubule networks within astrocytes grown in serum-free conditions adopted a tightly packed filamentous conformation that orientated itself along the cell process axis (Fig 20C & 20D); such tightly packed filamentous forms were not observed in control cells (Fig 20A & 20B) nor in Reelin treated cells (Fig 20E & 20F). To quantitate this, ten random cell counts were performed for each of the experimental conditions described and then were analyzed in a one-way ANOVA, followed by the Tukey Test to establish the statistical significance of the differences between the ratios of flat to ruffled cells amongst treatment groups. There were no significant differences between control (95% flat to 5% ruffled) and Reelin treated cells (80% flat to 20% ruffled) (Fig 22), however, a significant difference was found between control cells and serum deprived cells (28% flat to 72% ruffled) ($P< 0.01$), and between Reelin treated cells and serum deprived cells (Fig 20) ($P< 0.01$). To confirm that the observed change in cell morphology was not due to impending cell death, the Carboxyfluorescein diacetate (CFDA)/ propidium iodide (PI) cell viability assay was performed on cells subjected to identical experimental conditions. None of the astrocytes were observed to take up the PI dye (Fig 23) and thus we concluded that the observed change in astrocytic morphology was due, in part, to alterations of the astrocytic cytoskeleton, rather than due to cellular injury, presaging cellular death. These results

## Figure 22: Recombinant Reelin Reduces Membrane Ruffling in NT2/A Cells in Response to SFM

Ten counts were taken for each treatment condition and each count was of ~ 200 cells total. The ratio of flat to ruffled was determined for each cell count and was expressed as a ratio. Treatment 1 represents SFM treated cells, Treatment 2 represents cells treated with SFM supplemented with recombinant reelin enriched 293 cell media, and Treatment 3 represents control treated cells. The ratio of the number of flat to ruffled cells within each treatment group was counted. The average of the mean ratios (Y-axis) was plotted against treatment conditions (x-axis). The bar represents mean values ± Standard Error of the Means. According to the Tukey Test, there is no significant difference between control cells and cells treated with recombinant reelin ($P > 0.5$); however, there is a significant difference between control cells and cells treated with SFM ($P < .01$), and a significant difference was found between cells treated with recombinant reelin and cells treated with SFM ($P < .01$).

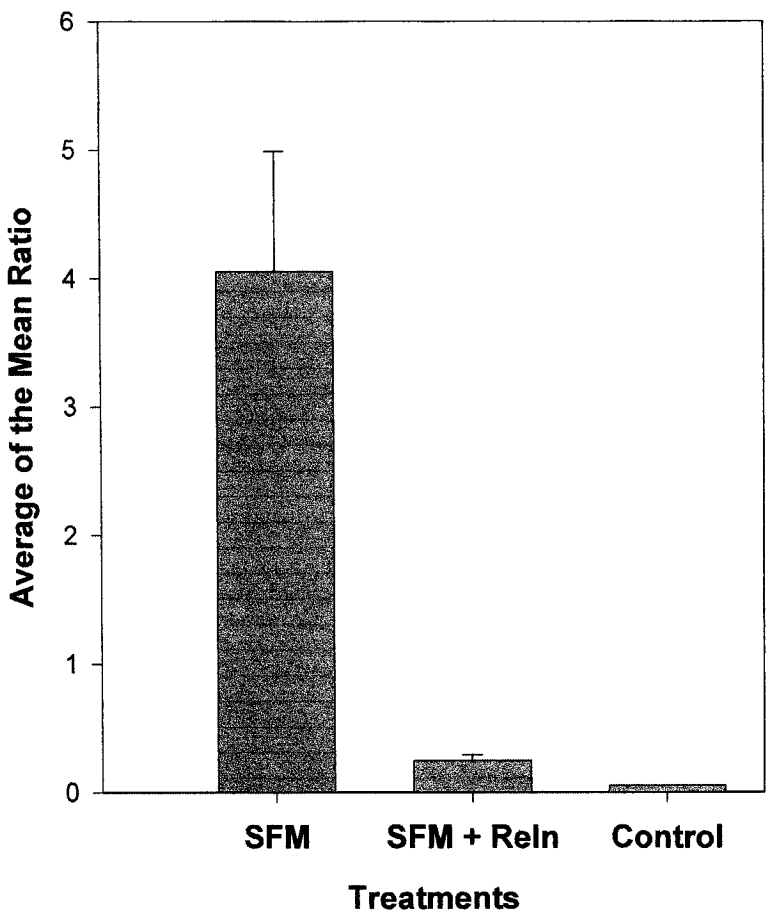
6
5
4
3
2
1
0
Average of the Mean Ratio
SFM
SFM + Reln
Control
Treatments

## Figure 23: SFM Induces Membrane Ruffling, Not Cell Death in NT2/A

Pure fifteen week old NT2/A grown in 6-well poly-D-lysine coated plates were pre-washed twice in PBS then treated for 72 hours with the following: 2 ml of SFM supplemented with 5% heat-inactivated FBS (Control, A & A′); 2 ml of SFM (Serum Free Media, B & B′); or with 2 ml of SFM supplemented with 75 µl of 293 medium containing recombinant reelin (Reelin Treated, C & C′), which was added fresh daily. Following the 72-hour incubation at 37°C, cells were used in the CFDA/PI viability assay as described in material and methods. Fluorescent cells were viewed within a 30-minute time frame, with the Axiovert 220M fluorescence microscope. Representative images are shown from triplicate results. Magnification x200 for A, B C; x400 for A′, B′, & C′.

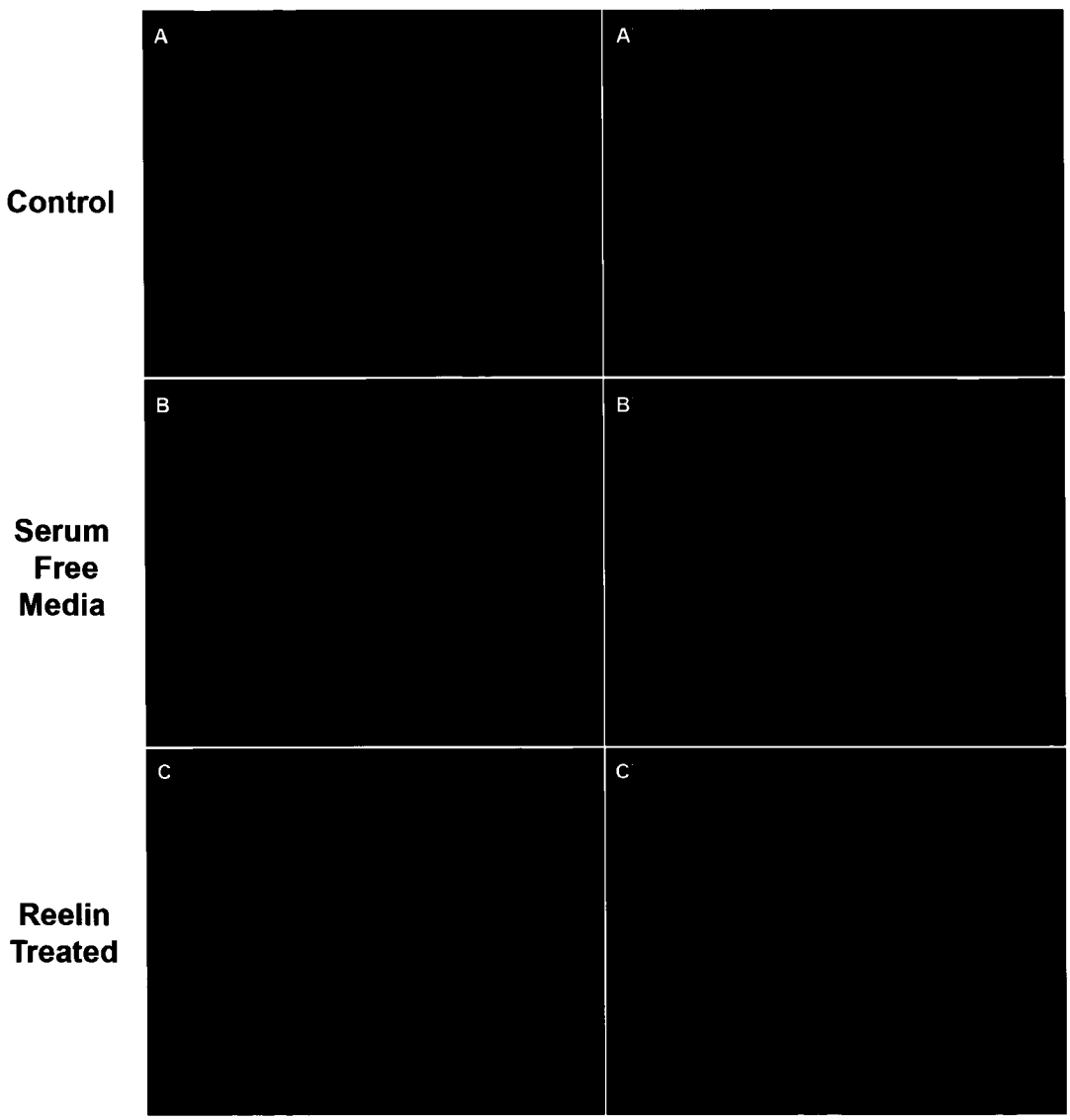
A
A
Control
B
B
Serum
Free
Media
C
C
Reelin
Treated

support a model in which Reelin signalling via the lipoprotein receptors triggers Dab1 phosphorylation, resulting in the maintenance of a flat, polygonal morphology in NT2/A.

# 4.0 Discussion

## 4.1 Key Findings

Reelin is a secreted glycoprotein that has been shown to signal via the lipoprotein receptors ApoER2 and VLDLR to induce the phosphorylation of Dab1 on tyrosyl residues 198 and 220 in primary mouse neuronal cultures (Rice DS et al. 1998; Trommsdorff M et al. 1999; Keshvara L et al. 2001). Recently, the Reelin signalling machinery has been identified within radial glial cells during development (Forster E et al. 2002; Luque JM et al. 2003). However, to date there has been no studies showing the presence of Reelin and downstream signalling components in astrocytes of the adult brain. Using a combination of molecular and cell biology techniques, RT-PCR, immunoblotting and immunohistochemistry, the presence of Reelin (Fig 8), its receptors (Fig 9, Fig 13& Fig 14) and downstream signalling component Dab1 (Fig 16 & Fig 17) have been established in mature NT2/A. Furthermore, a functional Reelin signalling pathway has been established in cells treated with recombinant Reelin (Fig 18 & Fig 19), with the subsequent tyrosyl phosphorylation of Dab1 on residues 198 and 220. In order to investigate the significance of Reelin signalling within this system, experiments were carried out to evaluate the cytoskeletal response of NT2/A cells exposed to SFM or SFM supplemented with recombinant Reelin (Fig 20 & Fig 21). These results established that the presence of Reelin significantly reduced the degree of membrane ruffling incurred by exposure to SFM (Fig 22).

All experiments were carried out on Human neurons and astrocytes derived from NT2/D1 cells. The NT2/D1 precursor cells have been shown to undergo both neuronal and glial differentiation in response to treatment with retinoic acid (Sandhu JK et al. 2002; Bani-Yaghoub M et al. 1999; Andrews PW 1984), producing fully functional

mature, astrocytes (Sandhu JK et al. 2002) and mature, neurons, which are capable of forming functional synapses when grown on a monolayer of NT2/A (Hartley RS et al. 1999). An advantage of this system is that neurons and astrocytes can be propagated and studied independently as pure cultures or as mixed co-cultures. As reported previously (Sandhu JK et al. 2002; Hartley RS et al. 1999), *pure* cultures of NT2/N did not survive more than 8 weeks post-differentiation *in vitro* (Personal observation, data not shown), whereas both NT2- N/A co-cultures and pure NT2/A cultures were perfectly viable and could be maintained *in vitro* for up to 30 weeks (Personal observation, data not shown).

Pure glial and neuronal cultures were used to determine the specificity of ApoER2 splicing variants per cell type (Fig 9 & Fig 11). However, since pure NT2/N cannot survive for very long in an *in vitro* environment without the presence of astrocytes, neurons were harvested from NT2 co-cultures and used as the source of neuronal protein and mRNA for all other experiments. Pure NT2/A cultures were used as the source of glial protein and mRNA for all experiments. These cells were easily identified by light microscopy (Fig 5C & 5C′) from NT2 co-cultures (Fig 5D & 5D′). Since synaptic connections between NT2/N were first detected after 4 weeks of maturation (within NT2 co-cultures), further increasing by 8 weeks of maturation (Hartley RS et al. 1999), we used fully matured, 15 week old NT2\N cells. Fifteen week old astrocytes were stained with the glial markers- glutamine synthase, GFAP, and vimentin (Fig 6) to confirm their identity and, similarly, neurons from NT2 co-cultures were characterized by staining with the neuron-specific marker MAP 2a + 2b (Fig 7). As such, this cell model system appears to replicate the development process occurring *in vivo* and to produce fully functional cells.

## 4.2 Reelin Signalling in Radial Glia and in Adult Brain

### 4.2(a) Reelin in Radial Glia

To date there have been no studies that have investigated the role of the Reelin signalling pathway in astrocytes of the adult brain. All studies have focused on either neurons or radial glial cells of the developing brain and neurons of the adult brain. In the developing brain, Forster E et al. (2002) were the first to show that the neuronal migration defects observed in the dentate gyrus of *reeler* and *scrambler/yotari* mutants are caused, in part, by malformations of the radial glial scaffold. This phenotype was assumed to be due to defective Reeling signalling in neurons. Subsequently, in 2003, a study by Luque JM et al. (2003) established, by double-labelling immunofluoresence experiments, the presence of the Reelin receptor machinery, including lipoprotein receptors ApoER2 and VLDLR along with cytoplasmic adaptor protein Dab1, in radial glial precursors, as well as in postmitotic neurons during cortical development. Thus, Reelins effects are not neuron-specific since it is capable of binding to receptors on target radial glial cells and that the subsequent downstream signalling was required for proper glial morphology and biochemical maturation during development (Weiss KH et al. 2003). Our observations are consistent with this study that the receptors are expressed throughout development and in mature cells (Fig 10 & Fig 12).

### 4.2(b) Reelin Pathway in Adult Astrocytes

We have shown for the first time that NT2/A and neurons are both capable of producing and secreting the 400 kDa glycoprotein Reelin and its various processed products (Fig 8) after 15 weeks of maturation. Furthermore, RT-PCR analysis has revealed that NT2/A contain transcripts for three of Reelins receptors ApoER2, VLDLR

(Trommsdorff M et al. 1999) and α3β1-integrin (Dulabon L et al. 2000) (Fig 9). Reelins receptors have previously been characterized in neurons only (Trommsdorff M et al. 1999; Dulabon L et al. 2000; & Senzaki K et al. 1999), but to date there have been no studies showing their expression in astrocytes of the adult brain. In addition, the RT-PCR study demonstrated the presence of alternatively spliced transcripts of the ApoER2 gene in the NT2 cell model system (Fig 10-12), consistent with the current literature (Brandes C et al. 1997; Korschineck I et al. 2001; & Kim DH et al. 1996).

Initially we performed a time-course experiment to determine whether there was any variation in splicing patterns across NT2 differentiation (Fig 10), since RA first induces the transient formation of radial glia (Walker et al. 2004) and subsequently neurons and astrocytes within the first few weeks of treatment (Sandhu et al. 2002; Andrews PW 1984). The results showed that the expression of the ApoER2 transcripts was fairly consistent throughout the time course of NT2 differentiation, but for two exceptions. Firstly, the ApoER2- Ex15/18 primers generated a 382 base pair variant (lacking both exon 15 and exon 18) in the undifferentiated cells, which disappeared over the course of development (Fig 10) and secondly, a similar pattern of expression was observed in NT2/A using the ApoER2- Ex6a/18 primers, which generated a 1,530 bp fragment (Fig 12). Significantly, the 102 bp variant of ApoER2, containing the consensus site for furin cleavage, appeared to be exclusively expressed in the astrocyte, and not in neuronal cultures (Fig 11 & Fig 12). Furin cleavage of this splice variant results in the secretion of a soluble fragment consisting of the entire ligand-binding domain of ApoER2 (Koch S et al. 2002). This variant transcript was translated and the soluble fragment was secreted exclusively in the media of NT2/A (Fig 15). We also

established that the other variants, observed at the transcriptional level, carried through to the protein level (Fig 13). Thus, there was one main variant of the receptor expressed in undifferentiated cells, at least 3 different proteins expressed by NT2/A over the period of maturation (protein extracted at 1, 2, 5, 10, & 15 weeks) and 2 variants were expressed by NT2/N. From these results, we concluded that Reelin and 3 different splicing variants of ApoER2 are actively transcribed and expressed in mature NT2/A.

Dab1 is a crucial component of the Reelin/ApoER2 signalling pathway (Trommsdorff M et al. 1999) and we observed that the cytosolic adaptor protein Dab1 was not only transcribed and abundantly expressed within NT2/A (Fig 16 & Fig 17), but we also found Dab1 to be actively phosphorylated on tyrosyl residues 198 (Fig 18) and 220 (Fig 19) in response to the Reelin signal. Thus our results have clearly demonstrated Reelin and ApoER2, along with the downstream effecter molecule Dab1 to be present and functional within NT2/A. It appears that Reelin in addition to having an effect upon glial cells during development also has an effect upon the morphology of mature NT2/A (Fig 20 & Fig 21).

### 4.2(c) Secretion of Dominant Negative Receptor Fragment

The functional significance of the ability of astrocytes to secrete the soluble-fragment, which acts as a dominant negative inhibitor of Reelin binding (Koch S et al. 2002) remains to be establish. However, since NT2/A appear to produce and secrete this soluble fragment (Fig 12 & Fig 15), it is tempting to speculate that it could modulate the effects of Reelin upon neurons, thereby negatively regulating Reelin signalling within the NT2 cell model system and possibly in the brain. This soluble, secreted fragment has been shown to actively inhibit Reelin-induced Dab1 phosphorylation in addition to

abolishing the background phosphorylation of Dab1 seen in non-stimulated neurons (Koch S et al. 2002), suggesting that this fragment mimics the effects of the Receptor Associated Protein (RAP, a high affinity ligand for the LDL receptor family) in a neuronal cell model system. Our finding of this secreted fragment in the media of NT2/A and not NT2/N (Fig 15 A) is a novel finding that suggests that ApoER2 expressing astrocytes might play a far more complex role in modulating Reelin signalling than previously thought possible.

## 4.3 Possible Roles of Reelin in the Adult Brain

### 4.3(a) Dendritic Outgrowth

The existence and function of Reelin in the adult brain wasn't discovered until a study by Martinez-Cerdeno V et al. (2002) established that substantial amounts of Reelin protein and mRNA are present in the brains of adult rodents (Martinez-Cerdeno V et al. 2002). After birth, reelin and its signalling molecules continue to be expressed in hippocampal pyramidal and interneurons of the mature human cortex (Deguchi K et al. 2003). A study by Niu S et al 2004, clearly showed that Reelin regulates the length and complexity of dendrites of hippocampal neurons through the activation of the ApoER2/VLDLR/Dab1 signalling pathway in the adult brain, in a SFK dependent manner.

### 4.3(b) Long Term Potentiation

A study by Weeber EJ et al. (2002) further investigated the functional significance of Reelin and its receptors ApoER2 and VLDLR at the physiological level in

the adult mouse brain. They used an associative fear-conditioned learning paradigm to evaluate both short and long term memory in knockout animals. These studies demonstrated that baseline synaptic transmission at Schaffer collateral synapses was not affected, since the input-output functions for the stimulation of the CA1 area did not vary between wild type (WT) and knockout mice. The lack of receptors also did not affect paired pulse facilitation, which is a form of short-term synaptic plasticity. However, LTP induction was completely blocked by the Receptor Associated Protein (RAP, a 39-kDa protein that can bind to members of the LDL receptor family and subsequently inhibit the binding and uptake of the receptors' ligands (Herz J et al. 1991)), in WT mice suggesting that these receptors may play a role in modulating the synaptic plasticity that underlies long-term hippocampus-dependent associative learning. To examine the effects of Reelin on LTP induction, hippocampal slices were perfused with either recombinant Reelin or control medium prior to LTP induction. Reelin significantly augmented LTP induction in the slices, whereas the ablation of either of Reelin's receptors abrogated this LTP-inducing affect of Reelin. Based on these findings, Weeber EJ et al. (2002) proposed that Reelin plays a direct role in the modulation of synaptic plasticity in the adult brain and that these affects upon synaptic plasticity are most likely to be mediated through an NMDA dependent mechanism.

These findings clearly identified Reelin as a key player in facilitating LTP in the hippocampus of the adult brain. Subsequently, Beffert U et al. (2004) analyzed the consequences of mutants harbouring compound genetic disruptions involving components of either the Reelin or Cdk-5 (cyclin-dependent kinase 5) signalling pathways on the modulation of synaptic transmission. Cdk-5 is a homologue of the

cyclin-dependent kinase family of seronine/threonine kinases and is regulated by the activators p35 and p39, which are both expressed exclusively in the brain (Tsai LH et al. 1994; Lew J et al. 1994). Like *reeler* mutants, Cdk-5 deficient mice have neuronal migration abnormalities, producing a phenotype that includes an inverted cortical plate and abnormal cell positioning in the hippocampus and the cerebellum (Oshima T et al. 1996). Beffert U et al. (2004) demonstrated that in ApoER2, VLDLR, p35 and p39 deficient mice Reelin-dependent LTP enhancement was completely abolished (Beffert et al. 2004), even though the overall machinery necessary for LTP induction remained intact in these animals. These findings suggested that the modulation of synaptic plasticity in the hippocampus by Reelin is dependent upon the Reelin receptors ApoER2 and VLDLR and it relies on the Cdk-5 activators p35 and p39.

There is an emerging view that astrocytes play a role in facilitating LTP in the hippocampus. Recent advancements in the field of glial research have shown that the glutamate released from astrocytes has the ability to activate extrasynaptic NMDA receptors of hippocampal pyramidal neurons (Araque A et al. 1998). Furthermore the calcium-binding synaptotagmin membrane protein *Syts IV* has been found to act as a calcium sensor required for glutamate release in astrocytes, with *syt4* knockout mice displaying a deficit in hippocampal based memory. Since it has been established that LTP is strongly inhibited in *reeler* adults, and that Reelin is required to maintain a proper radial glial scaffold during neuronal development, it is tempting to speculate that in the adult brain a change in astrocytic morphology could contribute to the loss of synaptic plasticity seen in *reeler* and *yotari/scrambler* mice. Since astrocytes play a prominent role in the modulation of neuronal communication (Piet R et al. 2004), and are capable of

acting as a third partner in synaptic transmission, it is not inconceivable that a change in astrocytic morphology, due to reduced Reelin signalling could alter the dynamics of synaptic transmission in the adult brain. Further studies will be needed to investigate whether the loss of LTP seen in *reeler* and *yotari/scrambler* mice is indeed due to alteration of astrocytic morphology in the adult brain. In light of recent studies, which have identified the importance of astrocytes in the modulation of synaptic transmission, our findings would be consistent with a model in which the secreted glycoprotein Reelin is required in NT2/A to help maintain correct astrocytic morphology at the synapse.

## 4.4 Role of Astrocytes in Synaptic Transmission

Astrocytes have previously been thought to play a supportive role within the CNS, to regulate and optimize the environment within which neurons function. As such, astrocytes actively remove neurotransmitters released during synaptic transmission, in addition to neuronal waste and metabolic by-products (Nedergaard M et al. 2003). Astrocytes are also responsible for delivering glucose and metabolic substrates to neurons and for maintaining tight control of local ion and pH homeostasis (Nedergaard M et al. 2003). However, over the past decade astrocytes have been shown to play key roles in the modulation of synaptic transmission and have been shown to respond to the synaptic release of neurotransmitter with elevations in the intracellular $Ca^{2+}$ concentration ($[Ca^{2+}]_i$) (Porter JT & McCarthy KD 1996). A turning point in glial cell research came with the discovery that cultured astrocytes in response to elevated $[Ca^{2+}]_i$ release gliotransmitters that can directly stimulate the postsynaptic neuron and can feed back onto the presynaptic terminal either to enhance or to depress further release of neurotransmitter (Newman EA

2003). This release of gliotransmitters is an important means by which glia can modulate the release of neurotransmitters from presynaptic terminals. It has recently been proposed that astrocytes could act as a detector of neuronal activity, since they are capable of responding differently to high and low levels of synaptic activity (Fellin T & Carmignoto G 2004). The authors suggest the following model, whereby "low synaptic activity triggers $[Ca^{2+}]_i$, elevations which remain restricted to activated astrocyte processes. This short-distance message evokes a calcium dependent release of neuroactive agents that may work as a feedback mechanism to locally affect neuronal transmission. Whereas high neuronal activity triggers a calcium signal that propagates to other processes and possibly to other astrocytes. This long-distance message works as a feed-forward mechanism to transfer information on neuronal activity to other cells remote from the initial site of activation at the astrocyte process"(Fellin T & Carmignoto G 2004). Thus, astrocytes are starting to emerge as an integral unit with neurons, that plays a distinctive role in brain function.

## 4.5 Astrocyte Morphology in the Adult Brain

We have demonstrated that membrane ruffling triggered by SFM in NT2/A can be significantly reduced by the presence of recombinant Reelin in culture (Fig 20-22). Thus the secreted glycoprotein Reelin appears to play a role in the determination of astrocyte morphology. Reelin is not the first molecule that has been observed to play a role in the regulation of astrocyte morphology. Studies by Ramakers GJ & Moolenaar WH (1998), and Goldman JE & Chiu FC (1984) have shown that certain factors, such as the mitogenic factor lysophosphatidic acid (LPA) as well as cAMP-raising agents such as

forskolin, can either induce or rapidly reverse astrocyte stellation in an *in vitro* environment. Treatment of pure rat glial cultures with LPA resulted in the reversal of cAMP-induced stellation through a RhoA mediated signalling pathway (Ramakers GJ & Moolenaar WH 1998). Furthermore, these findings supported a model in which basal RhoA activity was necessary to maintain cytoskeletal 'tension', in addition to glial morphology. RhoA is a member of the Ras homology family of small GTPases, which cycle from their active (GTP-bound) to their inactive (GDP-bound) conformation by hydrolyzing GTP to GDP. Specific guanine exchange factors (GEFs) reactivate the GTPases by catalyzing the replacement of GDP with a new GTP.

A connection between Reelin and RhoA signalling has been established by Stockinger W et al. (2000) who studied the molecular mechanism of Reelin mediated activation of RhoA. They demonstrated that the 59 amino acid insertion (encoded by exon 18) in the cytoplasmic tail of ApoER2 interacts with the JNK (c-Jun $NH_2$-terminal kinase)-interacting proteins, JIP-1 and JIP-2, both of which are members of the JIP group of mitogen-activated protein kinase scaffolding proteins (Yasuda J et al. 1999). JIP-1 has been shown to interact with RhoGEF, an exchange factor for the small GTPase RhoA (Meyer D et al. 1999). Thus, it is plausible that Reelin signalling via the ApoER2 receptor could activate JIP1 proteins, and in turn RhoGEF, which could then directly link the Reelin signalling to a RhoA dependent pathway involved in the organization of the cytoskeleton (Fig 2). If, on the other hand, the observed morphological changes in NT2/A are dependent upon a Reelin/Dab1 signalling pathway, then it is most likely to be transmitted via the Dab1- Src - PI3K and PKB/Akt kinase signalling cascade, which results in the inhibition of GSK-3β and suppresses the phosphorylation of the

microtubule associated protein tau (Beffert U et al 2002). The activation of either pathway can cause alterations to the cells cytoskeleton, and thus either pathway could be responsible for producing the observed morphological changes in NT2/A. Further biochemical studies will be needed in order to elucidate, whether the observed morphological changes in NT2/A is via a Dab1 or RhoA dependent mechanism.

## 4.6 Summary

Taken together our data supports the notion that Reelin signals via the ApoER2 lipoprotein receptor to facilitate Dab1 phosphorylation on tyrosyl residues 198 and 220 in mature human NT2/A (Fig 17 & Fig 18). These results provide direct evidence that in the NT2 cell model system, ApoER2 transcripts are differentially spliced between astrocytes and neurons (Fig 10 & Fig 11). The biological significance of this finding is not presently known, however, it is enticing to speculate that the observed variation found between glial and neuronal cell types could provide a mechanism by which cells can generate alternative intracellular responses to signals propagated by one signalling ligand. It was also interesting to find that mature human NT2/A produce a secreted soluble fragment (Fig 14A & 14B) that has been shown to act as a dominant negative receptor that inhibits Reelin signalling in mouse primary neurons (Koch S et al. 2002). This soluble peptide could provide a way for astrocytes to depress neuronal signalling within a co-culture environment; providing a possible inhibitory role for astrocytes in the Reelin-signalling pathway, within the NT2 cell model system.

Putting all of these findings together, we know Reelin is required in adult brain for the induction of LTP in the hippocampus; we know that astrocytes also play a role in the modulation of synaptic plasticity; we know that there is a functional Reelin signalling

pathway within NT2/A and we know that during development Reelin is required for proper glial morphology and biochemical maturation. In light of these findings it may not be too far fetched to predict that the observed Reelin signalling in astrocytes, via regulation of cell morphology could be a means by which astrocytes modulate synaptic transmission, especially since the geometry of the contact between the neuronal synapse and the astrocytic membrane is such a key factor in determining the shape of action of astrocyte glutamate release (Fellin T & Carmignoto G 2004). Suggestive of such a role for NT2/A in the modulation of LTP via glutamate release, is the findings of a recent study by Sandhu JK et al. (2002), which identified the presence of two functional, sodium dependent glutamate transporters- GLAST/EAAT- 1 (astrocyte specific glutamate and aspartate transporter) and GLT-1/EAAT-1 (glutamate transporter-1), on the surface of NT2/A. This study additionally, demonstrated the presence and functionality of glutamine synthase (an enzyme involved in the conversion of glutamate to glutamine), supportive to the idea that NT2/A can actively uptake and process glutamate, however further studies will be required to determine whether or not NT2/A release glutamate in response to synaptic transmission by NT2/N.

# 5.0 References

## 5.0 References


1. Alcantara S, Ruiz M, D'Arcangelo G, Ezan F, de Lecea L, Curran T, Sotelo C, Soriano E (1998) Regional and cellular patterns of reelin mRNA expression in the forebrain of the developing and adult mouse. Neurosci. 18(19): 7779-7799
2. Andersen OM, Benhayon D, Curran T, Willnow TE (2003) Differential Binding of Ligands to the Apolipoprotein E Receptor 2. Biochem. 42: 9355-9364
3. Andrews PW (1984) Retinoic acid induces neuronal differentiation of a cloned human embryonal carcinoma cell line in vitro. Dev. Biol. 103: 285-293
4. Andrews PW (1984) Retinoic acid induces neuronal differentiation of a cloned human embryonal carcinoma cell line in vitro. Dev Biol. 103(2): 285-293
5. Araque A, Sanzgiri RP, Parpura V, Haydon PG (1998) Calcium elevation in astrocytes causes an NMDA receptor-dependent increase in the frequency of miniature synaptic currents in cultured hippocampal neurons. J Neurosci. 18(17): 6822-6829
6. Arnaud L, Ballif BA, Forster E, Cooper JA (2003) Fyn Tyrosine Kinase is a Critical Regulator of Disabled-1 during Brain Development. Curr. Biol. 13: 9-17
7. Assadi AH, Zhang G, Beffert U, McNeil RS, Renfro AL, Niu S, Quattrocchi CC, Antalffy BA, Sheldon M, Armstrong DD, Wynshaw-Boris A, Herz J, D'Arcangelo G, Clark GD (2003) Interaction of reelin signaling and Lis1 in brain development. Nat Genet. 35(3): 270-276
8. Ballif BA, Arnaud L, Cooper JA (2003) Tyrosine phosphorylation of Disabled-1 is essential for Reelin-stimulated activation of Akt and Src family kinases. Mol. Brain Res. 117: 152-159

9. Bani-Yaghoub M, Felker JM, Naus CC (1999) Human NT2/D1 cells differentiate into functional astrocytes. Neuroreport 10(18): 3843-3846

10. Beffert U, Morfini G, Bock HH, Reyna H, Brady ST, Herz J (2002) reelin-mediated Signalling Locally Regulates Protein Kinase B/Akt and Glycogen Synthase Kinase 3β. JBC 277 (51): 49958-49964

11. Beffert U, Weeber EJ, Morfini G, Ko J, Brady ST, Tsai LH, Sweatt D, Herz J (2004) Reelin and Cyclin-Dependent Kinase 5-Dependent Signals Cooperate in Regulating Neuronal Migration and Synaptic Transmission. J of Neurosci. 24 (8): 1897-1906

12. Benhayon D, Magdaleno S, Curran T (2003) Binding of purified reelin to ApoER2 and VLDLR mediates tyrosine phosphorylation of Disabled-1. Mol. Brain Res. 112: 33-45

13. Bock HH, Herz J (2003) Reelin Activates Src Family Tyrosine Kinases in Neurons. Curr. Biol. 13: 18-26

14. Bock HH, Jossin Y, Bergner O, Herz J (2004) Apolipoprotein E receptors are required for Reelin-induced proteasomal defradation of the neuronal adaptor protein Disabled-1. JBC. E-PUB, Manuscript M401770200

15. Bock HH, Jossin Y, Liu P, Forster E, May P, Goffinet AM, Herz J (2003a) Phosphatidylinositol 3-kinase interacts with the adaptor protein Dab1 in response to Reelin signaling and is required for normal cortical lamination. JBC 278(40): 38772-38779

16. Bologa L, Cole R, Chiappelli F, Saneto RP, De Vellis J (1988) Expression of glial fibrillary acidic protein by differentiated astrocytes is regulated by serum antagonistic factors. Brain Res. 457(2): 295-302

17. Bradford MM (1976) A rapid and sensitive method for the quantitation of microgram quantities of protein utilizing the principle of protein-dye binding. Anal Biochem. 72: 248-254

18. Brandes C, Novak S, Stockinger W, Herz J, Schneider WJ, Nimpf J (1997) Avian and murine LR8B and human apolipoprotein E receptor 2: differentially spliced products from corresponding genes. Genomics 42(2): 185-191

19. Brich J, Shie FS, Howell BW, Li R, Tus K, Wakeland EK, Jin LW, Mumby M, Churchill G, Herz J, Cooper JA (2003) Genetic Modulation of Tau Phosphorylation in the Mouse. J of Neurosci. 23 (1): 187-192

20. Cantley LC (2002) The phosphoinositide 3-kinase pathway. Science 296(5573): 1655-1657

21. Caviness VS Jr, Rakic P (1978) Mechanisms of cortical development: a view from mutations in mice. Annu Rev Neurosci.1: 297-326

22. Ciesielski-Treska J, Bader MF, Aunis D (1982) Microtubular organization in flat epitheloid and stellate process-bearing astrocytes in culture. Neurochem Res. 7(3): 275-286

23. Compton SJ, Jones CG (1985) Mechanism of dye response and interference in the Bradford protein assay. Anal Biochem. 151(2): 369-374

24. Curran T, D'Arcangelo G, Goffinet A (1995) Reeler gene discrepancies. Nat Genet. 11(1): 12-13

25. D'Arcangelo G, Homayouni R, Keshvara L, Rice DS, Sheldon M, Curran T (1999) Reelin is a ligand for lipoprotein receptors. Neuron 24(2): 471-479

26. D'Arcangelo G, Miao GG, Chen SC, Soares HD, Morgan JI, Curran T (1995) A protein related to extracellular matrix proteins deleted in the mouse mutant reeler. Nat. 74(6524): 719-723

27. D'Arcangelo G, Nakajima K, Miyata T, Ogawa M, Mikoshiba K, Curran T (1997) Reelin is a secreted glycoprotein recognized by the CR-50 monoclonal antibody. J Neurosci. 17(1): 23-31

28. Deguchi K, Inoue K, Avila WE, Lopez-Terrada D, Antalffy BA, Quattrocchi CC, Sheldon M, Mikoshiba K, D'Arcangelo G, Armstrong DL (2003) Reelin and disabled-1 expression in developing and mature human cortical neurons. J Neuropathol Exp Neurol. 62(6): 676-684

29. DeSilva U, D'Arcangelo G, Braden VV, Chen J, Miao GG, Curran T, Green ED (1997) The human reelin gene: isolation, sequencing, and mapping on chromosome 7. Genome Res. 7(2): 157-164

30. Drakew A, Deller T, Heimrich B, Gebhardt C, Del Turco D, Tielsch A, Forster E, Herz J, Frotscher M (2002) Dentate Granule Cells in Reeler Mutants and VLDLR and ApoER2 Knockout Mice. Exp. Neurol. 176: 12-24

31. Dulabon L, Olson EC, Taglienti MG, Eisenhuth S, McGrath B, Walsh CA, Kreidberg JA, Anton ES (2000) Reelin binds alpha3beta1 integrin and inhibits neuronal migration. Neuron 27(1): 33-44

32. Falconer DS (1952) A totally sex-linked gene in the house mouse. J Genet. 50: 192-201

33. Fellin T, Carmignoto G (2004) Neurone-to-astrocyte signalling in the brain represents a distinct multifunctional unit. J Physiol. 559(Pt 1): 3-15

34. Forster E, Tielsch A, Saum B, Weiss KH, Johanssen C, Graus-Porta D, Muller U, Frotscher M (2002) Reelin, Disabled 1, and beta 1 integrins are required for the formation of the radial glial scaffold in the hippocampus. PNAS 99(20): 13178-13183

35. Frotscher M, Haas CA, Forster E (2003) Reelin controls granule cell migration in the dentate gyrus by acting on the radial glial scaffold. Cereb Cortex. 13(6): 634-640

36. Goetschy JF, Ulrich G, Aunis D, Ciesielski-Treska J (1986) The organization and solubility properties of intermediate filaments and microtubules of cortical astrocytes in culture. J of Neruocyt. 15: 375-387

37. Goldman JE, Chiu FC (1984) Dibutyryl cyclic AMP causes intermediate filament accumulation and actin reorganization in astrocytes. Brain Res. 306(1-2): 85-95

38. Gotthardt M, Trommsdorff M, Nevitt MF, Shelton J, Richardson JA, Stockinger W, Nimpf J, Herz J (2000) Interactions of the low density lipoprotein receptor gene family with cytosolic adaptor and scaffold proteins suggest diverse biological functions in cellular communication and signal transduction. JBC 275(33): 25616-25624

39. Gotthardt M, Trommsdorff M, Nevitt MF, Shelton J, Richardson JA, Stockinger W, Nimpf J, Herz J (2000) Interactions of the low density lipoprotein receptor gene family with cytosolic adaptor and scaffold proteins suggest diverse

biological functions in cellular communication and signal transduction. J BC 275(33): 25616-25624

40. Grant SG, O'Dell TJ, Karl KA, Stein PL, Soriano P, Kandel ER (1992) Impaired long-term potentiation, spatial learning, and hippocampal development in fyn mutant mice. Science 258(5090): 1903-1910

41. Hartfuss E, Forster E, Bock HH, Hack MA, Leprince P, Luque JM, Herz J, Frotscher M, Gotz M (2003) Reelin signaling directly affects radial glia morphology and biochemical maturation. Develop. 130(19): 4597-4609

42. Hartley RS, Margulis M, Fishman PS, Lee VM, Tang CM (1999) Functional synapses are formed between human NTera2 (NT2N, hNT) neurons grown on astrocytes. J Comp Neurol. 407(1): 1-10

43. Herz J, Beffert U (2000) Apolipoprotein E receptors: linking brain development and Alzheimer's disease. Nat Rev Neurosci. 1(1): 51-58

44. Herz J, Goldstein JL, Strickland DK, Ho YK, Brown MS (1991) 39-kDa protein modulates binding of ligands to low density lipoprotein receptor-related protein/alpha 2-macroglobulin receptor. JBC 266(31): 21232-21238

45. Herz J, Gotthardt M, Willnow TE (2000) Cellular signalling by lipoprotein receptors. Curr Opin Lipidol. 11(2): 161-166

46. Herz J, Hamann U, Rogne S, Myklebost O, Gausepohl H, Stanley KK (1988) Surface location and high affinity for calcium of a 500-kd liver membrane protein closely related to the LDL-receptor suggest a physiological role as lipoprotein receptor. EMBO J. 7(13): 4119-4127

47. Hiesberger T, Trommsdorff M, Howell BW, Goffinet A, Mumby MC, Cooper JA, Herz J (1999) Direct Binding of reelin to VLDL Receptor and ApoE Receptor 2 Induces Tyrosine Phosphorylation of Disabled-1 and Modulates Tau Phosphorylation. Neuron 24: 481-489

48. Hirotsune S, Fleck MW, Gambello MJ, Bix GJ, Chen A, Clark GD, Ledbetter DH, McBain CJ, Wynshaw-Boris A (1998) Graded reduction of Pafah1b1 (Lis1) activity results in neuronal migration defects and early embryonic lethality. Nat Genet. 19(4): 333-339

49. Howell BW, Gertler FB, Cooper JA (1997) Mouse disabled (mDab1): a Src binding protein implicated in neuronal development. EMBO J. 16(1): 121-132

50. Howell BW, Hawkes R, Soriano P, Cooper JA (1997a) Neuronal position in the developing brain is regulated by mouse disabled-1. Nature 389(6652): 733-737

51. Howell BW, Herrick TM, Hildebrand JD, Zhang Y, Cooper JA (2000) Dab 1 tyrosine phosphorylation sites relay positional signals during mouse brain development. Curr. Biol. 10: 877-885

52. Howell BW, Lanier LM, Frank R, Gertler FB, Cooper JA (1999) The Disabled 1 Phosphotyrosine-Binding Domain Binds to the Internalization Signals of Transmembrane Glycoproteins and to Phospholipids. Mol. Cell. Bio. 19 (7): 5179-5188

53. Ihara K, Muraguchi S, Kato M, Shimizu T, Shirakawa M, Kuroda S, Kaibuchi K, Hakoshima T (1998) Crystal structure of human RhoA in a dominantly active form complexed with a GTP analogue. JBC 273(16): 9656-66

54. Ikeda Y, Terashima T (1997) Expression of reelin, the gene responsible for the reeler mutation, in embryonic development and adulthood in the mouse. Dev Dyn. 210(2): 157-172

55. Jossin Y, Ignatova N, Hiesberger T, Herz J, Lambert de Rouvroit C, Goffinet AM (2004) The central fragment of Reelin, generated by proteolytic processing in vivo, is critical to its function during cortical plate development. J Neurosci. 24(2): 514-521

56. Kim DH, Iijima H, Goto K, Sakai J, Ishii H, Kim HJ, Suzuki H, Kondo H, Saeki S, Yamamoto T (1996) Human Apolipoprotein E Receptor 2. JBC 271(14): 8373-8380

57. Kim DH, Magoori K, Inoue TR, Mao CC, Kim HJ, Suzuki H, Fujita T, Endo Y, Saeki S, Yamamoto TT (1997) Exon/intron organization, chromosome localization, alternative splicing, and transcription units of the human apolipoprotein E receptor 2 gene. JBC 272(13): 8498-8504

58. Keshvara L, Benhayon D, Magdaleno S, Curran T (2001) Identification of Reelin-induced Sites of Tyrosyl phosphorylation on Disabled 1. JBC 276 (19): 1608-1604

59. Koch S, Strasser V, Hauser C, Fasching D, Brandes C, Bajari TM, Schneider WJ, Nimpf J (2002) A secreted soluble form of ApoE receptor 2 acts as a dominant-negative receptor and inhibits Reelin signalling. EMBO 21 (22): 5996-6004

60. Korschineck I, Ziegler S, Breuss J, Lang I, Lorenz M, Kaun C, Ambros PF, Binder BR (2001) Identification of a novel exon in apolipoprotein E receptor 2

leading to alternatively spliced mRNAs found in cells of the vascular wall but not in neuronal tissue. JBC 276(16): 13192-13197

61. Kubo KI, Mikoshiba K, Nakajima K (2002) Secreted Reelin molecules form homodimers. Neurosci. Res. 43: 381-388

62. Lee VM, Andrews PW (1986) Differentiation of NTERA-2 clonal human embryonal carcinoma cells into neurons involves the induction of all three neurofilament proteins. J Neurosci. 6(2): 514-521

63. Lew J, Huang QQ, Qi Z, Winkfein RJ, Aebersold R, Hunt T, Wang JH (1994) A brain-specific activator of cyclin-dependent kinase 5. Nat. 371(6496): 423-426

64. Luque JM, Morante-Oria J, Fairen A (2003) Localization of ApoER2, VLDLR and Dab1 in radial glia: groundwork for a new model of reelin action during cortical development. Brain Res Dev Brain Res. 140(2): 195-203

65. Mahley RW (1998) Apolipoprotein E: cholesterol transport protein with expanding role in cell biology. Science 240(4852): 622-630

66. Maness PF (1992) Nonreceptor protein tyrosine kinases associated with neuronal development. Dev Neurosci. 14(4): 257-270

67. Marin-Padilla M (1978) Dual origin of the mammalian neocortex and evolution of the cortical plate. Anat Embryol (Berl). 152(2): 109-126

68. Martinez-Cerdeno V, Galazo MJ, Cavada C, Clasca F (2002) Reelin immunoreactivity in the adult primate brain: intracellular localization in projecting and local circuit neurons of the cerebral cortex, hippocampus and subcortical regions. Cereb Cortex. 12(12): 1298-1311

69. Massaro EJ, Elstein KH, Zucker RM, Bair KW (1989) Limitations of the fluorescent probe viability assay. Mol Toxicol. 2(4): 271-284

70. Matsuo ES, Shin RW, Billingsley ML, Van deVoorde A, O'Connor M, Trojanowski JQ, Lee VM (1994) Biopsy-derived adult human brain tau is phosphorylated at many of the same sites as Alzheimer's disease paired helical filament tau. Neuron 13(4): 989-1002

71. May P, Herz J (2003) LDL Receptor-related Proteins in Neurodevelopment. Traffic 4: 291-301

72. Merrick SE, Trojanowski JQ, Lee VM (1997) Selective destruction of stable microtubules and axons by inhibitors of protein serine/threonine phosphatases in cultured human neurons. J Neurosci. 17(15): 5726-5737

73. Meyer D, Liu A, Margolis B (1999) Interaction of c-Jun amino-terminal kinase interacting protein-1 with p190 rhoGEF and its localization in differentiated neurons. JBC 274(49): 35113-35118

74. Mi H, Haeberle H, Barres BA (2001) Induction of astrocyte differentiation by endothelial cells. J Neurosci. 21(5): 1538-1547

75. Michler-Stuke A, Wolff JR, Bottenstein JE (1984) Factors Influencing Astrocyte Growth and Development in Defined Media. Int. J. Devl. Neurosci. 2(6): 575-584

76. Moonen G, Cam Y, Sensenbrenner M, Mandel P (1975) Variability of the effects of serum-free medium, dibutyryl-cyclic AMP or theophylline on the morphology of cultured new-born rat astroblasts. Cell Tissue Res. 163(3): 365-372

77. Nedergaard M, Ransom B, Goldman SA (2003) New roles for astrocytes: redefining the functional architecture of the brain. Trends Neurosci. 26(10): 523-530

78. Newman EA (2003) New roles for astrocytes: Regulation of synaptic transmission. Trends Neurosci. 26(10): 536-542

79. Niu S, Renfro A, Quattrocchi CC, Sheldon M, D'Arcangelo G (2004) Reelin Promotes Hippocampal Dendrite Development through the VLDLR/ApoER2-Dab1 Pathway. Neuron 41: 71-84

80. Nolte J (1999) The Human Brain: An introduction to its functional anatomy. Copyright © 1999 by Mosby, Inc. Fourth Edition, 30-35

81. Novak S, Hiesberger T, Schneider WJ, Nimpf J (1996) A new low density lipoprotein receptor homologue with 8 ligand binding repeats in brain of chicken and mouse. JBC 271(20): 11732-11736

82. Ogawa M, Miyata T, Nakajima K, Yagyu K, Seike M, Ikenaka K, Yamamoto H, Mikoshiba K (1995) The reeler gene-associated antigen on Cajal-Retzius neurons is a crucial molecule for laminar organization of cortical neurons. Neuron 14(5): 899-912

83. Ohshima T, Ward JM, Huh CG, Longenecker G, Veeranna, Pant HC, Brady RO, Martin LJ, Kulkarni AB (1996) Targeted disruption of the cyclin-dependent kinase 5 gene results in abnormal corticogenesis, neuronal pathology and perinatal death. PNAS 93(20): 11173-11178

84. Pappas GD, Kriho V, Pesold C (2001) Reelin in the extracellular matrix and dendritic spines of the cortex and hippocampus: a comparison between wild type

and heterozygous *reeler* mice by immunoelectron micrcoscopy. J of Neurocyt. 30: 413-425

85. Pawson T, Scott JD (1997) Signalling through scaffold, anchoring, and adaptor proteins. Science 278(5346): 2075-2080

86. Piet R, Poulain DA, Oliet SH (2004) Contribution of astrocytes to synaptic transmission in the rat supraoptic nucleus. Neurochem Int. 45(2-3): 251-257

87. Pleasure SJ, Lee VM (1993) NTera 2 cells: a human cell line, which displays characteristics, expected of a human committed neuronal progenitor cell. J Neurosci Res. 35(6): 585-602

88. Pleasure SJ, Page C, Lee VMY (1992) Pure, postmitotic, polarized human neurons derived from Ntera 2 cells provide a system for expressing exogenous proteins in terminally differentiated neurons. J of Neurosci. 12: 1802-1815

89. Porter JT, McCarthy KD (1996) Hippocampal astrocytes in situ respond to glutamate released from synaptic terminals. J Neurosci. 16(16): 5073-5081

90. Rakic P, Caviness VS Jr (1995) Cortical development: view from neurological mutants two decades later. Neuron 14(6): 1101-1104

91. Ramakers GJ, Moolenaar WH (1998) Regulation of astrocyte morphology by RhoA and lysophosphatidic acid. Exp Cell Res. 245(2): 252-262

92. Rechsteiner M, Rogers SW (1996) PEST sequences and regulation by proteolysis. Trends Biochem Sci. 21(7): 267-271

93. Reichenbach A, Siegel A, Senitz D, Smith TG Jr (1992) A comparative fractal analysis of various mammalian astroglial cell types. Neuroimage 1(1): 69-77

94. Reiner O, Carrozzo R, Shen Y, Wehnert M, Faustinella F, Dobyns WB, Caskey CT, Ledbetter DH (1993) Isolation of a Miller-Dieker lissencephaly gene containing G protein beta-subunit-like repeats. Nat. 364(6439): 717-721

95. Rice DS, Sheldon M, D'Arcangelo G, Nakajima K, Goldowitz D, Curran T (1998) Disabled-1 acts downstream of Reelin in a signaling pathway that controls laminar organization in the mammalian brain. Develop. 125(18): 3719-3729

96. Royaux I, Lambert de Rouvroit C, D'Arcangelo G, Demirov D, Goffinet AM (1997) Genomic organization of the mouse reelin gene. Genomics 46(2): 240-250

97. Safavi-Abbasi S, Wolff JR, Missler M (2001) Rapid morphological changes in astrocytes are accompanied by redistribution but not by quantitative changes of cytoskeletal proteins. Glia 36(1): 102-115

98. Sandhu JK, Sikorska M, Walker PR (2002) Characterization of astrocytes derived from human NTera-2/D1 embryonal carcinoma cells. J Neurosci Res. 68(5): 604-614

99. Sapir T, Elbaum M, Reiner O (1997) Reduction of microtubule catastrophe events by LIS1, platelet-activating factor acetylhydrolase subunit. EMBO J 16(23): 6977-6984

100. Schneider WJ, Nimpf J, Bujo H (1997) Novel members of the low density lipoprotein receptor superfamily and their potential roles in lipid metabolism. Curr Opin Lipidol. 8(5): 315-319

101. Senzaki K, Ogawa M, Yagi T (1999) Proteins of the CNR family are multiple receptors for Reelin. Cell 99(6): 635-647

102. Sheldon M, Rice DS, D'Arcangelo G, Yoneshima H, Nakajima K, Mikoshiba K, Howell BW, Cooper JA, Goldowitz D, Curran T (1997) Scrambler and yotari disrupt the disabled gene and produce a reeler-like phenotype in mice. Nat. 389(6652): 730-733

103. Slezak M, Pfrieger FW (2003) New roles for astrocytes: regulation of CNS synaptogenesis. Trends Neurosci. 26(10): 531-535

104. Stockinger W, Brandes C, Fasching D, Hermann M, Gotthardt M, Herz J, Schneider WJ, Nimpf J (2000) The reelin receptor ApoER2 recruits JNK-interacting proteins-1 and -2. JBC 275(33): 25625-25632

105. Stockinger W, Hengstschlager-Ottnad E, Novak S, Matus A, Huttinger M, Bauer J, Lassmann H, Schneider WJ, Nimpf J (1998) The low density lipoprotein receptor gene family. Differential expression of two alpha2-macroglobulin receptors in the brain. JBC 273(48): 32213-32221

106. Strasser V, Fasching D, Hauser C, Mayer H, Bock HH, Hiesberger T, Herz J, Weeber EJ, Sweatt JD, Pramatarova A, Howell B, Schneider WJ, Nimpf J (2004) Receptor Clustering Is Involved in Reelin Signalling. Mol. Cell. Biol. 24 (3): 1378-1386

107. Sun XM, Soutar AK (1999) Expression in vitro of alternatively spliced variants of the messenger RNA for human apolipoprotein E receptor-2 identified in human tissues by ribonuclease protection assays. Eur J Biochem. 262(1): 230-239

108. Sun XM, Soutar AK (2003) The Transmembrane Domain and PXXP Motifs of ApoE Receptor 2 Exclude It from Carrying out Clathrin-mediated Endocytosis. JBC 278 (22): 19926-19932

109. Sweet HO, Bronson RT, Johnson KR, Cook SA, Davisson MT (1996) Scrambler, a new neurological mutation of the mouse with abnormalities of neuronal migration. Mamm Genome. 7(11): 798-802

110. Tamagno E, Aragno M, Parola M, Parola S, Brignardello E, Boccuzzi G, Danni O (2000) NT2 neurons, a classical model for Alzheimer's disease, are highly susceptible to oxidative stress. Neuroreport 11(9): 1865-1869

111. Trommsdorff M, Borg JP, Margolis B, Herz J (1998) Interaction of cytosolic adaptor proteins with neuronal apolipoprotein E receptors and the amyloid precursor protein. JBC 273(50): 33556-33560

112. Trommsdorff M, Gotthardt M, Hiesberger T, Shelton J, Stockinger W, Nimpf J, Hammer RE, Richardson JA, Herz J (1999) Reeler/Disabled-like Disruption of Neuronal Migration in Knockout Mice Lacking the VLDL Receptor and ApoE Receptor 2. Cell 97: 689-701

113. Tsai LH, Delalle I, Caviness VS Jr, Chae T, Harlow E (1994) p35 is a neural-specific regulatory subunit of cyclin-dependent kinase 5. Nat. 371(6496): 419-423

114. Walker PR, Ly D, Liu QY, Smith B, Sodja C, Ribecco M, Sikorska M (2004) Genome-wide Expression Profiling of Neurogenesis in Relation to Cell Cycle Exit In " The Cell Cycle in the CNS", Ed., Janigro D. Human Press (In Press).

115. Ware ML, Fox JW, Gonzalez JL, Davis NM, Lambert de Rouvroit C, Russo CJ, Chua SC Jr, Goffinet AM, Walsh CA (1997) Aberrant splicing of a mouse disabled homolog, mdab1, in the scrambler mouse. Neuron 19(2): 239-249

116. Weeber EJ, Beffert U, Jones C, Christian JM, Forster E, Sweatt JD, Herz J (2002) Reelin and ApoE Receptors Cooperate to Enhance Hippocampal Synaptic Plasticity and Learning. JBC 277 (42): 39944-39952

117. Weeber EJ, Beffert U, Jones C, Christian JM, Forster E, Sweatt JD, Herz J (2002) Reelin and ApoE Receptors Cooperate to Enhance Hippocampal Synaptic Plasticity and Learning. JBC 277 (42): 39944-39952

118. Weiss KH, Johanssen C, Tielsch A, Herz J, Deller T, Frotscher M, Forster E (2003) Malformation of the radial glial scaffold in the dentate gyrus of reeler mice, scrambler mice, and ApoER2/VLDLR-deficient mice. J Comp Neurol. 460(1): 56-65

119. Wu VW, Schwartz JP (1998) Cell culture models for reactive gliosis: new perspectives. J Neurosci Res. 51(6): 675-681

120. Xu L, Sapolsky RM, Giffard RG (2001) Differential sensitivity of murine astrocytes and neurons from different brain regions to injury. Exp Neurol. 169(2): 416-424

121. Yasuda J, Whitmarsh AJ, Cavanagh J, Sharma M, Davis RJ (1999) The JIP group of mitogen-activated protein kinase scaffold proteins. Mol Cell Biol. 19(10): 7245-7254

122. Yoneshima H, Nagata E, Matsumoto M, Yamada M, Nakajima K, Miyata T, Ogawa M, Mikoshiba K (1997) A novel neurological mutant mouse, yotari, which exhibits reeler-like phenotype but expresses CR-50 antigen/reelin. Neurosci Res. 29(3): 217-223

123. Zhang Q, Fukuda M, Van Bockstaele E, Pascual O, Haydon PG (2004) Synaptotagmin IV regulates glial glutamate release. PNAS 101(25): 9441-9446